This is to certify that the
dissertation entitled

CLIMATE TRENDS AND SYNOPTIC PATTERNS
ASSOCIATED WITH MAJOR PRECIPITATION EVENTS
OF THE SOUTHERN APPALACHIANS

presented by

Ryan P. Shadbolt

has been accepted towards fulfillment
of the requirements for the

Ph.D. degree in Geography

Jay R Harman
Major Professor's Signature

July 21, 2009
Date

CLIMATE TRENDS AND SYNOPTIC PATTERNS ASSOCIATED WITH MAJOR PRECIPITATION EVENTS OF THE SOUTHERN APPALACHIANS

By

Ryan P. Shadbolt

A DISSERTATION

Submitted to
Michigan State University
in partial fulfillment of the requirements
for the degree of

DOCTOR OF PHILOSOPHY

Geography

2009

ABSTRACT

CLIMATE TRENDS AND SYNOPTIC PATTERNS ASSOCIATED WITH MAJOR PRECIPITATION EVENTS OF THE SOUTHERN APPALACHIANS

By

Ryan P. Shadbolt

This study focuses on the southern Appalachians, a region of pronounced biodiversity. While environmental change in the area is documented, our understanding of associated regional climate change remains less certain. For this reason, surface observations of minimum, maximum, and mean temperature, total precipitation, and total snowfall from 463 stations within the region were obtained from the National Climatic Data Center's Cooperative Observer Program to facilitate the construction of a baseline climatology focused on temporal trends and spatial clusters.

First-order temporal trends show that the southern Appalachian region experienced statistically significant cooling trends during 1931-2006, although two-phase regression results also reveal that statistically significant warming trends emerged during recent decades. This warming was most evident in wintertime and minimum temperatures with January temperatures warming as much as 4.00°C between the mid 1970s and 2006. Overall, diurnal and annual temperature ranges decreased, while annual precipitation increased over the study period. Snowfall totals decreased at low and mid elevations and a statistically significant increase occurred at high elevations. The recent warming and decreasing temperature ranges for this locale support trends presented within recent reports from Intergovernmental Panel on Climate Change and the United States Global Change Research Program. The effectiveness of the cluster analysis was

limited by the availability and spatial resolution of the observation stations. However, the resulting clusters still depicted relationships between stations of similar geographic locations and elevations and up to five climate regimes were defined for the region.

Additionally, a study of synoptic patterns during 1437 major precipitation events spanning 1979-2006 revealed up to 11 common synoptic patterns. The synoptic patterns were created by objective, subjective, and hybrid clustering approaches. The results from the objective approach differed from the subjective approach, and patterns uncovered by the hybrid approach had similarities to both the objective and subjective approaches. Since results varied depending on the cluster approach used, it is recommended that future studies should not rely solely on one approach when clustering synoptic patterns.

A temporal analysis showed that some synoptic patterns became more or less frequent over the 1979-2006 period and some trends were statistically significant. Precipitation events associated with low-pressure and frontal systems became more frequent, whereas precipitation events associated primarily with orographic lifting or thermodynamics became less common. The results from this dissertation build upon those from previous studies and provide a more complete summary of the region's recent climate, one that should help inform future climate studies of the region and inform those who manage the region's ecosystems.

ACKNOWLEDGEMENTS

Many individuals helped make the completion of this dissertation and my Ph.D. program possible. I am grateful to all Geography faculty, staff, and graduate students at Michigan State University and have enjoyed being a member of the department. I wish to thank the department's willing staff: Sharon Ruggles, Judy Reginek, and Claudia Brown. Tech supporters, Jim Brown and Wilson Ndovie, frequently assisted me with computer issues. The virtual course coordinator, Beth Weisenborn, was of great assistance during my time instructing the online version of the Geography of the U.S. and Canada course. The past and present graduate program coordinators, Dr. Randy Schaetzl and Dr. Antoinette WinklerPrins were always happily available to lend advice during the course of my M.A. and Ph.D. programs.

During my time at MSU, I was fortunate to receive funding from a variety of sources. I am appreciative of the Geography Department for the teaching and research assistantship opportunities I was awarded through the years. I am also thankful for the research opportunities offered to me by Dr. Julie Winkler, Dr. Joe Messina, and Dr. Ashton Shortridge. Dr. Jay Charney, Dr. Brian Potter, Dr. Warren Heilman, and Xindi Bian also graciously offered me research positions at the U.S. Forest Service office during some summer months as well.

In particular, completing this dissertation would not have been possible without the participation of my five committee members. Dr. Jeff Andresen, Dr. Catherine Yansa, and Dr. Jay Charney each provided valuable recommendations during the early stages of solidifying the objectives for this research project. Dr. Pang-Ning Tan provided essential suggestions for the cluster analysis portions of the study. My advisor, Dr. Jay Harman, deserves a large portion of the credit for sparking my interest in the southern Appalachian region, and ultimately, the initiation of this study. I have had the pleasure to accompany him on three separate field trips to the region and was taught to view it through the eyes of a geographer. His thoughtful questions, suggestions, and dedicated editing helped improve the text of this document with each passing revision.

Lastly, and most importantly, I wish to thank my family and friends for their patience and never-ending support throughout the years of my Ph.D. program. My wife, Jennifer Lamb, has been beside me every step of the way and I look forward to the future travels of our journey. I am certain at least a few trips to the southern Appalachians will be included in the itinerary.

TABLE OF CONTENTS

LIST OF TABLES

LIST OF FIGURES

CHAPTER 1

INTRODUCTION

1.1. Overview and Statement of Problem

With a relief greater than 1500 m in many areas, the southern Appalachian region offers a variety of microclimates with weather conditions comparable to those spanning from Georgia to Canada (Figure 1.1). Thousands of plant and animal species exist in the region, some of which live no place else in the world. Located along the TN and NC border, Great Smoky Mountains National Park (GSMNP; see Figure 1.2), for example, contains the largest expanse of old-growth forest east of the Mississippi River. According to the National Park Service (NPS), an estimated 100,000 species of living organisms reside within GSMNP and new species are frequently discovered (NPS, 2009).

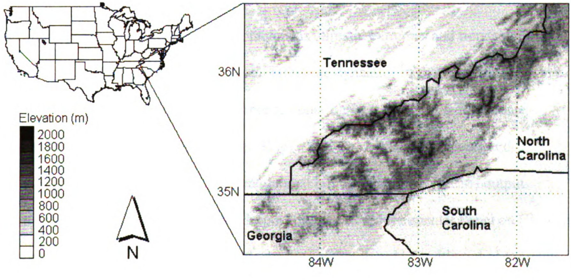

Figure 1.1. Southern Appalachian study area. Shaded elevation values are included as meters above sea level.

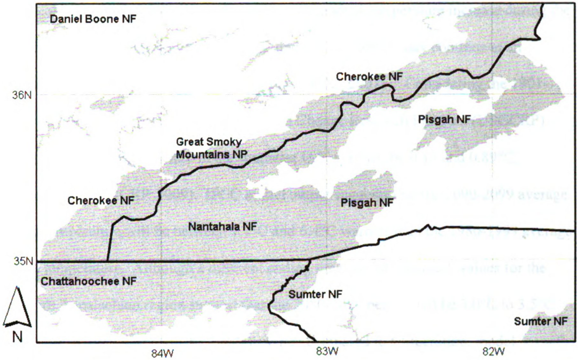

Figure 1.2. Study region with gray areas depicting federally-owned lands. Locations of Great Smoky Mountains National Park and nearby national forests are labeled.

While the region has demonstrated resilience over time, it is vulnerable to natural and anthropogenic disturbances. Such factors as climatic extremes and trends, wildfires, air pollution, deforestation, and insects all affect the dynamics of the vegetation in ways that are often poorly understood. Possible regional impacts resulting from climate change are also receiving attention (e.g., Kupfer and Cairns, 1996; Delcourt and Delcourt, 2001; Delcourt, 2002). Recent general circulation model (GCM) output summarized in the Fourth Assessment Report by the Intergovernmental Panel on Climate Change (IPCC) suggests warming trends for the southeastern U.S., although the models vary on the magnitude of warming. In addition, while some models predict wetter conditions in the southeastern U.S. by 2100, other models suggest drier conditions (IPCC, 2007a).

Analyses of global climate have shown a gradual temperature increase during the twentieth century ranging between 0.56°C and 0.92°C, which may continue at an increasing rate during the twenty-first century (IPCC, 2007a). Considering the 1901-2008 and 1970-2008 periods, the U.S. Global Change Research Program (USGCRP) found that annual temperature in the southeast U.S. warmed by 0.17 and 0.89°C, respectively (USGCRP, 2009). IPCC model output suggests that the 2090-2099 average global temperature will be between 1.1°C and 6.4°C warmer than the 1980-1999 average global temperature. Although a different ending time period was used, values for the southern Appalachian region suggest that the 2080-2099 period will be 3.0°C to 3.5°C warmer than 1980-1999 (IPCC, 2007a). When compared to temperature, model projections of precipitation from the Fourth Assessment Report display less agreement. In general, precipitation is expected to increase in mid-latitude regions (e.g., the Great Lakes) while decreasing in regions closer to the equator (e.g., Mexico). The southern Appalachians lie in between these two extremes, and climate models disagree over whether precipitation will increase, decrease, or remain close to current levels (IPCC, 2007a). The USGCRP did not make firm projections regarding the region's precipitation, although the report did point out that precipitation in the region did increase over the 1901-2008 period. In recent decades, rainfall was received in heavier amounts, but during fewer overall events. The result created the opportunity for more drought periods during the past few decades (USGCRP, 2009)

Amidst this uncertainty about future climates, an elaboration of temperature and precipitation trends of the recent past, as well as an in-depth description of synoptic patterns affecting the region's precipitation, remain lacking in the scientific literature.

These limitations constrain the ability of climate scientists to put climate projections emerging from GCMs into a scientific context. As a result, the ability to assess the likely consequences on the regional moisture climatology of changing synoptic patterns projected by model output is compromised, a problem made even worse by climatic complexity introduced by the extreme topographic variety within the region. Thus, I propose to construct a synoptic climatological inventory of the southern Appalachian region in order to elaborate the region's complex moisture climatology. A baseline temporal and spatial analysis of the region's temperature and precipitation will also be included to provide a context in which to compare results from global and regional climate model projections.

1.2. Ecological Change in the Region

Although debate exists over whether or not the southern Appalachians served as a refuge for plant and animal species during the last glacial advance (Deevey, 1949; Braun, 1950; Delcourt, 2002), there is consensus that over time the area has become a place of high biodiversity. However, the species richness of the southern Appalachians could be adversely impacted by a period of accelerated warming. A temperature increase of 1.5°C to 2.5°C (well within the range presented by the IPCC) is expected to put approximately 20 to 30 percent of the world's species at risk for extinction (IPCC, 2007b). Poleward and upward shifts in habitats are expected, leaving high-elevation species and endemic species (those found nowhere else) of the southern Appalachians particularly at risk (Delcourt, 2002). These high-elevation environments may be thought of as "sky islands" with similar ecosystems existing on each isolated mountain peak. Although sky island terminology has commonly been used to describe a species-rich area near the union of the Arizona, New Mexico, and Mexico borders (e.g., Heald, 1967; Kupfer et al., 2005; Skroch, 2009), the southern Appalachian region also possesses a species-rich, high-elevation island characteristic and has also received attention (e.g., Kupfer and Cairns 1996; Allen and Kupfer, 2000; 2001; Delcourt and Delcourt, 2001; Delcourt, 2002). Future warming trends may result in low-elevation species moving upward and eventually replacing high-elevation species since those species currently adapted to the highest elevations would have already reached the physical limits of their respective ranges.

Natural and anthropogenic causes have had detrimental effects on wildlife in the region already. Some species, such as Fraser fir (*Abies fraseri*) are endemic to region. The tree species has been impacted greatly by the exotic balsam woolly adelgid insect (Busing et al., 1988), as well as by high ozone levels (Aneja et al., 1991), and acid rain (Aneja et al., 1992). With the addition of increasing temperatures, Fraser fir is one example of a species that could disappear entirely by 2100 (Delcourt, 2002). Some of the most biodiverse and unique areas of the southern Appalachian high elevations are grassy balds (Mark, 1958; Houk, 2009). These balds, and likely all of the wildlife they contain, are also expected to continue disappearing as temperatures increase. In addition to the loss of diversity, a longstanding view has been that old-growth forests are carbon-neutral environments. However, two recent studies proposed that old-growth forests actually continue to sequester carbon in boreal, temperate (Luyssaert et al., 2008), and tropical (Lewis et al., 2009) climates. If true, any loss of the region's old-growth forest due to a warming climate could contribute to a feedback cycle and lead to additional warming.

1.3. Research Goals

The rationale for this study has two main considerations. First, studies of the region's ecology suggest that species richness is being affected by recent climate change and the trend will continue if global warming continues at the projected pace. Biodiversity is what sets the southern Appalachians, and particularly GSMNP, apart from other areas nearby, and it may be in jeopardy given this warming. The possible extinction of high-elevation and endemic species only raises the biological stakes. Second, climate projection results presented in the IPCC's Fourth Assessment Report and the USGCRP's 2009 report are tentative and uncertain for this region and a review of past climatological literature for the region suggests that additional research is needed to improve our scientific knowledge of the region's climate.

In order to address the need for additional climate research for this region, my specific goals for this dissertation include: 1) examining the region's temperature and precipitation values over time to highlight any temporal trends and test any existing trends for statistical significance, 2) spatially analyzing the region's station observations to note whether or not multiple distinct climate regimes exist, and if so, how many, 3) conducting a climatological inventory of synoptic patterns occurring during major precipitation events within the region using several approaches and testing the frequency trends of each synoptic pattern for statistical significance, and 4) comparing the results from the various approaches used.

To improve current knowledge of the region's future climate, researchers must first fully understand the region's climate of the recent past. As a result, I deemed a thorough investigation of recent climate of the southern Appalachians as necessary. In particular, climate scientists need an updated and expanded climatology of temperature, precipitation, and snowfall, as well as a broadened understanding of the synoptic origins of precipitation in order to obtain knowledge of conditions during the recent past. With the results provided here, those of us in the climate community should be better equipped to recognize future changes in the climate and synoptic patterns that influence the species-rich southern Appalachians.

1.4. Organization of the Dissertation

In Chapter 2, I provide a review of relevant literature covering previous baseline and synoptic climatologies, the history and methods of cluster analysis used in climatological research, and climate studies that used objective or subjective clustering techniques. Also within Chapter 2, I provide a list of specific research questions and objectives that I will address through this study. Chapter 3 includes a description of the study area and the datasets used. In that chapter I also describe my methods for carrying out the temporal and spatial baseline climatology and the synoptic climatology. In Chapter 4, the results and discussion of the temporal analysis are presented. The results and discussion of the spatial analysis are presented in Chapter 5. Results and discussion of the synoptic climatology are presented in Chapter 6. Lastly, in Chapter 7, I revisit the research questions, provide recommendations for future research, and share final remarks. Appendices A-E follow the dissertation and include supplemental material.

CHAPTER 2

LITERATURE REVIEW

2.1. General Climatologies of the Region

According to Köppen's well-known climate classification system, the southern Appalachian region is included within the Cfa, or "humid subtropical," category. Typically, Cfa regions are located between 25° and 40° latitude, along eastern sections of continents (Ahrens, 2003). These regions are characterized by hot, humid summers (i.e., dewpoints often exceed 23°C) and mild winters (i.e., average temperature of the coldest month below 18°C, and above -3°C). Precipitation is frequent and widespread. Annual totals usually range between 800 and 1650 mm (Ahrens, 2003). However, the complex topography of the southern Appalachians likely encompasses more climatic zones than just Cfa. Topographic shape, slope, aspect, and elevation create a variety of microclimates (Hack and Goodlett, 1960), and thus, the region experiences temperature and precipitation averages that can differ from those discussed above.

Using recorded precipitation data spanning 1936-1949, Whittaker (1952) showed that the southern Appalachian region had some of the highest annual precipitation totals in the eastern U.S. Precipitation in valley regions (e.g., Gatlinburg, TN, Elkmont, TN, and Maryville, TN) ranged from 50-60 inches (1270-1524 mm) annually and increased with elevation up to 80 inches (2032 mm) or more. Whittaker's dataset also revealed that precipitation maxima typically occurred during late winter/early spring and late summer, while minima occurred in late spring and early autumn.

Smallshaw (1953) presented three precipitation studies conducted by the

Tennessee Valley Authority (TVA) and the U.S. Weather Bureau. Annual precipitation values across the southern Appalachian region ranged from 39 inches (991 mm) in the valleys to 93 inches (2362 mm) on the ridges. The first study included stations scattered throughout the Newfound Gap region of GSMNP during the years 1946-1950. Precipitation totals increased abruptly with elevation up to about 3000-3500 ft (914-1067 m) and then continued to increase with elevation, but at a slower rate. However, the second and third studies demonstrated that not all areas in the Appalachians followed the pattern of increasing precipitation with increasing elevation. Snake Mountain, NC, and Clinch Mountain, VA, both received less precipitation near the peaks than in the surrounding valleys. In both cases, the smaller amount of precipitation was attributed to "a combination of updraft and carry-over of moisture-laden air because of the steep upper slope and the narrow crest of the ridge[s]" (Smallshaw, 1953; p. 587). In addition, a funneling effect could have occurred as wind passed the mountain peaks. The funneling effect may have accelerated wind speeds and impacted the amount of precipitation the gages collected. As a result, the TVA moved precipitation gages from peaks in order to avoid any future funneling effect.

Shanks (1954) used data from four stations within GSMNP during the years 1946-1950 to describe how temperature and precipitation varied with increasing elevation within the park. Stations included were: Park Headquarters (445 m), Alum Cave parking lot (1158 m), Newfound Gap (1524 m), and Clingman's Dome (1920 m). Over the five-year period, annual precipitation at the lowest station averaged 57.8 inches (1468.1 mm). Precipitation increased with increasing elevation, with the highest station averaging 90.9 inches (2308.9 mm). The five-year mean annual temperature profile for the stations showed that the average rate of decrease with altitude was 2.23°F/1000 ft (4.06°C/1000 m), which was similar to the results found by others (see Table 2 provided in Hicks, 1979). These lapse rate values tended to be less than the "normal lapse rate" usually given as 6.5°C/1000 m (Ahrens, 2003). However, the humid conditions and low continentality of the southeastern U.S. probably accounted for the region's smaller lapse rate (Hicks, 1979). Shanks found July to be the warmest month at all elevations, while the coldest month varied between November and December for low elevations and March for the highest station. These classic works by Whittaker (1952), Smallshaw (1953), and Shanks (1954) continue to be cited in reference to southern Appalachian climate. For similar classic overviews of the region's vegetation, the reader is referred to Braun (1950) and Whittaker (1956).

Mark (1958) created a climatology spanning a 26-year period (1931-1956) and included three stations: Asheville, NC (671 m), Banner Elk, NC (1131 m), and Mount Mitchell, NC (2022 m). Daily mean temperature fell to a minimum in January for Asheville (4.6°C) and Banner Elk (1.5°C), while the minimum for Mount Mitchell (-2.6°C) was in February. In agreement with Shanks (1954), Mark (1958) found that the daily mean temperature maximum occurred in July for all three stations (Asheville, 23.6°C; Banner Elk, 19.3°C; Mount Mitchell, 15.2°C). Annual precipitation increased with increasing elevation (Asheville, 956 mm; Banner Elk, 1301 mm; Mount Mitchell, 1830 mm). Substantial precipitation occurred at all times of the year, with dry periods in late spring and autumn. Snowfall began in October and continued through May, with maximum snowfall occurring in February for Asheville (annual total of 79 mm), January for Banner Elk (annual total of 224 mm), and March for Mount Mitchell (annual total of

378 mm). On average, Asheville received precipitation 128 days per year, while Banner Elk received precipitation on 117 days, and Mount Mitchell 145 days.

In order to study intense rainfall in GSMNP, Bogucki (1972) used rain gages at 20 locations during 1937-1968. Station elevations ranged from 280 to 1935 m. A total of 293 intense rain events were recorded, with 71 percent of events occurring between April and September. Intense rain events were defined as one or more inches received in one hour, or defined as three or more inches received in 24 hours. Annual average precipitation ranged from 55.19 inches (1401.83 mm) in Gatlinburg, TN, to 75.73 inches (1923.54 mm) at Clingman's Dome. Additional results were inconclusive as neither total precipitation nor elevation had a direct relationship on the number of intense rainfalls recorded at a particular gage.

In the surrounding area of GSMNP, Hicks (1979) used 1975-1976 summer observations from nine communities: Gatlinburg, TN (443 m and 445 m), Oconaluftee, NC (640 m), Cataloochee, NC (798 m), Sevierville, TN (283 m), Pigeon Forge, TN (314 m), Jones Cove, TN (360 m), Pittman Center, TN (411 m), Cosby, TN (524 m), and Cataloochee Branch, NC (1463 m). In addition, five stations were used within Greenbrier Cove: low-elevation cove (760 m), high-elevation cove (1040 m), oak-heath deciduous (1040 m), oak-heath deciduous (1030 m), and hemlock (1030 m). Linear relationships were determined based on temperature and precipitation data. The resulting temperature relationship with elevation was expressed as:

$$y = -0.0046x + 23.68 \text{ (where } r = -0.98\text{).}$$

The resulting precipitation relationship with elevation was expressed as:

$$y = 0.065x + 62.58 \text{ (where } r = 0.72).$$

Note that these relationships were based on stations at elevations less than 1500 m. As indicated by Smallshaw (1953), at higher elevations precipitation tended to increase upward at a slower rate suggesting that the true relationship between precipitation and elevation may not be linear.

More recently, Bolstad et al. (1998) used 13 local stations located at the Coweeta Hydrological Lab near Otto, NC, as well as 35 regional stations from the National Climatic Data Center (NCDC) to analyze temperature lapse rates in order to create a regression model. Station elevations ranged from 239 to 1967 m. Lapse rates varied between 3°C/1000 m and 7°C/1000 m depending on time of day. Daily maximum temperatures above canopy on south-facing slopes were 1.4°C warmer on average compared to north-facing slopes. Regional regression models provided more accurate estimates compared to models created from local observations or estimates created from kriging.

Lastly, Gaffin and Hotz (2000) used 30 years (1961-1990) of station data from the NCDC's Cooperative Observing Program (COOP) to create a spatial climatology of precipitation. The highest average amount of annual precipitation (>2000 mm) was received in the southwest portion of NC, near SC and GA. An annual precipitation minimum (1000 mm) was present near Asheville, NC, and was probably the result of downslope flow. During winter months, the spatial pattern of one maximum was most prominent. However, from May through August a second maximum was present near the area of GSMNP. In agreement with other studies, the driest times of the year occurred in spring and autumn, while the wettest time of year was summer.

While many climatological studies have been conducted within this region, many are older studies that often utilized short periods of record and/or incorporated data from a small number of stations (e.g., Whittaker, 1952; Smallshaw, 1953; Shanks, 1954; Mark, 1958; Bogucki, 1972; Hicks, 1979; Bolstad et al., 1998). Gaffin and Hotz (2000) presented the longest spatial climatology of precipitation and used a larger station network, but temporal variability was not discussed. Of the studies listed, only one station covered snowfall (Mark, 1958). Although these past studies are informative, they have not adequately covered recent decades, which in turn has not allowed for a sufficient and up-to-date temporal and spatial climatology of the region's temperature, precipitation, and snowfall.

2.2. Synoptic Patterns Impacting Southern Appalachian Precipitation

Miller's (1946) classic study presented two types of cool-season Atlantic Coast cyclones. Using data spanning 1929-1939 (October to April only) from 208 cyclone cases, he classified the cyclones as Type A or Type B. Type A cyclones frequently formed along the eastern coast. Usually, a large high-pressure system and cold air mass were present over much of the continental U.S., while a warm air mass was located over the western Atlantic where the cyclones originated. Precipitation was mostly limited to the areas ahead of the warm front and within the comma cloud region. Due to the maritime moisture involved, these cyclones had the potential to result in heavy precipitation; however, the cyclone movement was typically to the northeast, so in many cases they did not impact the southern Appalachians. The annual average frequency of Type A cyclones reached a maximum in November, decreased to a minimum in January, and then had a secondary maximum in March.

Miller's (1946) Type B cyclones formed over the southeastern U.S. along the southern portion of another mature cyclone, which was usually occluded and positioned near the Great Lakes region. Like Type A cyclones, precipitation with Type B cyclones could exist ahead of the warm front and within the comma surrounding the low, but also along the cold front and with the existing mature cyclone to the north. Therefore, precipitation with Type B cyclones was more widespread. Type B cyclones were more likely to have a warm sector that traversed the southern Appalachians. Another common feature of Type B cyclones was cold-air damming, where a shallow layer of cold air was present on the eastern side of the Appalachians (Richwein, 1980; Bell and Bosart, 1988). The annual average frequency of Type B cyclones reached a maximum in January, decreased to a minimum in February, and then had a secondary maximum in March.

In rare cases, some Atlantic Coast cyclones exhibited characteristics similar to both Type A and Type B cyclones. Bosart's (1975) addendum to Miller (1946) included three more cyclone types studied during the years 1964-1972. Type C cyclones were similar to Type B except that the secondary low was absent and a strong, cold anticyclone was present to the east. Type D cyclones were similar to Type A, though they were weaker systems that did not intensify during the northeast propagation. The cyclones were more elongated and usually short-lived. Lastly, Type E cyclones were characterized by an east-west frontal zone orientation with the low located north of the southern

Appalachians and south of New England. The systems moved rapidly eastward and an anticyclone was present to the northeast. While Miller (1946) and Bosart (1975) both highlighted the importance of Atlantic Coast cyclones on climate of the eastern U.S., they did not, however, discuss other cyclone types that also impact the region.

Klein (1957), Reitan (1974), and Zishka and Smith (1980) presented frequencies and origins of cyclones for North America. One important result from these papers was the noted decrease in cyclone frequency during the middle portion of the last century. Whether or not a direct link existed between the decreases in cyclone frequency and documented global cooling of the same time period is unclear, as these authors did not address it, though subsequent studies suggested such a relationship was present (van Loon and Williams 1976a, 1976b; Harvey 1978; Diaz and Quayle, 1978).

Over the 1951-1970 period, Reitan (1974) found 4.4 cyclone events on average traversing the southern Appalachian region during January, 2.9 events in April, 0.9 events in July, and 1.8 in October, depicting an annual pattern. The cyclones were of the three classic types: Alberta cyclones, Colorado cyclones, and Atlantic Coast cyclones. Results between Reitan (1974) and Klein (1957) were similar; however, Klein's earlier time periods (1901-1914 and 1924-1937) revealed the Alberta cyclone type as the most frequent, whereas Reitan's results showed Colorado cyclones as more common. In both cases, though, these cyclone types were more likely to affect the southern Appalachians during winter and early spring, whereas during the warmer portion of the year, the cyclone origins and paths were located farther north. Zishka and Smith's (1980) results of cyclogenesis and cyclone paths were similar to that of Reitan (1974), though Zishka and Smith focused only on January and July (1950-1977). The authors found that more cyclones were present during January and also that cyclones exhibited a lower minimum sea-level pressure on average during January (988 hPa for January and 1001 hPa for July).

O'Handley and Bosart (1996) described the impact of southern Appalachian topography on cyclones. Studying 40 winter cyclones spanning 1979-1986 (December through March), they discovered that frontal speed decreased by about 40 percent and that fronts often developed a "kink" in their shape just east of the southern Appalachians. In addition, thermal and pressure gradients were enhanced by the mountains, but once the fronts passed the mountains, the fronts became weaker.

Konrad (1997) studied 312 heavy rainfall events and found five patterns associated with heavy rainfall within the southeastern United States, although his patterns were more on meso-scale phenomena and he did not include composite maps of his patterns. Heavy precipitation events were defined as at least 50 mm of rainfall observed at one or more stations within a 6-hour period. In most cases, high mixing ratios were present at 700 hPa, while warm air advection was also present at 850 hPa. Pattern 1 had boundary-layer convergence about 400 km northwest of the heavy rain area. A low-pressure system with trailing cold front was probably present. Moisture and warmth moved in from the Gulf of Mexico and had the highest values at the point of greatest rainfall. Pattern 1 was most common in the western portion of the southern Appalachians.

Pattern 2 was common with slow-moving cold fronts. Boundary-layer convergence was located to the immediate northwest of the heavy rain location. Mean winds were stronger for this pattern compared to the others. High moisture and temperature advection values were, again, found near the point of highest precipitation. Pattern 2 systems were most common in the western portion of the Appalachians, and were also most frequent in May and June, as upper-level winds were still relatively strong.

Weaker winds, with boundary-layer convergence occurring 100 km southeast of the rainfall center, were common with Pattern 3. A weak, stationary frontal boundary was often present. This pattern was most common during the summer months, as upper-level winds were weaker. Frequent southerly/southeasterly flow resulted in frontal overrunning. Pattern 3 was common along the eastern and southern portions of the area.

Pattern 4 was often associated with an elongated area of low-level convergence. A low-pressure center moved north/northeast from the Gulf region. Moisture and warm air advection maxima were present to the east of the boundary-layer convergence as a result of southerly flow just east of the approaching low. Like Pattern 3, Pattern 4 was also most frequent in summer and along the eastern and southern portions of the region.

Pattern 5 was associated with two regions of convergence. The first was located to the northwest of the rainfall center and the other was located more than 400 km to the southeast. This pattern was less common and no well-defined surface features were identified. A weak front, with a northwest to southeast configuration, was sometimes present. The south/southwesterly flow was responsible for high moisture and temperature advection values near the point of highest rainfall.

With a focus on 500 hPa heights and surface fronts, Gaffin and Hotz (2000) discussed four subjective synoptic patterns associated with heavy precipitation in the region. The heavy rain events were determined by either 3 inches (76.2 mm) of rain in 6 hours and/or 4 inches (101.6 mm) of rain in 12 hours. The authors named the first pattern "Synoptic," which consisted of a strong low-pressure system with warm and cold fronts that traversed the area. Low-level winds were southerly, with southwesterly winds above 850 hPa. The Synoptic pattern was most common during the cold portion of the year, as the stronger westerlies played a larger role in determining the weather experienced in the southern Appalachians. The second pattern was "Frontal" and consisted of an east/west stationary front positioned over the region. The Frontal pattern was more common in the warmer portion of the year. Westerly winds tended to be weaker, which allowed for a stronger topographic influence on rainfall. The third pattern was "Meso High." The Bermuda High had a substantial influence on how much southerly airflow moved through the region. Precipitation was most frequent with Meso Highs when a stationary front was located to the north of the southern Appalachians. Lastly, "Tropical" patterns were simply heavy precipitation events associated with tropical cyclones that affected the region during summer and autumn months.

Diem (2006) supplied a summer precipitation and circulation analysis; however, his study area was limited to the north and central portions of GA. He found that prolonged wet periods were associated with mid-tropospheric troughing west of the study region, while dry periods had the trough located to the east. For wet conditions, large positive anomalies of 500 hPa and 850 hPa heights were located off the northeast coast, as negative height anomalies were present over the Midwest. During dry periods, Diem (2006) found that the height anomalies were located in the same general areas, but were of opposite sign. The study area was usually under an anticyclone or on the western side of a trough. The anticyclone was either of continental origin or an extension of the

Bermuda High. Spanning 1953-2002, Diem (2006) found that wet summers occurred during the 1960s and the early 1990s. Dry summers occurred during the mid 1950s, the mid 1970s to mid 1980s, and in the late 1990s.

Whereas many classic cyclone studies exist for North America (e.g., Miller, 1946; Klein, 1957; Reitan, 1974; Bosart, 1975; Zishka and Smith, 1980), only Gaffin and Hotz (2000) specifically addressed synoptic weather patterns impacting the southern Appalachians, and even that study focused solely on heavy precipitation events. Using surface fronts and 500 hPa heights, Gaffin and Hotz (2000) concluded with four subjectively-derived synoptic types (Synoptic, Frontal, Meso-High, and Tropical). Diem (2006) presented a 50-year temporal climatology of precipitation and circulation analysis, but his study area was geographically limited to a portion of GA. The studies discussed still do not cover origins of precipitation (synoptic or otherwise) received in the region during smaller precipitation events. The past studies also considered few synoptic variables and levels, which may have also limited the number of synoptic patterns found.

2.3. Methods of Cluster Analysis

2.3.1. Overview

In climatological research, cluster analysis is one preferred approach used to group items exhibiting similar characteristics. Cluster analysis can be used to objectively create synoptic patterns or climate regimes, both of which I have expressed as an interest to this study. Although cluster analysis was first introduced in the 1930s (e.g., Tyron, 1939), it was not until the middle portion of the twentieth century that technological improvements assisted in shortening the time required for computation. Prior to the

quantitative revolution in the 1960s, clusters were often formed either by entirely subjective means (visual examination) or by a rule-based algorithm (e.g., Köppen, 1923; Thornthwaite, 1931). The first climatological studies utilizing objective cluster analysis techniques surfaced during the late 1960s (e.g., Skaggs, 1969). Objective approaches have received more attention since that time, although subjective techniques still remain common in climate research for defining regions (e.g., Shadbolt et al., 2006; Walters et al., 2008) and synoptic patterns (e.g., Gaffin and Hotz, 2000; Walters and Winkler, 2001; Walters et al., in preparation). In Section 2.3, I provide information regarding the different clustering techniques available, methods used for determining the correct number of clusters, and some of the available distance measures used for clustering. In Section 2.4, I then provide a review of previous climate studies that used cluster analysis and are relevant to this study.

2.3.2. Hierarchical Clustering Techniques

Many objective cluster analysis techniques are available, but most can be broadly categorized as either hierarchical or non-hierarchical (i.e., partitional) in nature (Gong and Richman, 1995; Tan et al., 2006; Wilks, 2006). Hierarchical clustering begins by assuming each individual entity (i.e., data point) is a cluster, where the total number of entities and the initial number of clusters is k. Step 1 merges the two most similar entities together to create a new cluster and the total number of clusters then becomes k-1. This agglomerative process continues with each step until either all entities have been clustered into one cluster or the user terminates the clustering at a specified step to create a desired number of clusters. A hierarchical cluster result can be illustrated as a tree diagram or dendrogram and allows the user to consider nested or overlapping clusters if desired (Gong and Richman, 1995; Tan et al., 2006; Wilks, 2006).

Of hierarchical approaches available, those most commonly used are single linkage, complete linkage, group average, and Ward's method. Single linkage defines the proximity of two clusters by the linear distance between the two closest entities located in different clusters. In contrast, complete linkage defines the proximity as the distance between the farthest two points in different clusters. Group average considers all entities within each cluster by using the average pairwise proximity of all entity pairs between two clusters. Ward's method represents each cluster by a centroid, but also minimizes the sum of squared distances of each entity from its respective cluster centroid (Gong and Richman, 1995; Tan et al., 2006; Wilks, 2006).

2.3.3. Non-Hierarchical Clustering Techniques

The most widely-used non-hierarchical cluster approach is K-means (Gong and Richman, 1995; Tan et al., 2006; Wilks, 2006). Generally, K-means partitions entities into a user-specified number of clusters (*k*). K-means considers data centroids (K-medoid can also be used if a user strongly prefers using median instead of mean). To begin the K-means approach, the user must first determine the desired number of clusters (*k*) and the centroid locations. These locations (often referred to as "seed values") can be randomly chosen, although random initialization may yield different cluster results each time the analysis is performed. Poor initial centroid placement can also result in clusters that may not be particularly representative of the data, so users must consider initial centroid placement carefully when using K-means. Once the initial centroids are chosen, the user creates k clusters by assigning each entity to the closest centroid. Once all entities have been assigned, the centroids are computed again based on the entities within each cluster. In the next step, entities are assigned to the updated centroids and then the centroids are updated yet again. The process continues until either the centroids no longer change or the user terminates the clustering after a predetermined number of iterations (Gong and Richman, 1995; Tan et al., 2006; Wilks, 2006).

An extension to the K-means approach is bisecting K-means. In some ways the bisecting approach resembles a reversal of hierarchical clustering. Initially, all entities are clustered together. During the second step, the cluster is bisected to create two clusters. The third step involves one cluster being selected and bisected to create a total of three clusters. The process continues until k-1 bisections have occurred and k clusters have been created. Of course, this process creates the problem of determining which cluster to bisect at each step. Two approaches include either always selecting the largest cluster or selecting the cluster with the largest sum of squared errors. Once a cluster has been selected for bisection, the centroid is removed and two new centroid values must be determined (Tan et al., 2006).

2.3.4. Number of Clusters

While non-hierarchical clustering techniques suffer from the problems of approximating centroid location, neither non-hierarchical nor hierarchical approaches have a straightforward way of determining the correct number of clusters within a given dataset. Numerous statistical measures have been developed and some literature has been devoted exclusively to the subject (e.g., Milligan and Cooper, 1985). Most approaches involve calculating a particular statistic and then plotting those values on the vertical axis and the number of clusters on the horizontal axis. Ideally, a curve with a distinct peak or bend will result, or the curve may reach asymptotic behavior. The point at which the peak, bend, or asymptote occurs usually corresponds to the optimum number of clusters. Unfortunately, a distinct signal in the curve is not always present, which still leaves a subjective judgment call up to the researcher. To complicate the issue further, with so many different statistical measures available and none of them perfect, determining the best measure is difficult, particularly when different measures may provide a variety of results.

Milligan and Cooper (1985) examined 30 different statistics using artificial datasets with known numbers of distinct and non-overlapping clusters. Some statistics measured the cohesiveness of entities within each cluster, while others measured how different clusters were from each other, and some measured a combination of both. Results from Milligan and Cooper's (1985) study showed that all 30 statistics were not always perfect, with the number of clusters often under- or over-estimated. Such results are not encouraging given that the number of clusters is usually not known in advance, and, in a real world situation, clusters tend to be overlapping. With no known superior measure available, the best option is to consider multiple measures and compare results. If a map or plot of the data can be examined visually, that step may be helpful as well, although it can become cumbersome with large or multiple datasets.

2.3.5. Distance Measures

Cluster analysis assigns entities into clusters by considering the distance (or similarity) between all entities. Although many distance measures exist (e.g., Euclidean, Mahalanobis, City Block, Supremum, Chebyshev, and Correlative), no universal measure is used, so a researcher must determine which distance measure is best for a given dataset (Mimmack et al., 2001; Tan et al., 2006). The most popular measure used in climatological research has been Euclidean distance. A review by Gong and Richman (1995) revealed that roughly 85 percent of climatological cluster studies used Euclidean distance. Euclidean distance is calculated as the shortest possible distance between two entities. The calculation is repeated between all entities to create a distance vector or matrix, where if the number of entities is m, the resulting distance vector will have $m * (m - 1) / 2$ elements or the distance matrix will be an m x m symmetric matrix with zeros down the diagonal. Although Euclidean distance is easily calculated and frequently used, users should be aware that the measure does include two assumptions when two or more variables are to be clustered. First, Euclidean distance does not consider possible correlations between variables. Therefore, variables are weighted equally even when correlated variables are present. Secondly, Euclidean distance assumes that all variables are based on the same unit scale, which is frequently not the case (e.g., when considering temperature and precipitation). As a result, some variables may be inappropriately weighted more than others during clustering (Mimmack et al., 2001).

Although a thorough review highlights the popularity of Euclidean distance in climatological research (e.g., Gong and Richman, 1995), some studies have reported the benefits of using Mahalanobis distance and/or calculating principle components prior to using Euclidean distance when two or more variables are being clustered (e.g., Fovell and Fovell, 1993; Stephenson, 1997; Mimmack et al., 2001). To avoid the assumptions of the

Euclidean distance measure one may first use principle components analysis and then calculate Euclidean distance based on those component scores. The component scores can also be standardized so that unit scales are consistent. Alternatively, Mahalanobis distance can be used, since it attributes less weight to highly correlated variables and is able to account for variables of differing unit scales. However, in order to calculate Mahalanobis distance, one must first be able to invert the covariance matrix of the dataset. This criterion can be met only if the original data matrix is "full rank." To be full rank, a matrix cannot have more variables than observations and also no variable can be a linear combination of other variables (Mimmack et al., 2001). In events when a matrix is not full rank, it is possible to use either a pseudo-inverse that results in a truncated Mahalanobis distance (see Stephenson, 1997), or the principle components approach described previously can be used. Now that cluster methods have been discussed, past cluster studies that are relevant to this study will now be reviewed.

2.4. Relevant Cluster Studies

Stooksbury and Michaels (1991) clustered 449 stations within the southeastern U.S. based on 36 monthly temperature variables and 36 monthly precipitation variables spanning 1951-1980. Variables were standardized to give all variables equal weight. States included in the study were VA, TN, NC, SC, GA, FL, AL, and MS. The authors' hypothesis was that the conventional climate divisions that are based on county and state borders do not adequately capture homogeneous climate zones and that a cluster analysis may provide better results. Stooksbury and Michaels (1991) used Euclidean distance and a two-step clustering approach beginning with hierarchical clustering to determine the initial number of clusters and corresponding centroids. A partitioning cluster approach was then used to create a 24-cluster result and a 31-cluster result. Over 95 percent of stations were found to cluster with at least one spatially adjoining station. Although climatological differences between the clusters were not discussed in depth by Stooksbury and Michaels (1991), the southern Appalachian region was found to have at least four clusters. The "Western Appalachian & Valleys" cluster included the eastern side of TN and northern GA. The "Eastern Appalachian" cluster included a narrow swath along the extreme western edge of NC. The "Southside Virginia & Western North Carolina" cluster included the more interior portion of western NC. Lastly, the "Interior South Atlantic" cluster spanned portions of NC, SC, and northeastern GA.

Spanning 1949-1987, Gong and Richman (1995) considered summer precipitation for central and eastern North America in an effort to compare an assortment of cluster techniques. In most cases only two clusters existed for the southern Appalachian region. One cluster included TN, western NC, and northern GA, while a second cluster included the rest of NC, SC, and GA.

Fovell and Fovell (1993) used principle components analysis, group average linkage, and the 344 climate divisions created for the conterminous U.S. by the NCDC in order to improve upon Köppen's climate classification. The results of their study included 12 variables for temperature and 12 variables for precipitation. Cluster results included 14 and 25 clusters. Principle components analysis was used to eliminate correlation between variables and the values were standardized so that all variables had the same unit scale. Euclidean distance was then calculated. A climate division in northwest SC was omitted from analysis because it was considered a poor data point.

Fovell and Fovell's (1993) 14-cluster result showed eastern TN and western NC clustered together in the "E. Central" cluster, but the cluster included other areas as far away as MI. Another cluster ("Southeast") included eastern NC, SC, GA, and most the of the remaining southeastern states. Their 25-cluster result again clustered eastern TN and western NC into the E. Central category, which still included states much farther north. Eastern portions of NC, SC, and GA were clustered into a Southeast cluster. Northern GA, AL, and western TN were clustered into a second Southeast category. Clusters along the Gulf of Mexico and Atlantic coast were warmer and wetter than inland clusters. Of the inland clusters, the area including northern GA, AL, and western TN received substantial precipitation, especially in winter and spring. In the end, Fovell and Fovell (1993) classified most the southern Appalachian region as Köppen's Cfa category, with a few of the higher elevation regions categorized as Cfb.

Winkler (1992) studied hourly precipitation across the U.S. during 1967-1983 in order to determine any regional patterns in the diurnal receipt of heavy precipitation. Euclidean distance and average linkage were employed in a hierarchical cluster analysis. The data were segregated by season and then clustered. During winter, eastern TN, and most of NC, SC, and GA were clustered together. Heavy precipitation was found to be most common around sunrise. Spring clustered northeast TN and northwest NC together with a distinct nocturnal maximum and midday minimum. Southeast TN, southwest NC, the northern portions of SC and GA were also clustered together, but had no distinct diurnal pattern. For summer, a large eastern cluster including the southern Appalachian region had a prominent maximum during the mid-afternoon hours. Lastly, during autumn the majority of the southern Appalachian region fell into a cluster that still exhibited a

mid-afternoon maximum, but it was not as distinct as it was during summer. A portion of central and eastern TN also belonged to a cluster with a more midday precipitation maximum.

Although Davis and Rogers (1992) did not focus directly on the southern Appalachian region, they did use cluster analysis to create a spring and summer (April-September) synoptic climatology for VA. In their study, surface data were used from Washington, D.C., and synoptic data at the 850, 700, and 500 hPa levels from the surrounding area were also used. Davis and Rogers (1992) used the two-step clustering approach described earlier by Stooksbury and Michaels (1991) to create nine clusters. Cluster 1 represented a Bermuda High situation and was most common in July and August. A 500 hPa ridge was located inland with a trough located off the Atlantic coast. Cluster 2 had an anticyclone located over VA with an upper-level ridge present to the west. The situation was most common in late spring. Cluster 3 represented the passage of a surface cyclone to the north of VA during late spring months. A common mid-to-late summer occurrence was categorized as Cluster 4, where a deep, warm-core anticyclone was present. Cluster 5 had a surface low and large amplitude, short-wave trough located over New England or eastern Canada and was most common in late spring. Cluster 6 occurred almost entirely in April and was depicted as a recent cold frontal passage over the region. Occurring in spring, Cluster 7 was associated with an extra-tropical cyclone off the east coast and an anticyclone approaching from the west. Cluster 8 occurred in mid-to-late summer with a surface anticyclone to the northeast of VA resulting in onshore flow at low levels. Lastly, Cluster 9 occurred mostly in June and July, but was still common in other months. Westerly flow aloft was the most common quality associated with Cluster 9.

A consensus clustering technique was presented by Fovell (1997), where the author created a 4-cluster result for temperature and a 6-cluster result for precipitation and then overlaid the two maps, ultimately creating 14 clusters. A higher-order approach using seven temperature clusters and 15 precipitation clusters resulted in 26 consensus clusters. The author used data from the NCDC's 344 climate divisions spanning 1931-1981. Euclidean distance was used, but the author attempted to break the distance value into several terms including a component for mean, seasonality, and coseasonality. With the data standardized, the first two terms disappeared, leaving the coseasonality (or correlation) term. Group average linkage was the clustering approach used. For the 14-cluster result, eastern TN and western NC were clustered together. The remaining portion of NC, SC, and GA were also clustered together as a more wetter and warmer region. The 26-cluster result again had eastern TN and western NC as a cluster. Central NC was its own cluster. Eastern NC and all of SC and GA were also clustered. The differences between the clusters were not thoroughly discussed. In fact, Fovell (1997) concluded that perhaps the southeast region had been over-clustered and that merging of some the existing clusters could be justified.

When studying heavy precipitation for the southeastern U.S., Konrad (1997) used cluster analysis. He first clustered a variety of temperature, moisture, and lifting indices into three primary variables represented by vectors. The "A" vector represented the 500 hPa wind vector, while the "B" vector represented the area of greatest boundary-layer convergence or low-pressure center. Lastly, the "C" vector represented the nearest ridge of boundary-layer convergence or front. The cluster analysis used was the same two-step cluster approach described previously by Stooksbury and Michaels (1991). The five resulting cluster patterns were discussed previously in Section 2.2 of this chapter.

Walters and Winkler (2001) presented a climatology of 260 southerly low-level jet cases for central North America during the 1991-1992 warm seasons. The study did not directly focus on the southern Appalachian region, but the classification technique is still relevant because the authors subjectively clustered southerly low-level jets based on visual inspection of streamline curvature, latitudinal extent, and orientation of confluence and deformation zones. Twelve distinct southerly low-level jet patterns were defined. A subsequent study by Walters et al. (in preparation) followed the same approach to categorize 546 northerly low-level jet cases during 1991 into 16 different patterns.

Lastly, Walters et al. (2008) used principle components analysis and cluster analysis to investigate low-level jets and create regions with similar characteristics. Cluster techniques included using standardized principle component analysis scores. Three different hierarchical approaches were used (Ward's minimum variance, average linkage, and complete linkage). Variables included from each station in the clustering were low-level jet frequency, average jet speed, and average jet height, with each based on an eight-point compass. Results from the various cluster approaches were compared to visually outline clustered stations and create low-level jet regions. Regions were created for the annual scale, but also for each season. The southern Appalachian region was just off the eastern edge of the study area (Nashville, TN, was the easternmost station in the study).

Of these cluster analysis studies, each clustered relatively large areas. The southern Appalachian region was often limited to a small number of stations or climate division data points. Past studies covered temperature and/or precipitation, but snowfall was never included. Clusters were often created over a time period, but no consideration of possible temporal variability of the clusters was discussed. Most relevant studies for the region discussed above relied primarily on objective clustering techniques. Historically, however, subjective clustering techniques have been common in climatological research (e.g., Köppen, 1923; Thornthwaite, 1931), and some recent studies continue to use subjective approaches for defining climate regions or clustering synoptic patterns (e.g., Walters and Winkler, 2001; Walters et al., 2008; Walters et al., in preparation). A side-by-side comparison of objectively and subjectively-derived results was not attempted or discussed by the studies cited.

2.5. Research Questions and Objectives

In view of this survey of relevant literature cited here in Chapter 2, I wish to address four research questions in this study that previous studies have not fully answered. I will refer back to these research questions throughout subsequent chapters.

1) What is the temperature and precipitation climatology of the southern Appalachians?

2) How many climate regimes exist in this region?

3) What are the synoptic origins of precipitation here?

4) To what extent does the answer to Question 3 depend on whether an objective, subjective, or hybrid clustering approach is used

The purpose for Question 1 is to build upon studies referred to in Section 2.1. Question 2 also harks back to Section 2.1, but should also help bolster the previous results shared in Section 2.4 regarding the region's climate regimes. Studies in Section 2.2 have not fully described the region's synoptic climatology, hence the need for Question 3. Lastly, Question 4 was born out of results discussed in Section 2.4 in that those studies did not consider comparisons of various clustering approaches.

In order to answer the research questions, I will address a number of smaller objectives along the way. Objectives for the temporal and spatial analysis include: 1) selecting the region boundaries and time period of interest, 2) selecting and collecting the climate data, 3) making decisions about the temporal and spatial resolution of the data, 4) assessing the quality of the data and making adjustments in the dataset as needed, 5) analyzing the data for temporal and spatial trends, and 6) summarizing results.

Objectives for the synoptic climatology include: 1) selecting and collecting the appropriate data, 2) making decisions about the temporal and spatial resolution of the data, 3) assessing the quality of the data and making analytical adjustments, as needed, 4) determining criteria for a precipitation event, 5) plotting resulting synoptic pattern for each precipitation event, 6) summarizing the events into clusters based on objective, subjective, and hybrid approaches, 7) comparing and contrasting the results from the various approaches, and 8) analyzing the frequency of synoptic patterns during past years to monitor temporal variability.

As I will present in Chapters 4-6, my study considers additional stations and a longer time period, allowing for a more comprehensive look at temporal and spatial relationships that the historic studies may not have been able to obtain. My cluster study also focuses solely on climate data from stations located within the southern Appalachian region and the immediate surrounding area, allowing for a cluster representation of the area with a higher spatial resolution. The synoptic climatology created by objective, subjective, and hybrid approaches yields additional synoptic patterns not previously covered. However, before the specifics of the results are presented, I will first describe the study area, datasets, and methods used in Chapter 3.

CHAPTER 3

STUDY AREA, DATA, AND METHODS

3.1. Study Area

The southern Appalachians are often defined as the mountainous region in the eastern United States that remained unglaciated during the last glacial advance. Most studies focus on the southern states of TN, NC, SC, and GA, although other states (e.g., AL, MS, KY, VA, WV, MD, OH, PA, and NY) are sometimes considered part of the region, as well. For this study, a bounding rectangle of 34.50°N to 36.55°N and 81.50°W to 84.75°W including portions of TN, NC, SC, and GA was used to denote the study area of interest (Figure 1.1). The bounding coordinates yield a rectangular area and although the southern Appalachian mountain chain itself is not rectangular (the chain is oriented in a southwest to northeast direction), a rectangular area is advantageous when gridded data are used for map creation.

The study area has diverse topography including the Piedmont, Blue Ridge, and the Ridge and Valley provinces associated with the southern Appalachians (Figure 3.1). The Piedmont generally corresponds to the low-lying area below 500 m in the southeastern portion of the study area. The Blue Ridge includes areas above 500 m running from southwest to northeast. The Ridge and Valley province includes the low-lying areas on the northwest side of the Blue Ridge. A small portion of the Appalachian Plateau is present in the very northwestern portion of the map where elevations above 500 m are present (Figure 3.1). The complex topography of the region often leads to orographic lifting and enhanced rainfall totals in the area. In fact, some parts of the southern Appalachian region receive more precipitation than any other in the eastern U.S. Large portions of the study area are federally-owned. As illustrated in Chapter 1, these lands include GSMNP, and the Cherokee, Nantahala, Pisgah, Chattahoochee, Sumter, and Daniel Boone National Forests (Figure 1.2).

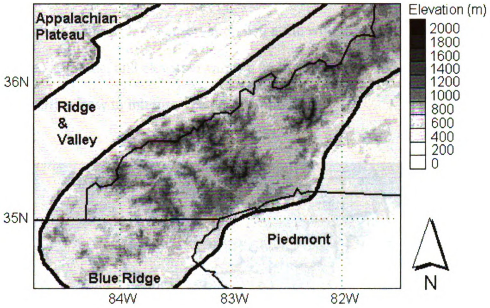

Figure 3.1. Study area bounded by 34.50°N to 36.55°N and 81.50°W to 84.75°W. Geographic provinces are labeled with approximate boundaries included. Elevation is shaded in gray based on meters above sea level.

3.2. Data for the Baseline Climatology

Climate data are generated by the Cooperative Observer Program (COOP) and are archived by the NCDC. Monthly variables initially considered here included: minimum temperature, maximum temperature, mean temperature, mean soil temperature, total precipitation, total snowfall, and total evaporation. Beginning in 1890, the COOP network is the largest and oldest weather observation network within the United States.

Volunteers use instruments provided by the National Weather Service (NWS) to record the information, which is then conveyed to the NCDC, where the data undergo quality control prior to being made available to the public (Winkler, 2004). More than 18,000 U.S. COOP stations with monthly data exist, 463 of which reside within the region selected for this study (Figure 3.2). Station data for the COOP network are available for free online at: http://cdo.ncdc.noaa.gov/CDO/cdo for users with an academic affiliation. Downloads include a file with the observation list, a file with the station list (includes station latitude, longitude, and elevation values), an inventory file, and an information file, which describes how to interpret the observation file.

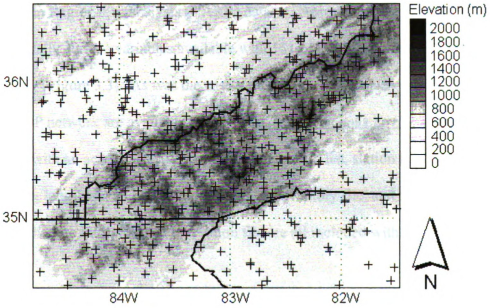

Figure 3.2. Study area with elevation shaded in gray. Plus signs represent locations of the 463 monthly COOP stations.

Elevation data used were from the National Elevation Dataset (NED) and were obtained at no cost from the United States Geological Survey (USGS) using the Seamless Data Distribution System (SDDS; available online at: http://seamless.usgs.gov). The

SDDS provides a seamless, high-resolution elevation dataset for the U.S. The dataset itself is a 1:24,000 scale Digital Elevation Model (DEM) for the 48 conterminous states. The projection is Geographic, with a resolution of one arc second. The horizontal datum is NAD83 and the vertical datum is NAVD88. Elevation units are in meters above sea level.

3.3. Data for the Synoptic Climatology

Daily precipitation totals are also available from the COOP dataset provided by the NCDC. Although precipitation data were available for earlier years, I chose the study period for the synoptic climatology as 1979-2006 to coincide with data availability of the North American Regional Reanalysis (NARR) dataset. Approximately 19,000 COOP stations have daily surface variables available with 151 of those included within my region of study (Figure 3.3). As was the case with the monthly dataset, station data for the daily COOP network are available online (http://cdo.ncdc.noaa.gov/CDO/cdo) at no cost for those with an academic affiliation. An observation list, station list (includes station latitude, longitude, and elevation values), an inventory file, and an information file that describes how to interpret the observation file are all included with the download.

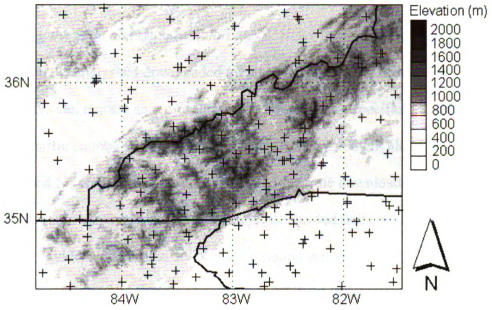

Figure 3.3. Study area with elevation shaded in gray. Plus signs represent locations of the 151 daily COOP stations.

The NARR dataset, created by the National Centers for Environmental Prediction (NCEP), is available for 1979 to the present (Mesinger et al., 2006). The NARR was preceded by the global reanalysis dataset that was available four times daily on a 2.5° x 2.5° grid for 17 atmospheric levels (Kalnay et al., 1996). In contrast, NARR data are available eight times daily on the 32 km Eta grid for 45 vertical levels. A map of the NARR grid domain is available at: http://nomads.ncdc.noaa.gov/images/grid-221.gif. NARR values are integrated from rawinsonde, dropsonde, pibals, aircraft, surface, and satellite observations, to arrive at a gridded dataset. Temperature, wind, moisture, and other variables are available for free download at: http://www.emc.ncep.noaa.gov/mmb/rreanl/. Due to the large size of the files, the data are available in a compressed, GRIdded Binary (GRIB) format.

3.4. Procedures for the Baseline Climatology

3.4.1. Acquiring the Data and Quality Control

To begin the analysis, I downloaded monthly COOP surface station data. For downloads, users can request an entire state, specific station(s), specific climate division(s), specific county(s), or a range of stations based on COOP identification numbers. To test for continuity, I initially attempted separate downloads by state, county, and climate division. An inspection of the station list showed that county information was often not provided and climate division information was frequently incorrect. Therefore, unless the COOP identification numbers of the desired stations are known in advance, one should download stations for an entire state. The variables I initially selected for this study were monthly and annual values of minimum temperature (MMNT), maximum temperature (MMXT), mean temperature, (MNTM), mean soil temperature (MOyz), total precipitation (TPCP), total snowfall (TSNW), and total evaporation (TEVP). The year range was selected as 1890-2006 since 1890 was the first year COOP data were available and 2006 was the most recent complete year at the time of download. The download process was repeated for each of the four states in the study region (TN, NC, SC, and GA).

All data were processed using Interface Description Language (IDL; available for purchase at: http://rsinc.com/idl/). The IDL source code for this project became quite lengthy, so it is not provided in this dissertation, but I can provide an electronic copy upon request. The National Elevation Dataset was downloaded as eight separate files. I combined the files using the IDL program elevation.pro. The dataset had a resolution of 10,980 rows and 15,304 columns within the study area. However, using such a large array slowed IDL execution time considerably during subsequent map creation. As will be discussed, I created numerous maps for this project, so the need for speedy processing time had to be balanced against the necessity for maintaining a sufficient elevation data resolution. After experimentation, I determined a compromise of counting every 50th elevation point. In the end, the elevation array used had 220 rows and 307 columns.

I created clean1.pro for the purpose of extracting only the stations within the study region from the TN, NC, SC, and GA files. Also included within clean1.pro was code to: 1) convert station latitude/longitude locations from minutes into decimal degrees, 2) count the total number of stations, which was 463 in this case, 3) create maps of the study area, elevation, and station locations (Figures 3.2), and 4) check the observations for errors. Although observations undergo quality control by the NCDC prior to release, some errors do remain present in the dataset, of which users must be cognizant. In some cases, more than one entry for an observation can be found. Frequently, these multiple entries consist of data entries and missing entries and a user can "combine" the two or more entries to create one complete observation. However, at other times the distinction of entries is not so clear (e.g., the entries report a non-missing value for the same month). To eliminate this problem, in all cases I only considered the first observation entry. Whenever a subsequent entry was found for the same observation, it was deleted. Regarding variables, although only MMNT, MXNT, MNTM, MOyz, TPCP, TSNW, and TEVP were requested, some entries for MO34 (i.e., mean soil temperature taken in bare ground at a depth of 50 cm) and MO54 (i.e., mean soil temperature taken in sod at a depth of 50 cm) were present in the data and were deleted. In the observation files, after each monthly data entry, a flag value is provided (Table 3.1).

Table 3.1. Possible flag values included with monthly COOP observations.

Flag	Description
A	Accumulated amount. Value may include data from previous month(s).
B	Adjusted Total. Monthly value based on proportional available data.
E	Estimated monthly or annual total.
I	Monthly means or totals based on incomplete time series.
M	Missing data element.
S	Amount is accumulating and will be included in a subsequent value.
T	Trace of precipitation or snowfall. Value = 00000.
+	Phenomenon occurred on several days.
	Flag not needed.

For consistency within the dataset, unless the flag was equal to "M," "T," or blank, the data entry was reset to missing ("-99999"). Although observations were available in some cases back to 1890, most stations had a later starting date. In addition, despite having been checked for errors and missing observations, the data were compromised by changes in station location and stations with short periods of record that needed to be addressed. For these reasons, I created cluster1.pro to initially analyze data in 10-year overlapping periods (e.g., 1930-1939, 1935-1944, etc., up through 1995-2004). Some stations had a short period of record in comparison to the entire study period chosen, and using 10-year overlapping periods allowed for many of those stations to be included when they would otherwise have been unusable for further analysis. Stations reporting observations 100 percent of the time were optimum, but not the norm. For this study, stations with observations available 90 percent or more of the time during a 10-year period were considered "good" stations. Stations with fewer than 90 percent of observations available were not used.

My analysis within cluster1.pro revealed that the mean soil temperature (MOyz) variable did not have a single station where data were available 90 percent or more of the time for a single 10-year period. In addition, the total evaporation (TEVP) variable never had more than seven stations with 90 percent of observations available in a given decade. As a result, I omitted those two variables from further analysis. Data characterizing other variables (minimum, maximum, and mean temperature, total precipitation, and total snowfall) were available 90 percent or more of the time at some stations beginning shortly after 1900, although it was not common until after 1930. Spatial analysis results presented here are for years spanning 1930-2004 when 10-year overlapping periods were used. In Chapter 5 I will present results from the decades of 1935-1944, 1965-1974, and 1995-2004 in order to provide spatial depictions for the beginning, middle, and end of the record.

I converted all variables to metric units (ºC for temperature variables and mm for precipitation variables) and then used simple correlation analysis to determine any linear temporal trends and test the resulting trends for statistical significance. Linear trends were calculated for all stations, by month, and by station elevation during 1931-2006. In many cases the series were not linear, so I performed a two-phase regression analysis (see Solow, 1987) in order to highlight years when statistically significant "breaks" in the trends were common.

Annual values are included within the COOP dataset, but values were rarely reported. Therefore, I calculated annual values as the mean of value from all 12 months of the year when all months had a non-missing value. Elevation categories were grouped as low (< 500 m), mid (500-999 m), and high (≥ 1000 m). Of the 463 monthly stations, 231 were in the low category, 167 were in the in mid category, and 65 were in the high category. Figure 3.4 includes station locations by the respective elevation grouping, as created by elev.pro. I will summarize the temporal results in Chapter 4 using mid-season months (January, April, July, and October) to represent seasonal values (other months are included in Appendix A). Spatial results for January and July are presented in Chapter 5 and results for April and October are included in Appendix B. Results will also be summarized by elevation category.

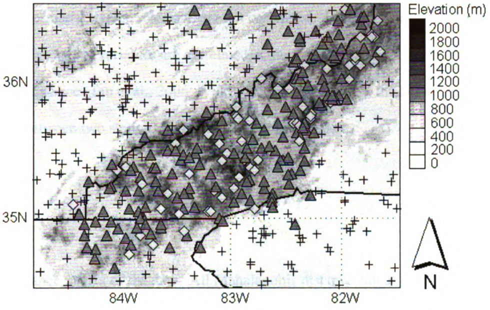

Figure 3.4. Study area with elevation shaded in gray and station locations plotted by elevation category. Black plus signs represent low-elevation stations located below 500 m. Dark gray triangles represent mid-elevation stations located between 500 and 999 m. Light gray diamonds represent high-elevation stations located at 1000 m or above.

3.4.2. Cluster Analysis

Although IDL provides commands for both non-hierarchical (CLUSTER_WTS) and hierarchical (CLUSTER_TREE) approaches, the approach I used here was a bisecting K-means algorithm, which borrows some of its methodology from both hierarchical and non-hierarchical methods. As discussed in Section 2.3.3., bisecting K-means obtains *k* clusters by first assuming all stations are within one cluster and then splits the cluster into two. Next, one cluster is selected for splitting and the process continues until k clusters are reached (Tan et al., 2006).

IDL does not directly provide source code to perform the bisecting K-means approach, but I was still able to perform the task using IDL and other software. To initiate clustering, I needed to provide a pairwise distance measure between the climate values at all stations. Euclidean distance is often used, but it is based on the assumptions that all variables use the same scale and are not correlated. In cases where variables are of varying scales and/or variables are correlated, a more appropriate choice is Mahalanobis distance (Tan et al., 2006; Wilks, 2006). Specifically, the Mahalanobis distance (D) between two stations (vectors) $\mathbf{x}$ and $\mathbf{y}$ is defined as:

$$D^2 = [\mathbf{x} - \mathbf{y}]^T [S]^{-1} [\mathbf{x} - \mathbf{y}]$$

S is the covariance matrix of the data. All Mahalanobis distance calculations were completed within cluster1.pro. Distance values were converted into similarity values using:

$$sim = \exp(-D^2)$$

Next, I performed bisecting K-means clustering using CLUstering TOolkit software (CLUTO; available online for free at: http://glaros.dtc.umn.edu/gkhome/cluto/cluto/download). The download includes a manual that gives a thorough description of how to use the various options and parameters within CLUTO (Karypis, 2003). In this case, similarity matrices based on

Mahalanobis distances were provided, so the CLUTO "scluster" command was appropriate with the general syntax:

scluster [optional parameters] GraphFile NClusters

GraphFile was the name of the file storing the similarity matrix and NClusters was the desired number of clusters. An example of a specific line command (to be typed as one line) I used is included as follows:

```
./scluster -clmethod=rbr -clustfile=cluster9/Jan_19301939.xls.clustering.10 Jan_19301939.xls 10
```

In this example, an optional call to "-clmethod" was used to signal that repeating bisections were to be used and a call to "-clustfile" was used to create a specific output file name. I performed the clustering for January during 1930-1939 and stations were bisected nine times to create 10 clusters. I created script files with edits made to the above command so that I could automate execution for all months and annual values, for all 10-year overlapping periods, for all climate variables individually and combined, and for 1-10 clusters.

As discussed in Chapter 2, one challenge of cluster analysis is determining the number of clusters that best represents the data. Some quantitative approaches are available and CLUTO provides seven different statistical measurements. These values either measure the cohesiveness within clusters, the difference between clusters, or some combination of both. The results from each measurement were compared. Plotting these values against the number of clusters results in a curve. Preferably the curve will reach asymptotic behavior and level off. The point at which the curve levels off highlights where additional clusters is not beneficial. I created such plots using cluster3.pro. The resulting plots from the statistics were not always consistent. At times, the resulting plots continued increasing beyond 10 clusters and did not level off. Other instances had a leveling off after the inclusion of only a few clusters. However, in most cases leveling off occurred at approximately five clusters. These results were further supported by the cluster maps themselves (created using cluster2.pro), because mapping five clusters often still revealed distinct patterns amongst the stations, with the addition of more clusters making the cluster maps more difficult to interpret. For these reasons, and to make the comparison of the maps easier, only the 5-cluster results will be shown in Chapter 5.

3.5. Procedures for the Synoptic Climatology

3.5.1. Acquiring the Data and Quality Control

In order to determine which specific meteorological (synoptic) scenarios account for precipitation in the region, I used COOP precipitation observations at the daily time scale. Similar to the monthly data, daily data were downloaded for the entire states of TN, NC, SC, and GA. In this case, the daily record of precipitation (PRCP) was the only desired variable. The year range was selected as 1979-2006 because the NARR dataset begins in 1979, and although data were available for 2007 at the time of download, much of the data values were still preliminary and had not all been fully checked via the NCDC's quality control process.

Again, data were processed using IDL. I created the program clean2.pro for the purpose of extracting the daily stations within the study area. The program completed the following tasks: 1) converted station latitude/longitude locations from minutes into decimal degrees, 2) counted the number of stations, which was 151 in this case, and 3) created a map of the study area, elevation, and stations locations (Figure 3.3). Next, I created precip.pro to check the observations for errors and determine the number and dates of precipitation events. The dataset was checked for any remaining preliminary observations, multiple observations for the same day, observations reporting the wrong variable (anything other than PRCP), observations reported in the wrong units, and observations reporting dates in an incorrect order. One preliminary observation was found and removed from further consideration. No instances of the other errors were found. One peculiarity discovered: some stations reported the time of observation as hour 24 when reported time is supposed to range between 0 and 23. Two flag values were provided with each observation (Tables 3.2-3.3).

Table 3.2. Possible flag 1 values included with daily COOP observations.

Flag	Description
A	Accumulated amount since last measurement.
B	Accumulated amount includes estimated values (since last measurement).
E	Estimated amount.
J	Value has been manually validated.
M	Missing data value (data value = -99999 for missing).
S	Included in a subsequent value. (data value = “00000” or “-99999”).
T	Trace (data value = 00000 for a trace).
(	Expert system edited value, not validated.
)	Expert system approved edited value.
	Flag not needed.

Table 3.3. Possible flag 2 values included with daily COOP observations.

Flag	Description
0	Valid data element.
1	Valid data element (from "unknown" source, pre-1982).
2	Invalid data element (subsequent value replaces original value).
3	Invalid data element (no replacement value follows).
4	Validity unknown (not checked).
5	Non-numeric data value has been replaced by a deciphered numeric value.
A	Substituted TOBS for TMAX or TMIN.
B	Time shifted value.
C	Precipitation estimated from snowfall.
D	Transposed digits.
E	Changed units.
F	Adjusted TMAX or TMIN by a multiple of + or -10 degrees.
G	Changed algebraic sign.
H	Moved decimal point.
I	Rescaling other than F, G, or H.
J	Subjectively derived value.
K	Extracted from an accumulated value.
L	Switched TMAX and/or TMIN.
M	Switched TOBS with TMAX or TMIN.
N	Substitution of "3 nearest station mean."
O	Switched snow and precipitation data value.
P	Added snowfall to snow depth.
Q	Switched snowfall and snow depth.
R	Precipitation not reported; estimated as "O."
S**	Manually edited value.
T	Failed internal consistency check.
U	Failed areal consistency check (beginning Oct. 1992).
**	Manually edited value derived by any of the procedures noted by Flags A-R.

Accumulated, estimated, and invalid observations were not desired, so I considered only those observations meeting the following flag criteria: Flag 1 had to be equal to "J," "M," "T," ")," or blank, while Flag 2 had to be equal to "0," "1," or blank. If any other flag values were present, the observation was discarded by resetting the observation to missing ("-99999") and Flag 1 to "M."

I determined precipitation events within precip.pro. Previous studies of the region have focused on "heavy" or "intense" precipitation events and used criteria such as: 3 inches (76.2 mm) or more of precipitation received at one or more stations in a day (Bogucki, 1972), 50 mm of precipitation received at one or more stations in a 6-hour

period (Konrad, 1997), or 3 inches (76.2 mm) of rain received in 6 hours and/or 4 inches (101.6 mm) of rain received in 12 hours (Gaffin and Hotz, 2000). However, my suspicion was that much of the precipitation received in the southern Appalachian region may actually result from smaller and lighter rain events. In fact, by considering the amount of precipitation received and the percentage of available stations reporting precipitation, I was able to determine that at least a trace of precipitation was received at one or more of the stations on 9096 out of the possible 10,227 days (88.9 percent) during the 1979-2006 study period (Table 3.4). Less stringent criteria were considered in order to be more inclusive of smaller events, but due to computation restraints, I ultimately chose my specification as 25 percent or more of the available stations reporting 0.5 inches (12.7 mm) or more of precipitation in a day. Given these criteria, over the 1979-2006 time period 1437 precipitation events were found (Table 3.4). A more in-depth discussion of the computation and virtual memory issues encountered will be covered in Section 3.5.2.

Table 3.4. Possible number of precipitation events. Event criteria include the percentage of available stations reporting (values along the topmost row) and amount of precipitation received in a day (values along the leftmost column). The criteria of 0.5 in (12.70 mm) or more of precipitation received by 25 percent or more of the available stations was selected for this study resulting in 1437 precipitation events (shown in bold).

	>0%	≥5%	≥10%	≥15%	≥20%	≥25%	≥30%	≥35%	≥40%	≥45%	≥50%
>0.0 in (0.00 mm)	9096	7238	6464	5905	5390	4921	4546	4151	3824	3496	3231
≥0.1 in (2.54 mm)	8126	5981	5135	4500	3967	3534	3176	2859	2591	2329	2097
≥0.2 in (5.08 mm)	7594	5219	4311	3649	3164	2771	2455	2135	1900	1663	1463
≥0.3 in (7.62 mm)	7164	4621	3698	3084	2602	2209	1881	1636	1436	1244	1093
≥0.4 in (10.16 mm)	6793	4117	3185	2562	2121	1762	1494	1278	1108	971	827
≥0.5 in (12.70 mm)	6426	3703	2743	2140	1719	**1437**	1190	1023	867	752	636
≥0.6 in (15.24 mm)	6080	3272	2311	1764	1426	1158	982	824	702	577	482
≥0.7 in (17.78 mm)	5776	2877	1978	1483	1176	951	787	658	542	439	371
≥0.8 in (20.32 mm)	5483	2534	1684	1245	971	795	635	521	421	354	287
≥0.9 in (22.86 mm)	5194	2202	1429	1040	808	643	517	432	336	284	218
≥1.0 in (25.40 mm)	4931	1922	1212	866	672	529	422	339	282	219	174

In contrast to the once-daily COOP data, NARR data are available eight times daily at 0000, 0300, 0600, 0900, 1200, 1500, 1800, and 2100 UTC. Because the daily COOP observation time varied amongst stations, only the last NARR observation of the day (2100 UTC) was considered in this study. NARR files are split by time period, so 365 files (or 366 for leap years) needed to be downloaded for each year. Despite being compressed into GRIB format, the files were still quite large and contained values for many variables at many vertical levels and at a horizontal resolution of 32 km. For this study, I wished to download the following variables: height, temperature, specific humidity, vertical velocity, and the u and v wind components at 850 hPa and 700 hPa and height, and the u and v wind components at 300 hPa. Fortunately, software exists for automating the download and variable extraction process. Instructions on how to complete these tasks are available at: http://www.cpc.ncep.noaa.gov/products/wesley/fast_downloading_grib.html. The instructions guide the user through the process of downloading the required software (perl, grep, cURL, get_inv.pl, and get_grib.pl). A sample script is also provided to assist in the automation process. A portion of the revised script that I created is included in Appendix C. Once all files were downloaded in GRIB format, an approach for uncompressing the data was needed. Various options for uncompressing GRIB files are available, but a fairly straightforward approach is available at: http://www.cpc.ncep.noaa.gov/products/wesley/wgrib.html. Software called "WGRIB" is available in the C programming language. I downloaded and compiled the WGRIB source code manually, but some compiled versions are available for direct download. Appendix C provides information regarding WGRIB and uncompressing GRIB files.

3.5.2. Clustering Synoptic Patterns

Objective and subjective approaches can be used for clustering synoptic patterns. I considered three different schemes for this study: 1) an objective approach, in which I created all clusters objectively using IDL and CLUTO, 2) a subjective approach, in which I visually examined and clustered all 1437 cases, and 3) a hybrid approach, wherein I initially created 50 objective clusters and then subjectively combined the clusters further.

For the objective approach I utilized CLUTO software to objectively cluster the synoptic patterns. CLUTO requires an input matrix of similarity values based on pairwise distances. The distance measure I used was Mahalanobis distance and I created the IDL program cluster4.pro for the calculations. To begin, a matrix with dimensions *Events* x *Variables* was required, where *Events* = 1437 (the number of precipitation events) and *Variables* = 1,450,095 (15 variables at all 96,673 grid points). In addition, some matrices required a dimension, *M*, where *M* = (*Events* * (*Events* – 1)) / 2. In this case, if *Events* = 1437, then *M* = 1,031,766. Unfortunately, these large numbers created execution problems due to memory allocation for each matrix. In order to remain within the computation and virtual memory limits of the IDL software and computer, it was necessary for me to decrease the overall size of the input dataset. I experimented with matrix dimensions until values were reached that the software and computer could handle successfully. In the end, I chose seven of the original 15 variables (850 hPa height, temperature, and dewpoint, 700 hPa height, temperature, and dewpoint, and 300 hPa height). In addition, rather than use the entire 349 x 277 horizontal grid provided within the NARR dataset, I selected a much smaller 8 x 9 subset (Figure 3.5).

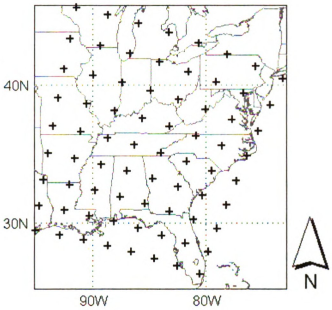

Figure 3.5. Subset of NARR grid points selected for objective cluster analysis.

I created the program extract.pro to extract the subset of grid points and variables. Also included in the program were conversions for Kelvin to Celsius temperature and specific humidity to dewpoint. Once the Mahalanobis distances and similarity values were created successfully, the values were used within CLUTO. Up to 100 clusters were created using the repeated bisections method discussed earlier. In addition, clusters were created using each of the seven statistical measures provided by CLUTO (Karypis, 2003; Zhao and Karypis, 2003) in an effort to determine the optimum number of clusters. Unfortunately, the results from the statistical measures were inconclusive because the plots (created by cluster5.pro) did not display a distinct pattern even when up to 100 objective clusters were used, so in the end I chose to run the objective analysis using the same number of clusters that was found during the subjective analysis.

For the subjective approach, I created maps for all 1437 events using events.pro. The synoptic patterns for each precipitation event were printed and then subjectively categorized by me to create clusters. Separate maps were created for each variable at the 850, 700, and 300 hPa level. I considered all levels and variables as I subjectively clustered, but the synoptic patterns were most distinct at the 850 hPa level. In order to quickly count the number of cases within all subjective and objective clusters, as well as determine seasonal distributions for all clusters, I created the programs cluster6.pro and cluster7.pro. Only the 850 hPa maps for the subjective and objective approaches will be shown in Chapter 6, but the 700 and 300 hPa maps are included in Appendix D.

In the hybrid approach, I used CLUTO and events.pro to initially cluster the synoptic patterns from the 1437 precipitation events into 50 objective clusters and create maps for each. Much like the subjective approach, I then visually clustered those 50 further, in order to end with a smaller number of clusters. The results from this hybrid approach were then compared to the subjective and objective results. All maps for the hybrid approach are included in Appendix E.

For each cluster, the associated synoptic data from all cases were averaged to create a composite map (using objective.pro, subjective.pro, and hybrid.pro). Comparison of the resulting synoptic patterns was done mostly in a qualitative way by describing the differences between the synoptic patterns. However, some quantitative comparisons are provided by referencing contour values on the maps, for example. Additionally, I calculated frequency values in cluster7.pro in order to show which synoptic patterns were more common than others and to highlight temporal changes that occurred over the 1979-2006 period. Frequency values were calculated for three overlapping periods of 1979-1992, 1986-1999, and 1993-2006. In addition, trends of the annual frequency values were tested for statistical significance. Results of the dissertation will now be presented in Chapters 4-6.

CHAPTER 4

RESULTS AND DISCUSSION OF THE TEMPORAL ANALYSIS

4.1. Overview

First-order changes for all variables during 1931-2006 are reported in Tables 4.1-4.5. In this chapter, I will present and discuss results for January, April, July, October, and Annual. Additional figures for other months are included in Appendix A. Please note that the ranges of y-axis values on the figures are not always the same for all months. I adjusted the y-axis values based on the inter- or intra-annual variability of temperature and precipitation. The results of this chapter build upon those from previous studies and provide new temporal information to more thoroughly answer Question 1 posed in Section 2.5.

Table 4.1. Temporal change in minimum temperature (°C) 1931-2006.

Elev	Jan	Feb	Mar	Apr	May	Jun	Jul	Aug	Sep	Oct	Nov	Dec	Annual
All	-2.67	-0.78	-0.17	-0.53	-0.61	-0.49	0.24	0.18	-0.48	-0.55	0.60	-1.19	-0.54
Low	-2.82	-1.11	-0.56	-1.06	-1.07	-0.98	-0.19	-0.23	-1.00	-1.05	0.16	-1.46	-0.93
Mid	-2.61	-0.56	0.09	-0.21	-0.28	-0.14	0.47	0.35	-0.12	-0.13	0.93	-1.00	-0.19
High	-3.42	-1.04	-0.49	-0.28	-0.62	-0.72	0.08	-0.04	-0.61	-0.53	0.71	-1.56	-0.70

Table 4.2. Temporal change in maximum temperature (°C) 1931-2006.

Elev	Jan	Feb	Mar	Apr	May	Jun	Jul	Aug	Sep	Oct	Nov	Dec	Annual
All	-2.22	-0.62	0.33	-0.00	-1.53	-2.18	-0.51	-0.46	-1.73	-1.80	0.22	-0.74	-0.91
Low	-2.46	-0.88	-0.01	-0.42	-2.02	-2.70	-0.99	-0.88	-2.13	-2.11	-0.08	-0.83	-1.28
Mid	-1.75	-0.24	0.73	0.53	-0.88	-1.57	-0.01	-0.01	-1.22	-1.24	0.72	-0.54	-0.25
High	-4.16	-2.31	-1.53	-1.79	-3.14	-3.64	-1.99	-2.39	-3.71	-4.03	-1.73	-2.63	-3.05

Table 4.3. Temporal change in mean temperature (°C) 1931-2006.

Elev	Jan	Feb	Mar	Apr	May	Jun	Jul	Aug	Sep	Oct	Nov	Dec	Annual
All	-2.45	-0.68	0.08	-0.27	-1.05	-1.33	-0.13	-0.13	-1.10	-1.17	0.40	-0.94	-0.74
Low	-2.64	-0.98	-0.28	-0.73	-1.54	-1.83	-0.58	-0.55	-1.56	-1.58	0.03	-1.12	-1.12
Mid	-2.16	-0.38	0.44	0.17	-0.54	-0.82	0.25	0.19	-0.64	-0.67	0.83	-0.75	-0.21
High	-3.78	-1.66	-1.00	-1.01	-1.79	-2.17	-0.95	-1.11	-2.12	-2.26	-0.48	-2.07	-1.78

Table 4.4. Temporal change in total precipitation (mm) 1931-2006.

Elev	Jan	Feb	Mar	Apr	May	Jun	Jul	Aug	Sep	Oct	Nov	Dec	Annual
All	-4.34	-11.86	-9.77	1.31	22.88	32.62	-27.02	-16.44	47.70	6.77	35.55	-18.24	59.19
Low	-8.57	-12.80	-9.52	1.71	22.82	31.33	-20.14	-12.27	45.06	11.88	29.87	-16.78	60.55
Mid	1.13	-8.50	-10.55	0.80	25.98	37.47	-32.40	-15.38	53.17	-1.00	43.93	-20.43	81.40
High	9.67	-8.35	5.05	16.85	17.07	46.07	-43.36	-33.62	59.25	8.55	54.43	-12.40	125.03

Table 4.5. Temporal change in total snowfall (mm) 1931-2006.

Elev	Jan	Feb	Mar	Apr	May	Jun	Jul	Aug	Sep	Oct	Nov	Dec	Annual
All	19.15	-5.25	-29.77	10.57	0.88	0.00	0.00	0.00	-0.06	-0.14	-8.23	-27.70	-45.28
Low	1.02	-13.00	-25.38	4.07	0.00	0.00	0.00	0.00	-0.11	0.09	-7.54	-30.48	-52.59
Mid	17.08	-19.10	-46.42	9.32	0.42	0.00	0.00	0.00	0.00	-0.27	-9.40	-38.45	-92.59
High	196.87	131.13	10.27	77.60	9.92	0.00	0.00	0.00	0.00	-0.19	-2.64	46.17	561.76

4.2. Temporal Results of Temperature

4.2.1. January

Time series plots for January show a very distinct pattern in minimum, maximum, and mean temperature (Figure 4.1). A distinct warming trend was present at all elevations beginning in the late 1970s and continued through the end of the series. In fact, results from a two-phase regression analysis highlight that statistically significant breaks ($p \leq 0.10$) in the time series occurred most often in the mid-to-late 1970s for cool season months and support the documented 1976/1977 climate shift found by others (Trenberth, 1990; IPCC, 2007a). In many cases, January temperatures warmed by as much as 4.00°C or more over the last few decades. Nonetheless, linear values show that an overall cooling trend occurred at all elevations over the entire 1931-2006 period. High elevations experienced the greatest amount of cooling with a drop of 3.42°C for minimum temperature, 4.16°C for maximum temperature, and 3.78°C for mean temperature, all of which were statistically significant at the $p \leq 0.01$ level. Low-elevation stations experienced the second-most cooling with changes of 2.82°C for minimum temperature (significant at the $p \leq 0.05$ level), 2.46°C for maximum temperature (significant at the $p \leq 0.05$ level), and 2.64°C for mean temperature (significant at the $p \leq 0.01$ level). Lastly, mid elevations had temperature drops of 2.61°C for minimum temperature (significant at the $p \leq 0.05$ level), 1.75°C for maximum temperature (significant at the $p \leq 0.10$ level), and 2.16°C for mean temperature (significant at the $p \leq 0.05$ level), respectively.

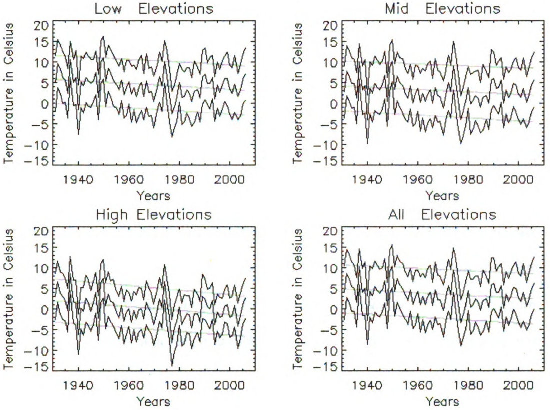

Figure 4.1. January minimum (bottom line), maximum (top line), and mean (center line) temperature in °C. A linear fit was calculated for each variable over 1931-2006. Results are included for low elevations (< 500 m; top left), mid elevations (500 – 999 m; top right), high elevations (≥ 1000 m; bottom left), and all elevations (bottom right).

While the 1931-2006 linear trends suggest that cooling occurred, the trends are also heavily influenced by the period of extended warmth at the beginning of the record. Although warm values were present at the end of the series as well, at the time of analysis, data were available through 2006 only. At the time of this writing (2009), however, preliminary data suggest that the years 2007 and 2008 were also warm and their addition will likely impact any subsequent long-term study. These monthly value results also suggest that substantial decreases in the daily temperature range may be present (e.g., temperature range values for high elevations were statistically significant at the $p \leq 0.05$ level), which could have an effect on the region's plant and animal species that rely on (or are vulnerable to) variation in diurnal temperature range.

4.2.2. April

Compared to January, temporal changes in temperature for April were more modest (Figure 4.2). Over 1931-2006, low-elevation stations had a decrease in minimum temperature (1.06°C; statistically significant at the $p \leq 0.05$ level), maximum temperature (0.42°C; not statistically significant), and mean temperature (0.73°C; not statistically significant). High-elevation stations also experienced some cooling across the board with 0.28°C for minimum temperature (not statistically significant), 1.79°C for maximum temperature (significant at the $p \leq 0.01$ level), and 1.01°C for mean temperature (not statistically significant). Changes at mid elevations were not statistically significant with a decrease in minimum temperature of 0.21°C. Maximum temperature increased by 0.53°C and mean temperature increased by 0.17°C. Such results suggest an overall increase in the diurnal temperature range at low elevations (not statistically significant)) and mid elevations (significant at $p \leq 0.10$ level) and a decrease in temperature range for high-elevation stations (significant at $p \leq 0.01$ level).

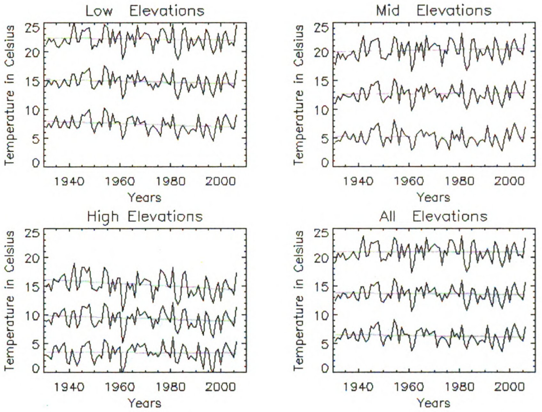

Figure 4.2. April minimum (bottom line), maximum (top line), and mean (center line) temperature in °C. A linear fit was calculated for each variable over 1931-2006. Results are included for low elevations (< 500 m; top left), mid elevations (500 – 999 m; top right), high elevations (≥ 1000 m; bottom left), and all elevations (bottom right).

4.2.3. July

Much like April, most temporal changes in temperature for July were smaller than they were during January (Figure 4.3). Two-phase regression results suggest that statistically significant breaks occurred in the 1960s, which corresponds to a period of cooler temperatures. Warm season temperatures have tended to rise since that time. Long-term deviations were not necessarily consistent across each variable or elevation. Low-elevation stations experienced cooling for all variables with 0.19°C for minimum temperature (not statistically significant), 0.99°C for maximum temperature (significant at the $p \leq 0.05$ level), and 0.58°C for mean temperature (not statistically significant). Mid-elevation stations had warming for minimum temperature (0.47°C) and mean temperature (0.25°C), and slight cooling for maximum temperature (0.01°C), none of which were statistically significant. Stations at high elevations had a small amount of warming for minimum temperature (0.08°C; not statistically significant) and more substantial cooling for maximum temperature (1.99°C; significant at the $p \leq 0.01$ level) and mean temperature (0.95°C; significant at the $p \leq 0.05$ level).

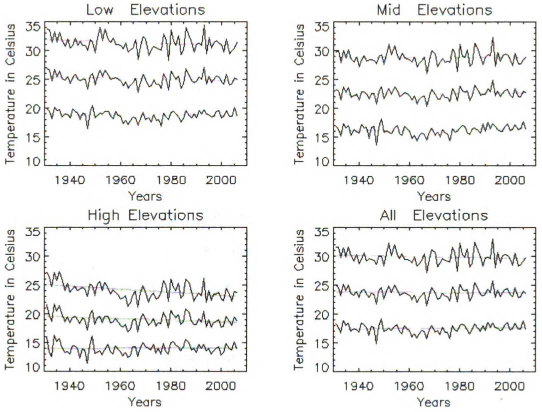

Figure 4.3. July minimum (bottom line), maximum (top line), and mean (center line) temperature in °C. A linear fit was calculated for each variable over 1931-2006. Results are included for low elevations (< 500 m; top left), mid elevations (500 – 999 m; top right), high elevations (≥ 1000 m; bottom left), and all elevations (bottom right).

In general, the overall trends for April (Figure 4.2) and July (Figure 4.3) were similar. Low- and mid-elevation stations exhibited relatively stable temperatures over time, with a very small amount of cooling during 1931-2006. In contrast, stations at high elevations had maximum temperatures during spring and summer decrease steadily over 1931-2006. Mean temperature at those locations also decreased to a lesser extent, while minimum temperatures remained stable. Diurnal temperature ranges during July decreased at low elevations (statistically significant at the $p \leq 0.10$ level), mid elevations (not statistically significant), and high elevations (statistically significant at the $p \leq 0.01$ level).

4.2.4. October

October (Figure 4.4) experienced regional cooling throughout the 1931-2006 period. High-elevation stations had cooling of 0.53°C for minimum temperature (not statistically significant), 4.03°C for maximum temperature (statistically significant at the $p \leq 0.01$ level), and 2.26°C for mean temperature (statistically significant at the $p \leq 0.01$ level). Stations at mid elevations encountered cooling of minimum temperature (0.13°C; not statistically significant), maximum temperature (1.24°C; statistically significant at the $p \leq 0.01$ level), and mean temperature (0.67°C; not statistically significant), as well. Low-elevation stations cooled by 1.05°C for minimum temperatures (not statistically significant), 2.11°C for maximum temperatures (statistically significant at the $p \leq 0.01$ level), and 1.58°C for mean temperatures (statistically significant at the $p \leq 0.01$ level), respectively. With minimum temperatures cooling less than maximum temperatures, diurnal temperature ranges likely decreased over the period at all elevations. In fact, temperature range values over time were statistically significant for low and mid elevations at the $p \leq 0.10$ level and at the $p \leq 0.01$ level for high elevations.

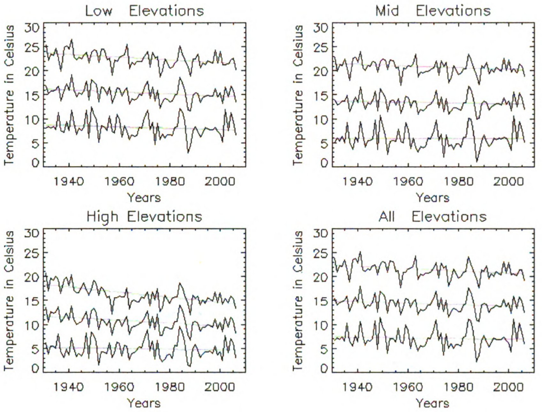

Figure 4.4. October minimum (bottom line), maximum (top line), and mean (center line) temperature in °C. A linear fit was calculated for each variable over 1931-2006. Results are included for low elevations (< 500 m; top left), mid elevations (500 – 999 m; top right), high elevations (≥ 1000 m; bottom left), and all elevations (bottom right).

4.2.5. Annual

Averages over the entire year showed a general cooling trend over the 1931-2006 period at all elevations (Figure 4.5). Minimum temperatures at low elevations dropped by 0.93°C (statistically significant at the $p \leq 0.01$ level), mid elevations dropped by 0.19°C (not statistically significant), and high elevations dropped by 0.70°C (statistically significant at the $p \leq 0.05$ level). Maximum temperatures cooled 1.28°C at low elevations (statistically significant at the $p \leq 0.01$ level), 0.25°C at mid elevations (not statistically significant), and 3.05°C at high elevations (statistically significant at the $p \leq 0.01$ level) while mean temperatures decreased by 1.12°C at low elevations (statistically significant at the $p \leq 0.01$ level), 0.21°C at mid elevations (not statistically significant), and 1.78°C at high elevations (statistically significant at the $p \leq 0.01$ level). These results show that the diurnal temperature range decreased at all elevations with low-elevation values statistically significant at the $p \leq 0.10$ level and high-elevation values significant at the $p \leq 0.01$ level.

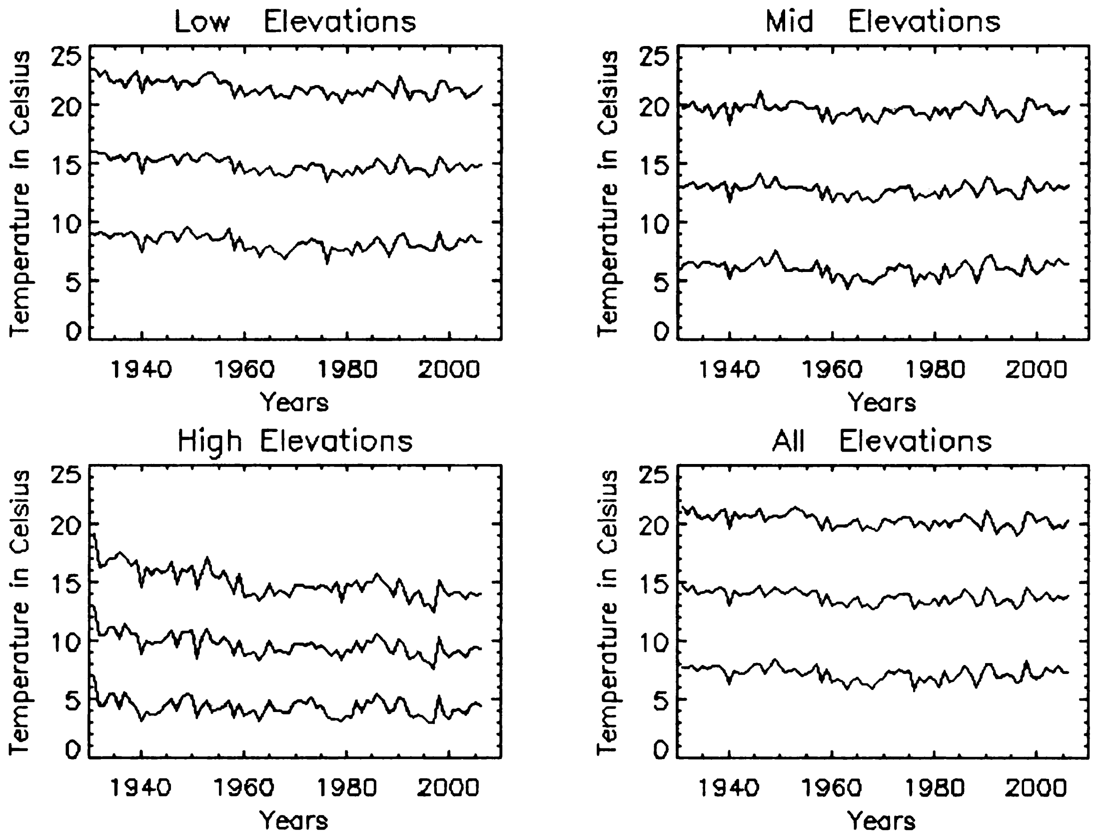

Figure 4.5. Annual values of minimum (bottom line), maximum (top line), and mean (center line) temperature in °C. A linear fit was calculated for each variable over 1931-2006. Results are included for low elevations (< 500 m; top left), mid elevations (500 – 999 m; top right), high elevations (≥ 1000 m; bottom left), and all elevations (bottom right).

In terms of seasonal trends presented in Figures 4.1-4.4 , the results here generally suggest that autumn and winter months warmed in recent decades, while spring and summer months cooled. These results imply that the overall annual cycle of temperature also may have decreased with time. At all elevations over the 1931-2006 period, the annual maximum for all temperature variables was reached in July and the minimum was reached in January (Figure 4.6). This figure also highlights the trend of generally decreasing temperature values with increasing elevation.

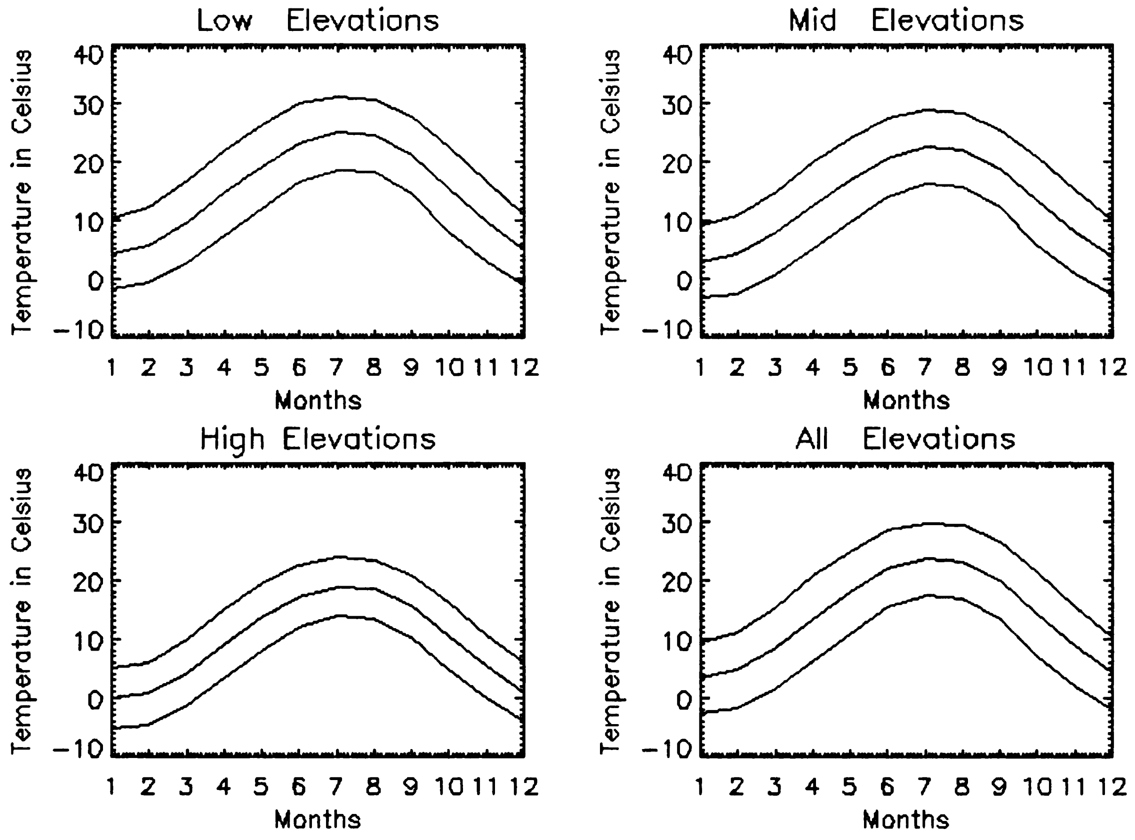

Figure 4.6. Intra-annual trends of minimum (bottom line), maximum (top line), and mean (center line) temperature in °C versus months of the year. Values were averaged over the entire 1931-2006 period. Results are included for low elevations (< 500 m; top left), mid elevations (500 – 999 m; top right), high elevations (≥ 1000 m; bottom left), and all elevations (bottom right).

4.3. Temporal Results of Precipitation and Snowfall

4.3.1. January

First-order changes in total precipitation and total snowfall from 1931-2006 are reported in Tables 4.4 and 4.5. Two-phase regression results did not highlight any common breaks in the time series for precipitation or snowfall. January precipitation for low-elevation stations decreased by 8.57 mm (Figure 4.7), while snowfall increased by 1.02 mm (Figure 4.8), neither of which was statistically significant. Precipitation and snowfall increased for mid and high stations with precipitation going up by 1.13 mm at mid elevations (not statistically significant) and 9.67 mm at high elevations (not statistically significant). Snowfall increased by 17.08 mm at mid elevations (not statistically significant) and 196.87 mm at high elevations (statistically significant at the $p \leq 0.01$ level).

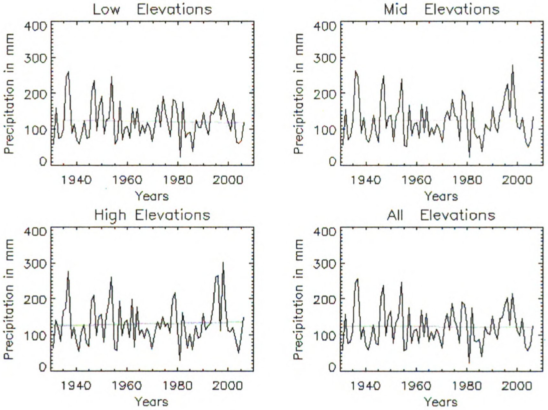

Figure 4.7. January precipitation in mm. A linear fit was calculated for 1931-2006. Results are included for low elevations (< 500 m; top left), mid elevations (500 – 999 m; top right), high elevations (≥ 1000 m; bottom left), and all elevations (bottom right).

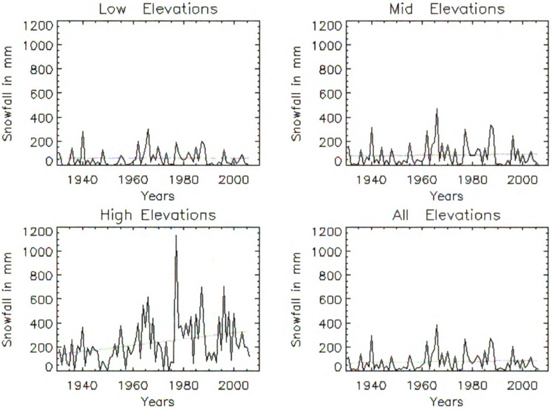

Figure 4.8. January snowfall in mm. A linear fit was calculated for 1931-2006. Results are included for low elevations (< 500 m; top left), mid elevations (500 – 999 m; top right), high elevations (≥ 1000 m; bottom left), and all elevations (bottom right).

4.3.2. April

April precipitation and snowfall increased at all elevations over the 1931-2006 period (Figures 4.9-4.10). Statistically insignificant increases of 1.71 mm (low elevations), 0.80 mm (mid elevations), and 16.85 mm (high elevations) occurred for precipitation, while 4.07 mm (low elevations), 9.32 mm (mid elevations), and 77.60 mm (high elevations) occurred for snowfall. The high-elevation snowfall increase was statistically significant at the $p \leq 0.10$ level.

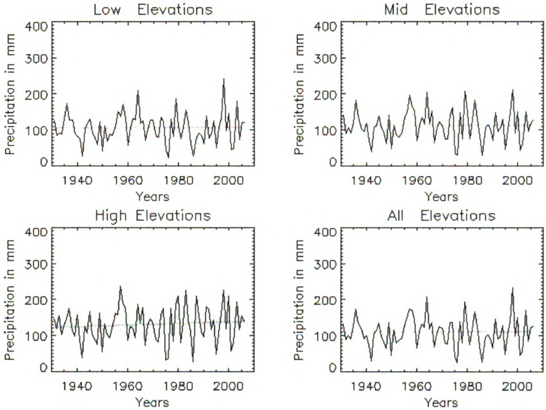

Figure 4.9. April precipitation in mm. A linear fit was calculated for 1931-2006. Results are included for low elevations (< 500 m; top left), mid elevations (500 – 999 m; top right), high elevations (≥ 1000 m; bottom left), and all elevations (bottom right).

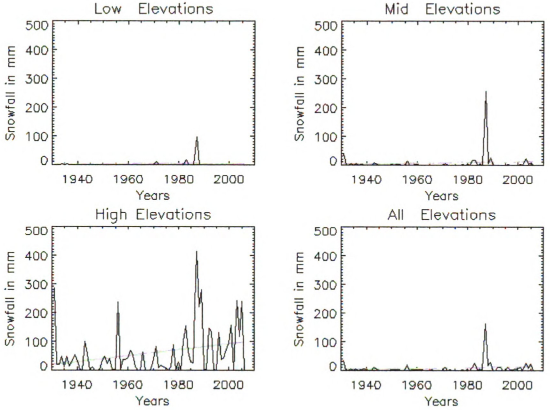

Figure 4.10. April snowfall in mm. A linear fit was calculated for 1931-2006. Results are included for low elevations (< 500 m; top left), mid elevations (500 – 999 m; top right), high elevations (≥ 1000 m; bottom left), and all elevations (bottom right).

4.3.3. July

No snowfall values were reported for July. July precipitation for 1931-2006 decreased at all elevations (Figure 4.11). Low-elevation stations dropped 20.14 mm (not statistically significant). Meanwhile, mid elevations decreased by 32.40 mm (statistically significant at the $p \leq 0.10$ level) and high elevations decreased by 43.36 mm (statistically significant at the $p \leq 0.05$ level).

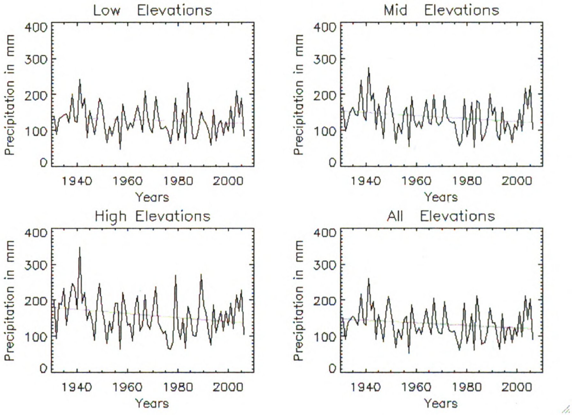

Figure 4.11. July precipitation in mm. A linear fit was calculated for 1931-2006. Results are included for low elevations (< 500 m; top left), mid elevations (500 – 999 m; top right), high elevations (≥ 1000 m; bottom left), and all elevations (bottom right).

4.3.4. October

Total precipitation over the study period for October (Figure 4.12) increased at low elevations (11.88 mm), decreased at mid elevations (1.00 mm), and increased at high elevations (8.55 mm). Snowfall totals (Figure 4.13) remained relatively steady with a small increase at low elevations of 0.09 mm, and a decrease at mid and high elevations of 0.27 and 0.19 mm, respectively. None of the precipitation or snowfall values for October were statistically significant.

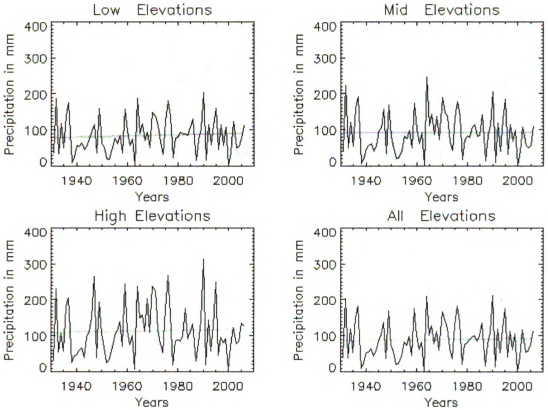

Figure 4.12. October precipitation in mm. A linear fit was calculated for 1931-2006. Results are included for low elevations (< 500 m; top left), mid elevations (500 – 999 m; top right), high elevations (≥ 1000 m; bottom left), and all elevations (bottom right).

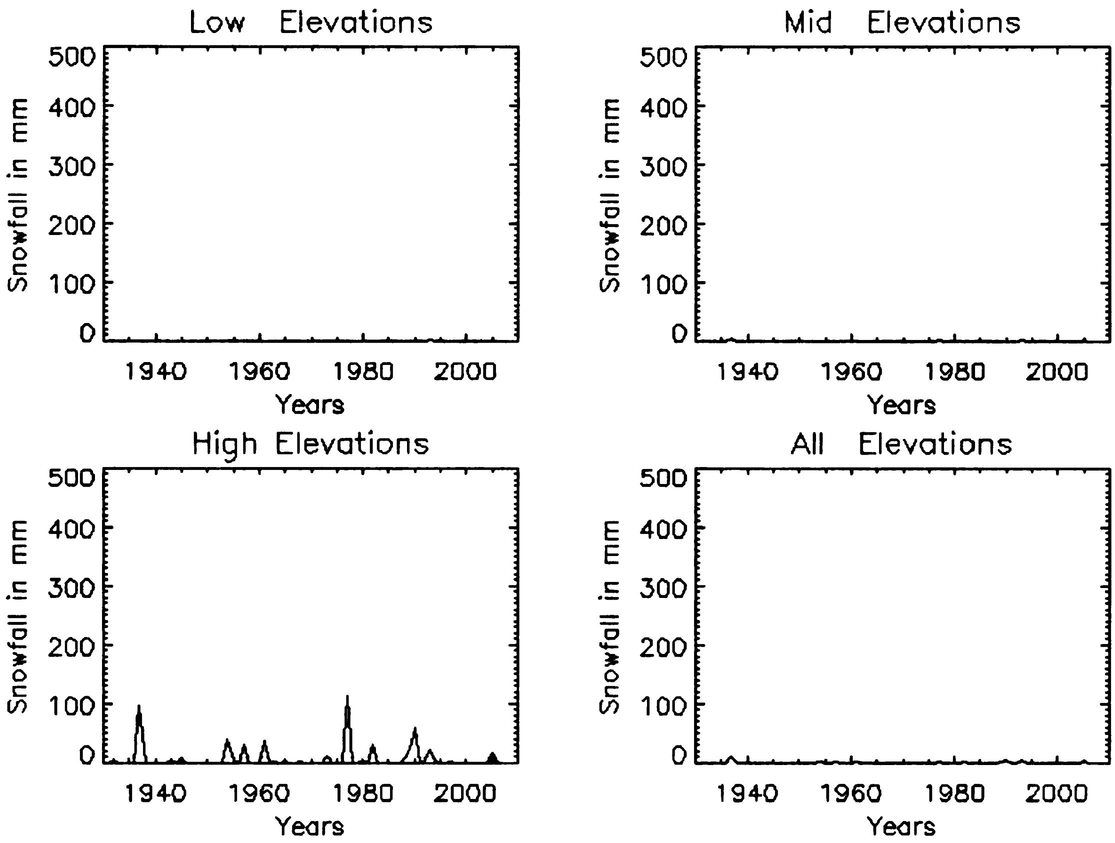

Figure 4.13. October snowfall in mm. A linear fit was calculated for 1931-2006. Results are included for low elevations (< 500 m; top left), mid elevations (500 – 999 m; top right), high elevations (≥ 1000 m; bottom left), and all elevations (bottom right).

4.3.5. Annual

When considering the values after averaging all 12 months, total precipitation (Figure 4.14) increased at all elevations over the study period (60.55 mm for low, 81.40 mm for mid, and 125.03 mm for high), although none of the values trends were statistically significant. Snowfall (Figure 4.15) decreased at low elevations (52.59 mm; not statistically significant) and mid elevations (92.59 mm; not statistically significant), while increasing substantially at high elevations (561.76 mm; statistically significant at the $p \leq 0.01$ level).

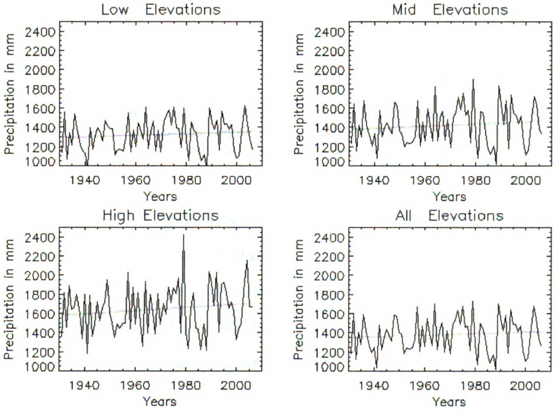

Figure 4.14. Annual values for precipitation in mm. A linear fit was calculated for 1931-2006. Results are included for low elevations (< 500 m; top left), mid elevations (500 – 999 m; top right), high elevations (≥ 1000 m; bottom left), and all elevations (bottom right).

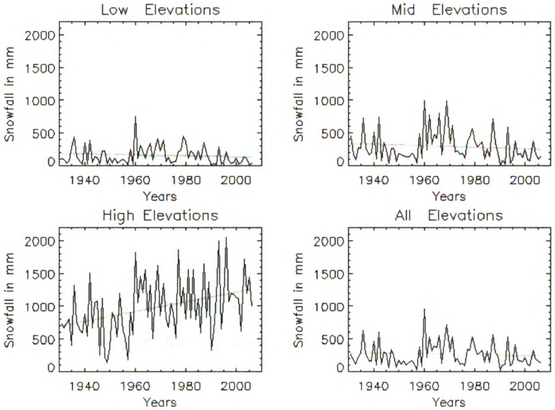

Figure 4.15. Annual values for snowfall in mm. A linear fit was calculated for 1931-2006. Results are included for low elevations (< 500 m; top left), mid elevations (500 – 999 m; top right), high elevations (≥ 1000 m; bottom left), and all elevations (bottom right).

Trends during 1931-2006 suggest that total precipitation diminished in winter months and the months of July and August. Annual precipitation values increased, however, and during months spanning April through June and September through November (Table 4.4 and Figures 4.7, 4.9, 4.11, 4.12, and 4.14). Annual snowfall totals decreased at low and mid elevations, while increasing at high elevations (Table 4.5 and Figures 4.8, 4.10, 4.13, and 4.15). Even at high elevations, snowfall decreased during some autumn months, while a shift toward additional snowfall during spring seemed to be the norm. When looking ahead, preliminary data for 2007 and 2008 suggest that much of the southeastern U.S. continues to be in a dry period. In some cases, Figures 4.7-4.15

already display this trend at the end of the series, as values often dropped off during the last year or two.

Intra-annual trends for 1931-2006 show that values of both precipitation and snowfall generally increased with increasing elevation and the snow season spanned from October until the following May (Figures 4.16-4.17). The annual snowfall maximum was experienced during January for stations at low and mid elevations. For high-elevation stations, the snowfall maximum was reached in February. In terms of total precipitation, low- and mid-elevation stations had a maximum in March with a secondary maximum in July. In contrast, high elevations had the largest maximum in July and a secondary maximum in March. At all elevations, the driest month of the year was October. A secondary precipitation minimum was present in April for low and mid elevations. High elevations actually had a second minimum in February and a third in April.

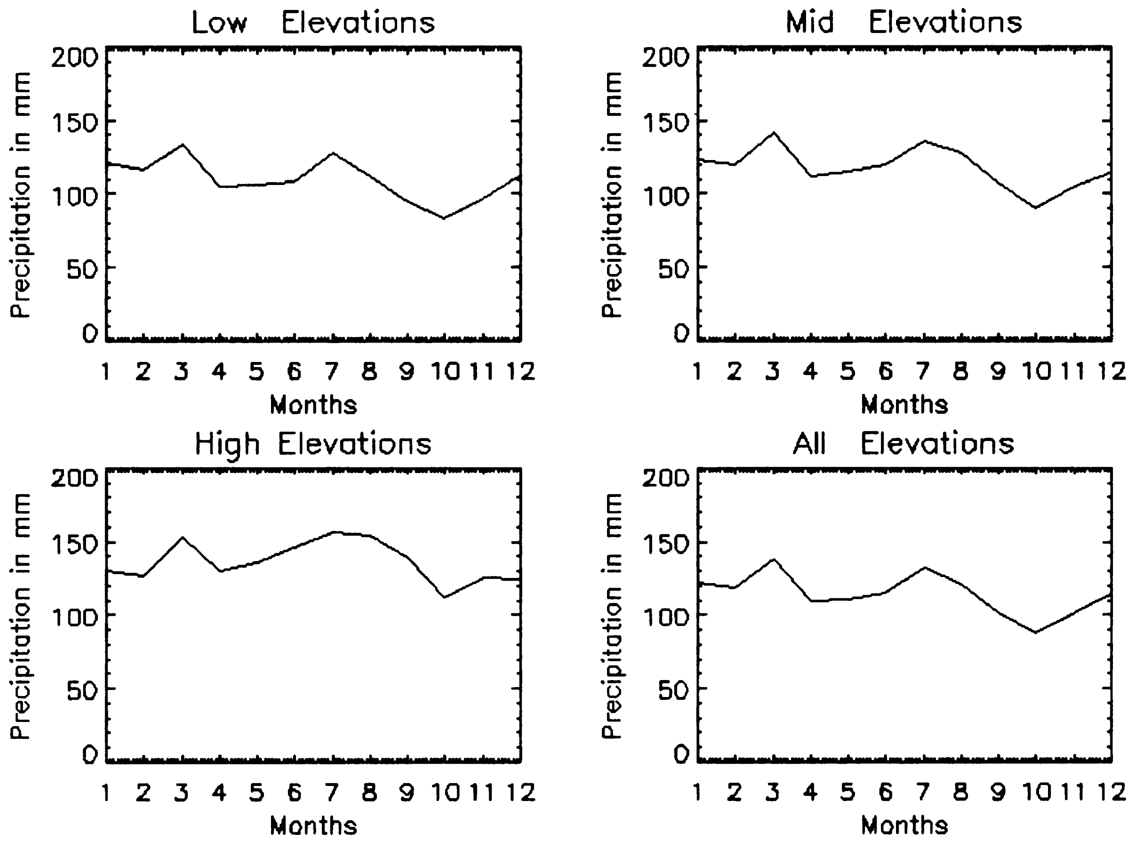

Figure 4.16. Intra-annual trends of total precipitation in mm versus months of the year. Values were averaged over the entire 1931-2006 period. Results are included for low elevations (< 500 m; top left), mid elevations (500 – 999 m; top right), high elevations (≥ 1000 m; bottom left), and all elevations (bottom right).

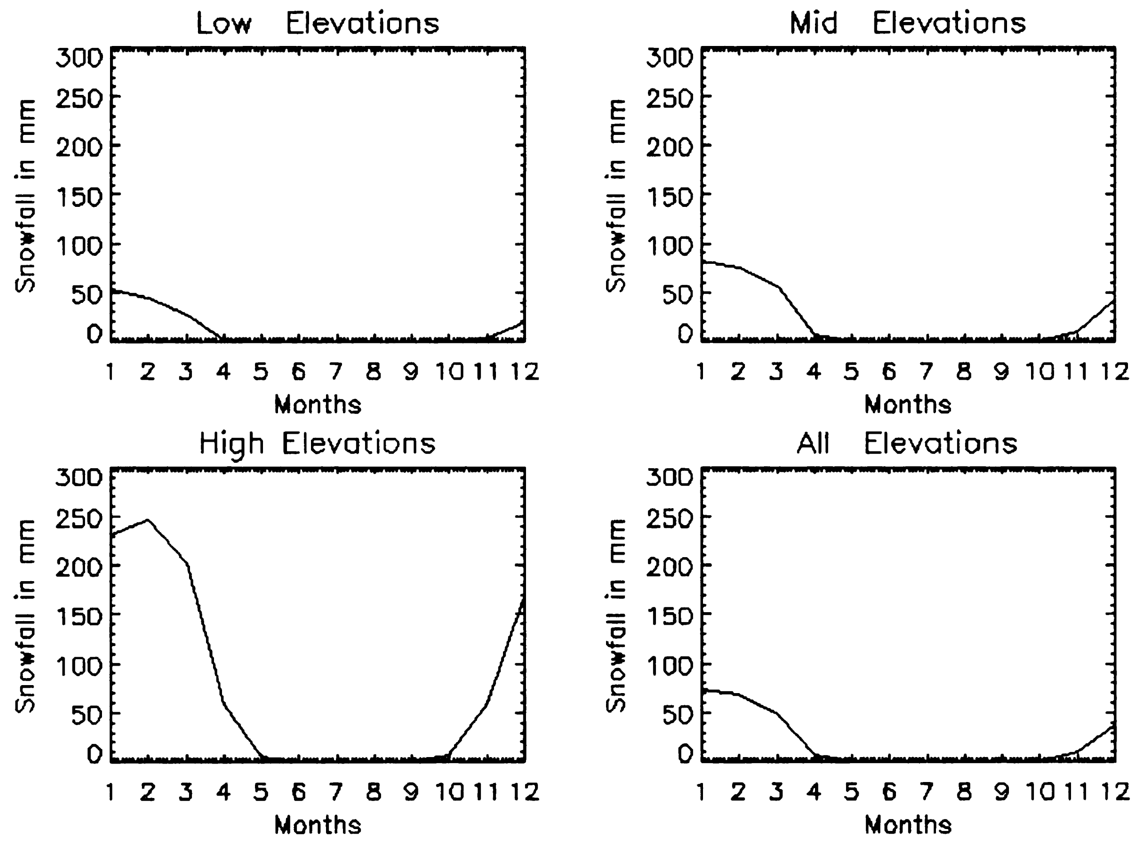

Figure 4.17. Intra-annual trends of total snowfall in mm versus months of the year. Values were averaged over the entire 1931-2006 period. Results are included for low elevations (< 500 m; top left), mid elevations (500 – 999 m; top right), high elevations (≥ 1000 m; bottom left), and all elevations (bottom right).

4.4. Discussion

In general, these results support Köppen's classification of this region as humid subtropical (Cfa). As a whole, the region experienced relatively hot and humid summers and mild winters (i.e., average temperature of the coldest month was below 18°C, and above -3°C). Annual precipitation generally fell within Köppen's specified range of 800 to 1650 mm. However, the results here were more similar to those found by Gaffin and Hotz (2000) in that the annual totals of precipitation I found were usually 1000 mm or greater even at low-elevation stations. Furthermore, in agreement with the previous studies discussed in Chapter 2 (e.g., Whittaker, 1952; Smallshaw, 1953; Shanks, 1954;

Mark, 1958; Bogucki, 1972; Hicks, 1979; Gaffin and Hotz, 2000), the results here also suggest that precipitation totals tended have a positive relationship with elevation. Across all elevations, the annual range in precipitation generally ranged from 1000 to 1700 mm. However, local-scale topographical variations in elevation, slope, shape, and aspect likely contributed to some values exceeding these averages. For instance, some high-elevation stations had precipitation totals of 2000 mm or more. Similar ranges and values were found in previous studies by Whittaker (1952), Smallshaw (1953), Shanks (1954), Mark (1958), Bogucki, (1972), Hicks (1979), and Gaffin and Hotz (2000).

Whittaker (1952) found that the annual precipitation peaks occurred during late winter/early spring and late summer, while the minima occurred in late spring and early autumn. Mark (1958) reported that dry periods usually occurred during late spring and autumn months. Gaffin and Hotz (2000) found spring and autumn to be the driest seasons while summer was the wettest season. Although Whittaker (1952), Mark (1958), and Gaffin and Hotz (2000) did not specify exact months, their broad results do agree with the intra-annual trends I illustrated in Figure 4.16. Diem's (2006) results show that dry periods during summer months in GA spanned the mid 1950s, the mid 1970s through the mid 1980s, and again during the late 1990s, while wet periods spanned the 1960s and early 1990s. My July maps in Figure 4.11 support those results. In addition, my results illustrated that wet summer periods were present from roughly the mid 1930s through 1950, the 1960s, and during the early 2000s. Observations at the very end of the series in Figure 4.11 and preliminary data not shown suggest that the region is currently in a dry period.

The only previous study to discuss snowfall was Mark (1958). Much like my results in Figure 4.17, he found that snowfall began in October and continued through May. His results relied on the three stations of Asheville, NC (671 m), Banner Elk, NC (1131 m), and Mount Mitchell, NC (2022 m), to represent low, mid, and high elevations. Mark's (1958) results showed that maximum snowfall occurred in February for Asheville (79 mm), January for Banner Elk (224 mm), and March for Mount Mitchell (378 mm). In contrast, I found that both low- and mid-elevation stations generally received peak snowfall during January, while high-elevations stations peaked in February (Figure 4.17), and the average snowfall values I found were somewhat lower (53 mm for low, 82 mm for mid, and 247 mm for high). However, the representative stations that Mark (1958) used do not coincide exactly with the elevation categories I specified. Following my scheme, Asheville, NC, would be a mid-elevation station, whereas both Banner Elk, NC, and Mount Mitchell, NC, would both be in the high-elevation category. These differences probably account for at least some of the variation in snowfall totals between our respective studies.

As was the case in previous studies (e.g., Shanks, 1954; Mark, 1958; Hicks, 1979; Bolstad et al., 1998), I found temperatures to decrease with increasing elevation (Figures 4.1-4.6). In agreement with Shanks (1954) and Mark (1958), I found July to be the warmest month at all elevations (Figure 4.6). I also found January to be the coolest month for all elevations. In contrast, Shanks (1954) found the coolest months at low elevations to be November and December and March to be coldest for high elevations, but Mark (1958) found the coldest temperatures for high elevations during February. In general, I found that minimum, maximum, and mean temperatures cooled overall during the 1931-2006 period, but warming did occur throughout the last few decades. My temperature values also suggest that the diurnal temperature range decreased, which is in agreement with results found by others in global studies (Karl et al., 1993; Easterling et al., 1997; IPCC, 2007a). In addition, my results show that cool-season temperatures warmed more than warm-season temperatures during the past few decades, which coincides with results from the USGCRP's 2009 report for the southeastern U.S. This result suggests that the range of the annual temperature cycle decreased. Other studies by Balling et al. (1998), the IPCC (2007a), and Stine et al. (2009) found this same general trend occurring globally.

In reference to Question 1, my results thus far have generally supported the findings reported by others, but some small differences are present. For instance, my precipitation values were somewhat higher than those classified by the Köppen classification for the region. I was able to be more specific than Whittaker (1952), Mark (1958), and Gaffin and Hotz (2000) in pinpointing the timing of annual precipitation maxima and minima. My snowfall values were somewhat lower than Mark's (1958), but this result may be explained by his inclusion of only three stations. Although my data agree with others regarding the timing of the annual temperature maximum (July), my minimum temperature results did differ from others (Shanks, 1954; Mark, 1958). My speculation is that these differences result from the fewer stations and shorter study periods utilized in earlier studies. My results show that temperature values generally had an inverse relationship with elevation, whereas precipitation and snowfall totals had a positive relationship with elevation.

In addition to building upon past studies, my study provides new information as well to assist with answering Question 1. Diurnal and annual temperature ranges in the region were found to be shrinking over the study period. Total precipitation increased over the study period. Snowfall totals decreased at low and mid elevations during most months. Snowfall totals increased at high elevations, where a decrease in snow totals during some autumn months were offset by a shift toward increased springtime snowfall.

CHAPTER 5

RESULTS AND DISCUSSION OF THE SPATIAL ANALYSIS

5.1. Overview

Table 5.1 shows the number of stations for each month (and annually) within each overlapping decade when at least 90 percent of the data were available for all variables (minimum, maximum, and mean temperature, total precipitation, and total snowfall). Few stations were available until after 1930. Although 463 monthly stations were used throughout the study, during the 1930-1939 decade 30 or fewer stations frequently reported data. In general, with each passing decade the number increased and in the final decade (1995-2004), the number of stations surpassed 70. Some noticeable exceptions to this trend were January and February during the 1955-1964 and 1960-1969 decades when fewer than 30 stations were available. During those decades, fewer stations reported snowfall totals and no known technological changes in snowfall measurement during that time have been documented.

Table 5.1. Number of stations with at least 90 percent of data available for minimum, maximum, mean temperature, total precipitation, and total snowfall.

Period	Jan	Feb	Mar	Apr	May	Jun	Jul	Aug	Sep	Oct	Nov	Dec	Ann
1890-1899	0	0	0	0	0	0	0	0	0	0	0	0	0
1895-1904	0	0	0	0	0	0	0	0	0	0	0	0	0
1900-1909	1	1	0	0	0	1	1	1	0	0	0	0	0
1905-1914	1	1	0	0	0	1	1	0	0	0	0	1	0
1910-1919	1	1	0	0	0	1	0	0	0	0	0	0	0
1915-1924	1	0	1	1	0	1	0	1	1	1	0	0	0
1920-1929	0	0	1	1	1	1	1	1	1	1	1	0	0
1925-1934	0	1	1	1	1	1	1	1	1	1	1	1	0
1930-1939	29	30	27	27	28	28	29	26	23	25	29	26	11
1935-1944	38	42	41	37	36	39	38	40	33	33	39	35	24
1940-1949	37	39	41	39	38	39	38	39	34	35	37	32	26
1945-1954	40	38	39	44	44	43	45	46	43	45	37	35	24
1950-1959	37	37	46	55	58	55	55	55	54	54	44	34	21
1955-1964	20	22	34	54	58	54	57	59	60	59	53	28	13
1960-1969	22	23	38	66	64	64	64	66	66	65	53	32	15
1965-1974	32	44	50	75	77	78	75	76	76	74	60	51	23
1970-1979	41	42	52	69	70	70	69	68	68	67	57	52	31
1975-1984	44	41	55	67	67	66	65	66	65	66	64	53	32
1980-1989	47	48	66	68	67	67	67	67	68	68	67	61	34
1985-1994	65	67	71	72	70	72	72	72	71	71	70	66	55
1990-1999	71	71	70	68	72	71	72	70	70	69	72	69	61
1995-2004	72	74	73	72	72	71	70	70	74	74	75	73	64

My initial intent for using 10-year overlapping periods was to not only study the stations in a spatial context, but also to determine whether any temporal change or variability was noticeable amongst the clusters over time. However, because the overall number and location of available stations changed substantially during the study period, the number and location of stations were probably the largest factors creating noticeable change amongst the clusters. For instance, few stations existed during early years of the study (the northwestern portion of the study area in particular) and inclusion of additional stations in later decades likely affected the clusters.

Cluster results for minimum, maximum, and mean temperature were quite similar, so only mean temperature is presented here. The 5-cluster result is shown and the 1935-

1944, 1965-1974, and 1995-2004 decades are used to represent periods near the beginning, middle, and end of the record. January and July maps are shown here to represent cool and warm season clusters. April and October clusters for representing the transition seasons are not discussed in this chapter, but the maps for those months are included in Appendix B. Results within this chapter yield spatial information to assist in answering Questions 1 and 2 from Section 2.5.

During the analysis, stations were ranked based on the "strength" of the corresponding cluster. When referring to the strongest cluster, I mean that stations within that cluster were statistically most similar. On the maps, stations in Cluster 1 (i.e., the strongest cluster) are depicted as a black dot. Stations in Cluster 2 are very dark gray plus signs. Stations in Cluster 3 are dark gray squares. Those in Cluster 4 are light gray triangles, and those in Cluster 5 (i.e., the weakest cluster) are very light gray diamonds. Although cluster strength is important, its evaluation is more crucial in studies using many clusters. Since I am only presenting five clusters in this study, in most cases all of the clusters are important, so I will not overly emphasize cluster strength or rank. As I will show, some groups of stations tended to cluster together frequently, but did not necessarily always cluster together at the same rank each time (e.g., in one time period a group of stations may be within Cluster 1 and in another time period the same stations may be within Cluster 3).

5.2. Spatial Results of Temperature

5.2.1. January

During 1935-1944, 38 stations were available (Figure 5.1). Results for most maps suggest cluster relationships with latitude and/or elevation. Cluster 3 (square) was located in the southeast and low-lying Piedmont portion of the area and was the warmest (6.12°C) cluster. Cluster 2 (plus sign) was at slightly higher elevations mostly along the southeast-facing side of the Blue Ridge (5.10°C). Cluster 4 (triangle) stations were comprised of the mid-elevation stations and had mean temperatures of 3.71°C. Cluster 5 (diamond) stations were located at mid-to-high elevations and had a lower temperature (1.87°C). Lastly, Cluster 1 (dot) consisted of one station at a high elevation that had the lowest temperature (-3.04°C).

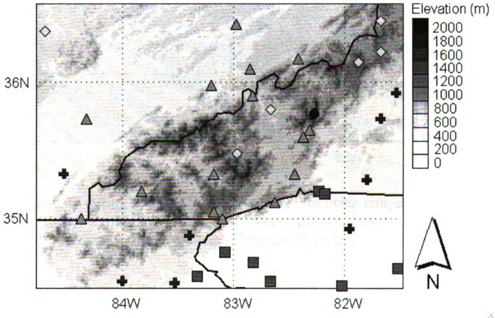

Figure 5.1. January during 1935-1944 with 5 clusters for mean temperature, where Cluster 1 (dot), Cluster 2 (plus sign), Cluster 3 (square), Cluster 4 (triangle), and Cluster 5 (diamond) represent station locations. Elevation in meters is shaded in gray.

Thirty-two stations were available during the 1965-1974 period (Figure 5.2). In the southeast portion, Cluster 2 was the warmest (6.16°C). Cluster 1 had some stations at slightly higher elevations along the Blue Ridge (4.74°C). Cluster 4 was comprised of mostly low- and mid-level stations (3.07°C). Cluster 3 stations were located at higher elevations (0.88°C) in the northeast portion of the study area, and Cluster 5 stations were generally at the highest elevations (-0.80°C).

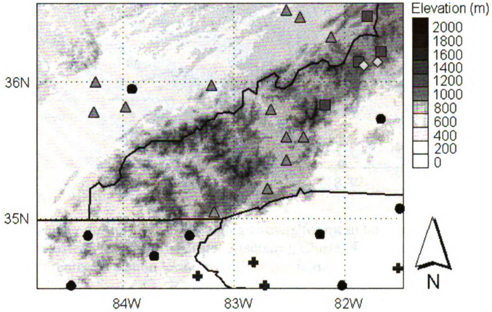

Figure 5.2. January during 1965-1974 with 5 clusters for mean temperature, where Cluster 1 (dot), Cluster 2 (plus sign), Cluster 3 (square), Cluster 4 (triangle), and Cluster 5 (diamond) represent station locations. Elevation in meters is shaded in gray.

For the 1995-2004 period, 72 stations were available (Figure 5.3). Cluster 2 was the warmest cluster (5.85°C) and was generally located in the southeast and lowest-lying areas. Cluster 1 was also mostly scattered along the southeast side of the Blue Ridge at slightly higher elevations (4.40°C). Cluster 3 was a large cluster comprised of more northerly and mid-level stations (3.00°C). Cluster 5 was also northerly with mid- to high-level stations (1.26°C). Lastly, Cluster 4 consisted of only two stations, but they were high-elevation stations (-2.60°C).

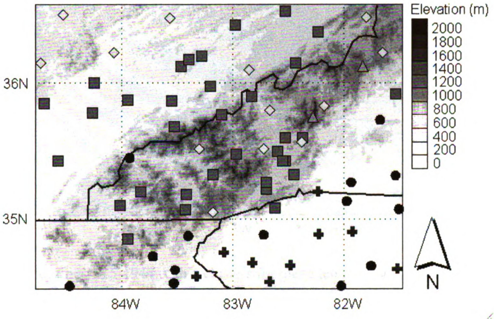

Figure 5.3. January during 1995-2004 with 5 clusters for mean temperature, where Cluster 1 (dot), Cluster 2 (plus sign), Cluster 3 (square), Cluster 4 (triangle), and Cluster 5 (diamond) represent station locations. Elevation in meters is shaded in gray.

5.2.2. July

During 1935-1944 for July, 38 stations were available (Figure 5.4). In this case, Cluster 1 was the coldest cluster (15.09°C) and included one high-elevation station. Cluster 4 was the second coolest cluster (20.89°C) and consisted of mid- to high-elevation stations. Mid-level stations were included in Cluster 2 and were somewhat warmer (23.00°C). Stations in low- to mid-elevation areas were in Cluster 3 (24.67°C). The warmest stations (26.04°C) were in Cluster 5. Most of these stations were located in the southeast area, but a few others lay at low elevations on the northwest side of the Blue Ridge.

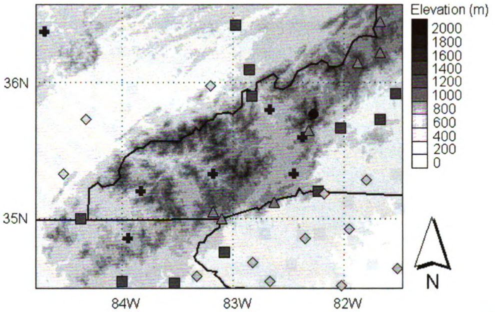

Figure 5.4. July during 1935-1944 with 5 clusters for mean temperature , where Cluster 1 (dot), Cluster 2 (plus sign), Cluster 3 (square), Cluster 4 (triangle), and Cluster 5 (diamond) represent station locations. Elevation in meters is shaded in gray.

Seventy-five stations reported during the 1965-1974 decade (Figure 5.5). The warmest cluster (25.38°C) was Cluster 3, with all stations at low elevations and most located to the southeast. Cluster 5 was also a warm cluster (23.95°C) and was comprised of stations at low and mid elevations on both sides of the Blue Ridge. Cluster 1 included mid-level and northerly stations (22.60°C), whereas Cluster 2 included mid- and high-elevation stations (21.51°C). The coolest cluster was Cluster 4, where temperatures averaged 19.13°C. Stations in Cluster 4 were generally at high elevations.

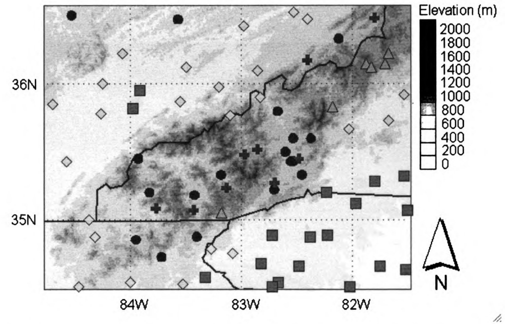

Figure 5.5. July during 1965-1974 with 5 clusters for mean temperature, where Cluster 1 (dot), Cluster 2 (plus sign), Cluster 3 (square), Cluster 4 (triangle), and Cluster 5 (diamond) represent station locations. Elevation in meters is shaded in gray.

For 1995-2004, 70 stations were available for July (Figure 5.6). The warm cluster (26.12°C), consisting of stations to the southeast and low elevations, was Cluster 4. Low- and mid-elevation stations were included in Cluster 3 and had an average temperature of 24.65°C. Stations at mid and high locations were grouped in Cluster 2 and were somewhat cooler (22.86°C). High-elevation stations were grouped into Clusters 1 and 5, with temperatures of 20.45°C and 16.03°C, respectively.

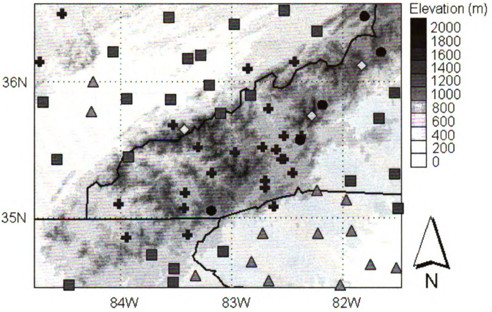

Figure 5.6. July during 1995-2004 with 5 clusters for mean temperature, where Cluster 1 (dot), Cluster 2 (plus sign), Cluster 3 (square), Cluster 4 (triangle), and Cluster 5 (diamond) represent station locations. Elevation in meters is shaded in gray.

5.3. Spatial Results of Precipitation

5.3.1 January

Unlike temperature, cluster patterns expressed in terms of precipitation tended to be less regionally homogeneous, which supports previous literature (Root and Schneider, 2001). For January during 1935-1944, there were 38 stations present (Figure 5.7). Cluster 1 had the lowest precipitation (90.49 mm). The cluster was located near the TN and NC border in low and mid elevations. Cluster 5 also had low precipitation (110.23 mm), but had stations scattered at varying locations and elevations. Cluster 3 had stations in low and mid elevations (129.29 mm). Cluster 2 had more precipitation (149.15 mm) and was mostly located on the south side of the Blue Ridge at low and mid elevations. Highest precipitation totals were associated with Cluster 4 (183.50 mm) at four stations near the union of the NC, SC, and GA borders located on the south side of the Blue Ridge at mid elevations.

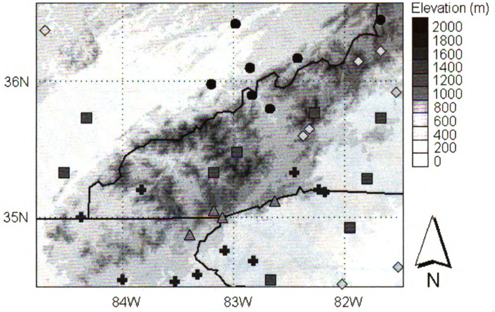

Figure 5.7. January during 1935-1944 with 5 clusters for total precipitation, where Cluster 1 (dot), Cluster 2 (plus sign), Cluster 3 (square), Cluster 4 (triangle), and Cluster 5 (diamond) represent station locations. Elevation in meters is shaded in gray.

Thirty-two stations were reporting during January 1965-1974 (Figure 5.8). The driest locations were associated with Cluster 5 (77.37 mm). Four of the stations in that cluster were located within a low-lying valley that cuts through the Blue Ridge in a northwest to southeast direction toward Asheville, NC. This valley was conveniently used for the placement of Interstate-40 and ultimately connects Knoxville, TN, and Asheville, NC. This "I-40 corridor" generally received less precipitation than the much higher elevations to its southwest and northeast. Cluster 2 was comprised of mid- and high-elevation stations mostly at northerly locations and was also dry (96.06 mm). Cluster 3 included some southeastern stations at low elevations, two stations in the Ridge and Valley province and two stations at higher elevations (110.60 mm). Some low and mid stations were in Cluster 4 (131.06 mm). Lastly, Cluster 1 had the highest precipitation total (153.81 mm) and was located in northern GA and near the SC and NC borders.

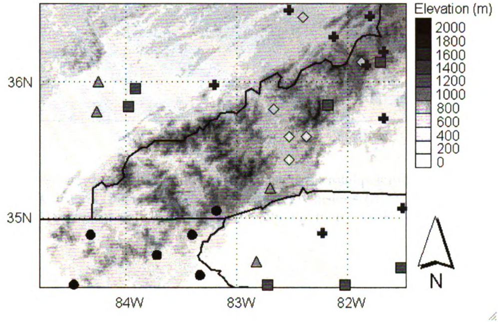

Figure 5.8. January during 1965-1974 with 5 clusters for total precipitation, where Cluster 1 (dot), Cluster 2 (plus sign), Cluster 3 (square), Cluster 4 (triangle), and Cluster 5 (diamond) represent station locations. Elevation in meters is shaded in gray.

During 1995-2004, 72 stations were available for January (Figure 5.9). Clusters 1 and 3 had the lowest precipitation totals (107.62 mm and 124.62 mm) and were located in low-lying northerly locations, along the I-40 corridor, and at low-lying southeastern locations. Cluster 2 was scattered at locations on both sides of the Blue Ridge (142.95 mm). Higher totals were present for Cluster 4 (161.50 mm) at mid-elevations locations along the Blue Ridge. The highest totals were associated with Cluster 5 (196.02 mm), where most stations were located in northeast GA and southwest NC.

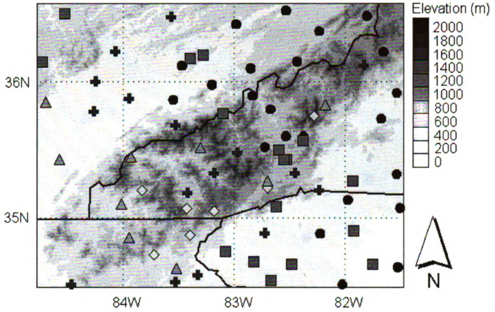

Figure 5.9. January during 1995-2004 with 5 clusters for total precipitation, where Cluster 1 (dot), Cluster 2 (plus sign), Cluster 3 (square), Cluster 4 (triangle), and Cluster 5 (diamond) represent station locations. Elevation in meters is shaded in gray.

5.3.2. July

During 1935-1944 there were 38 stations reporting for July (Figure 5.10). The driest locations were included in Cluster 1 mostly at low elevations (129.48 mm). Cluster 3 was mostly at mid elevations (149.67 mm), whereas Cluster 2 stations were at mid and high elevations (176.19 mm). Cluster 4 had two stations at mid-to-high elevations (210.19 mm) and Cluster 5 had three stations (249.43 mm). Two stations from Cluster 5 were located near the union of NC, SC, and GA and the third was located at a higher elevation.

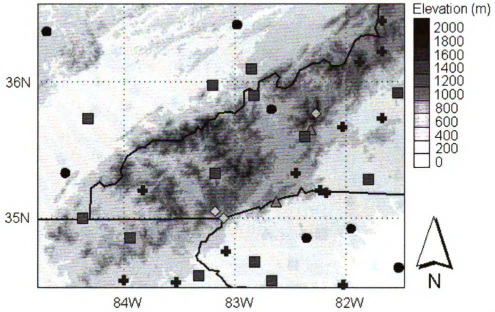

Figure 5.10. July during 1935-1944 with 5 clusters for total precipitation, where Cluster 1 (dot), Cluster 2 (plus sign), Cluster 3 (square), Cluster 4 (triangle), and Cluster 5 (diamond) represent station locations. Elevation in meters is shaded in gray.

Lower precipitation values were reported at 75 stations during 1965-1974 (Figure 5.11). In this case, the lowest values were included in Cluster 3 (96.01 mm) along the I-40 corridor and in the southeastern portion of the region. Low values were also present in Cluster 1 (127.76 mm) and Cluster 4 (115.29 mm) at low and mid elevations. Cluster 2 was also at low and mid elevations, but had somewhat higher precipitation totals (144.13 mm). The wettest region was Cluster 5 (166.92 mm) and mostly included stations in southwest NC and northeast GA.

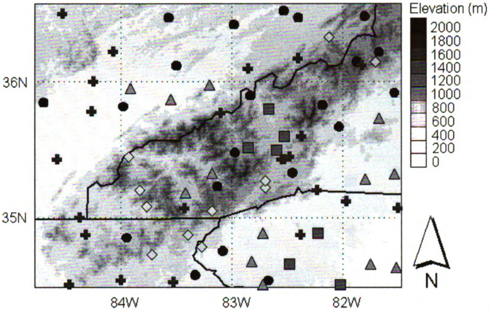

Figure 5.11. July during 1965-1974 with 5 clusters for total precipitation, where Cluster 1 (dot), Cluster 2 (plus sign), Cluster 3 (square), Cluster 4 (triangle), and Cluster 5 (diamond) represent station locations. Elevation in meters is shaded in gray.

Seventy stations reported during July for the 1995-2004 period (Figure 5.12). Cluster 4 was the driest cluster (94.24 mm) with stations located in the low-lying southeast portion of the area and some stations located at mid-to-high elevations along the Blue Ridge. Stations within Cluster 2 (107.39 mm) and Cluster 3 (121.45 mm) were mostly scattered at low and mid elevations. Cluster 1 had stations along the Blue Ridge and also within the Ridge and Valley province (138.17 mm). Cluster 5 had the highest totals (167.30 mm), but also had stations scattered in along the Blue Ridge and the Ridge and Valley province.

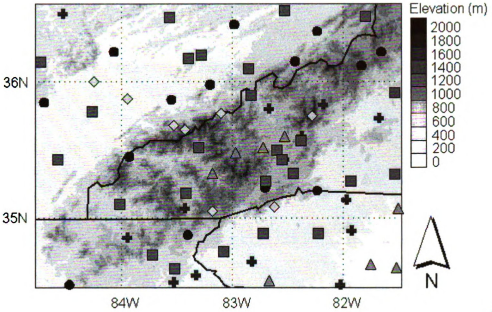

Figure 5.12. July during 1995-2004 with 5 clusters for total precipitation, where Cluster 1 (dot), Cluster 2 (plus sign), Cluster 3 (square), Cluster 4 (triangle), and Cluster 5 (diamond) represent station locations. Elevation in meters is shaded in gray.

5.4. Spatial Results of Snowfall

5.4.1. January

During 1935-1944, 38 stations reported snowfall (Figure 5.13). Stations that received the lowest totals (36.61 mm) were located either in the southeastern portion of the region or within the I-40 corridor and were included in Cluster 2. Cluster 3 included stations at low and mid elevations (56.27 mm). Stations mostly at mid elevations of the Blue Ridge were in Cluster 4 (75.81 mm). The highest values were generally reported at the highest elevations within Cluster 1 (258.28 mm) and Cluster 5 (127.04 mm).

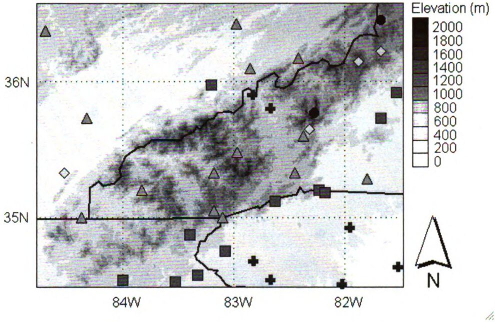

Figure 5.13. January during 1935-1944 with 5 clusters for total snowfall, where Cluster 1 (dot), Cluster 2 (plus sign), Cluster 3 (square), Cluster 4 (triangle), and Cluster 5 (diamond) represent station locations. Elevation in meters is shaded in gray.

Somewhat higher values were reported from 75 stations during 1965-1974 (Figure 5.14). Cluster 1 included the lowest values (54.18 mm). Stations within that cluster were all southern stations in either GA or SC. Cluster 5 and Cluster 2 had much higher values (102.41 mm and 139.21 mm) and included stations at mid elevations along the I-40 corridor and two stations in the Ridge and Valley province. Cluster 4 included stations at northern locations and mid-to-high elevations (187.92 mm). The highest totals were reported in Cluster 3 (289.50 mm) and included four northeast stations at high elevations.

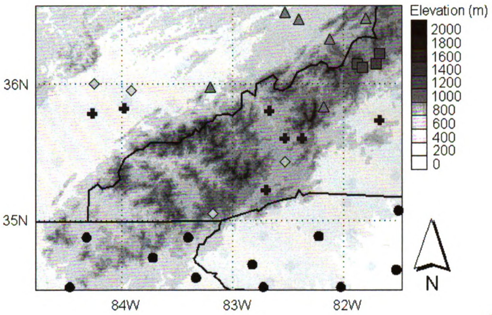

Figure 5.14. January during 1965-1974 with 5 clusters for total snowfall, where Cluster 1 (dot), Cluster 2 (plus sign), Cluster 3 (square), Cluster 4 (triangle), and Cluster 5 (diamond) represent station locations. Elevation in meters is shaded in gray.

Seventy stations reported snowfall during January for 1995-2004 (Figure 5.15). Small totals were reported in Cluster 1 (9.58 mm). Stations in that cluster were mostly at low elevations and/or at southern locations. Somewhat more snowfall was received by Cluster 2 stations (61.01 mm). Many of those stations were also located at low elevations, although a large percentage was located in the Ridge and Valley province of TN. Cluster 3 was comprised of northern stations and stations along the I-40 corridor (113.00 mm). The highest totals were reported by stations at high elevations and northeast locations. Those stations were included in Cluster 4 (239.02 mm) and Cluster 5 (516.51 mm).

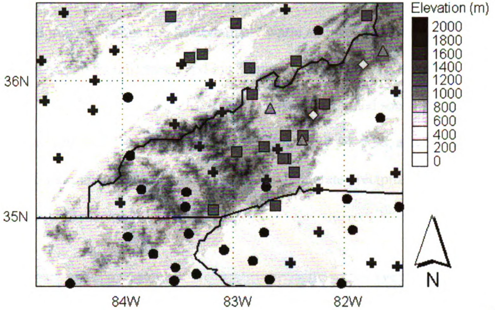

Figure 5.15. January during 1995-2004 with 5 clusters for total snowfall, where Cluster 1 (dot), Cluster 2 (plus sign), Cluster 3 (square), Cluster 4 (triangle), and Cluster 5 (diamond) represent station locations. Elevation in meters is shaded in gray.

5.5. Spatial Results for All Variables

5.5.1. January

Clusters based on all variables (minimum, maximum, and mean temperature, total precipitation, and total snowfall) were also considered. Cluster 2 was the coldest cluster (-3.59, 2.30, 8.19°C for minimum, mean, and maximum temperature) and largely included stations along the Blue Ridge (Figure 5.16). Cluster 2 also had precipitation and snowfall values of 115.13 and 93.41 mm. Cluster 5 consisted of high-elevation stations and was also cool (-2.76, 2.76, 8.26°C for minimum, mean, and maximum temperature), but also had the highest precipitation (147.37 mm) and snowfall (121.82 mm) values. Cluster 3 stations were mostly located near the I-40 corridor and had the lowest precipitation values (-2.16, 3.93, 10.03°C for minimum, mean, and maximum temperature, 95.78 mm for precipitation, and 66.88 mm for snowfall). Stations in Cluster 4 were at low and mid elevations and had relatively warm and wet conditions (-1.34, 4.95, and 11.25°C for minimum, mean, and maximum temperature, 142.28 mm for precipitation, and 61.92 mm for snowfall). Lastly, Cluster 1 included southerly stations at low elevations. Cluster 1 was the warmest of the clusters (0.54, 5.96, and 11.38°C for minimum, mean, and maximum temperature), and had moderate precipitation (141.12 mm), but low snowfall receipt (47.71 mm).

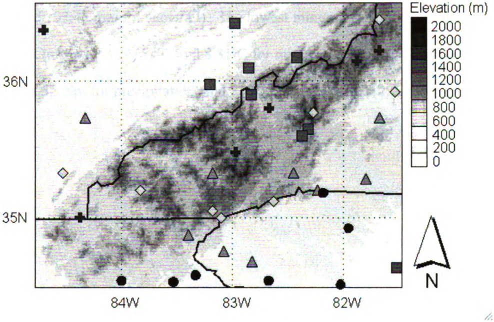

Figure 5.16. January during 1935-1944 with 5 clusters for all variables (minimum temperature, maximum temperature, mean temperature, total precipitation, and total snowfall), where Cluster 1 (dot), Cluster 2 (plus sign), Cluster 3 (square), Cluster 4 (triangle), and Cluster 5 (diamond) represent station locations. Elevation in meters is shaded in gray.

January clusters during 1965-1974 did not express any strong spatial patterns as all clusters had stations at varying locations and elevations (Figure 5.17). Cluster 1 had northerly stations with relatively cool temperatures and the highest snowfall total (-2.81, 2.53, and 7.84°C for minimum, mean, and maximum temperature, 100.32 mm for precipitation, and 201.88 mm for snowfall). Cluster 3 had the highest precipitation and lowest snowfall values (-1.86, 3.66, and 9.16°C for minimum, mean, and maximum temperature, 139.40 mm for precipitation, and 94.30 mm for snowfall). Cluster 4 had the highest mean and maximum temperatures (-2.22, 4.10, and 10.39°C for minimum, mean, and maximum temperature, 104.20 mm for precipitation, and 131.28 mm for snowfall). Cluster 2 had several stations in the I-40 corridor and the lowest precipitation value (-1.76, 3.98, and 9.69°C for minimum, mean, and maximum temperature, 87.84 mm for precipitation, and 103.46 mm for snowfall). The lowest minimum temperatures were associated with Cluster 5 (-3.24, 2.80, and 8.81°C for minimum, mean, and maximum temperature, 124.52 mm for precipitation, and 139.52 mm for snowfall).

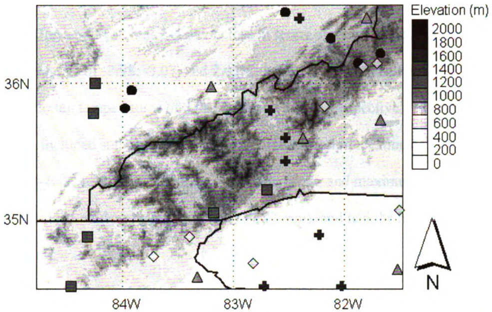

Figure 5.17. January during 1965-1974 with 5 clusters for all variables (minimum temperature, maximum temperature, mean temperature, total precipitation, and total snowfall), where Cluster 1 (dot), Cluster 2 (plus sign), Cluster 3 (square), Cluster 4 (triangle), and Cluster 5 (diamond) represent station locations. Elevation in meters is shaded in gray.

The 1995-2004 decade for January was comprised of five distinct climate regimes (Figure 5.18). Stations in Cluster 1 were all southeastern stations at low elevations within the Piedmont. This was the warmest cluster (-1.11, 5.35, and 11.77°C for minimum, mean, and maximum temperature). Cluster 1 was also relatively dry (120.30 mm for precipitation and 34.84 mm for snowfall). Cluster 2 mostly included stations along the I-40 corridor and stations to the north of that area. Overall, Cluster 2 was the driest cluster (110.04 mm for precipitation), although it did experience the second highest snowfall totals (73.41 mm). Cluster 3 was located near the NC, SC, and GA borders and had the highest precipitation total (178.39 mm), but lowest snowfall total (25.80 mm). Stations in Cluster 4 were located at low and mid elevations on the north and south sides of the

Blue Ridge. Moderate precipitation (139.53 mm) and low snowfall (48.12 mm) were associated with Cluster 4. Clusters 2-4 were close in terms of temperature, having minimum temperatures of -2.98, -3.07, and 2.45°C, mean temperatures of 3.01, 3.32, and 3.08°C, and maximum temperatures of 8.98, 9.68, and 8.59°C, respectively. Lastly, Cluster 5 mostly included stations at northerly and high-elevation locations. This regime was the coldest (-4.49, 1.48, and 7.43°C for minimum, mean, and maximum temperature), received moderate precipitation (134.87 mm), and had the highest snowfall totals (183.41 mm).

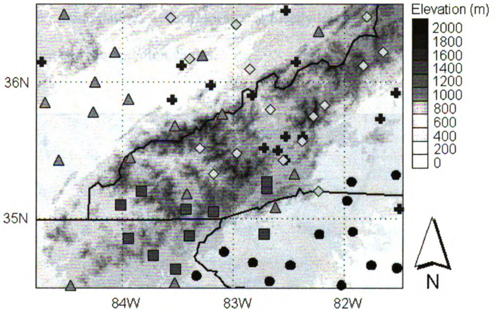

Figure 5.18. January during 1995-2004 with 5 clusters for all variables (minimum temperature, maximum temperature, mean temperature, total precipitation, and total snowfall), where Cluster 1 (dot), Cluster 2 (plus sign), Cluster 3 (square), Cluster 4 (triangle), and Cluster 5 (diamond) represent station locations. Elevation in meters is shaded in gray.

5.5.2. July

Since snowfall was not reported during July, clusters were based on the other four

variables. During July 1935-1944 (Figure 5.19) the coolest and wettest cluster was Cluster 5 (14.92, 20.15, and 25.38°C for minimum, mean, and maximum temperature, and 218.51 mm for precipitation). Stations in that cluster were all located along the Blue Ridge and often at high elevations. Cluster 2 was also cool (16.11, 22.71, and 29.32°C for minimum, mean, and maximum temperature), but had the lowest precipitation totals (146.67 mm). Cluster 1 (18.97, 25.23, and 31.49°C for minimum, mean, and maximum temperature, and 152.37 mm for precipitation), Cluster 3 (18.72, 24.68, and 30.55°C for minimum, mean, and maximum temperature, and 159.17 mm for precipitation), and Cluster 4 (19.21, 25.48, and 31.76°C for minimum, mean, and maximum temperature, and 157.30 mm for precipitation) were all located at mostly low elevations and had similar temperature and precipitation values.

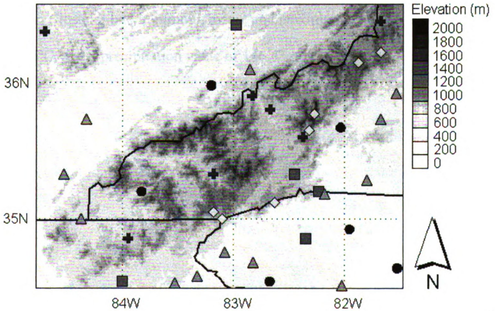

Figure 5.19. July during 1935-1944 with 5 clusters for all variables (minimum temperature, maximum temperature, mean temperature, total precipitation), where Cluster 1 (dot), Cluster 2 (plus sign), Cluster 3 (square), Cluster 4 (triangle), and Cluster 5 (diamond) represent station locations. Elevation in meters is shaded in gray.

Station coverage for July during 1965-1974 (Figure 5.20) was much better compared to the 1935-1944 period (Figure 5.19). The wettest cluster was Cluster 1 (15.85, 22.38, and 28.90°C for minimum, mean, and maximum temperature, and 161.84 mm for precipitation), where many of the stations were located near the intersection of NC, SC, and GA. The driest cluster was Cluster 5 (17.76, 23.12, and 28.46°C for minimum, mean, and maximum temperature, and 118.96 mm for precipitation), although the stations were scattered between high and low elevations. Cluster 4 was mostly comprised of stations along the Blue Ridge and had the lowest minimum and mean temperatures (15.47, 22.07, and 28.64°C for minimum, mean, and maximum temperature, and 124.87 mm for precipitation). Clusters 2 and 3 were the warmest clusters and were located primarily in the lowest-lying areas. Cluster 2 had a minimum, mean, and maximum temperature of 18.15, 24.53, and 30.89°C, with a precipitation value of 128.88 mm. Meanwhile, Cluster 3 had minimum, mean, and maximum temperatures of 17.86, 23.99, and 17.86°C, and a precipitation value of 146.43 mm.

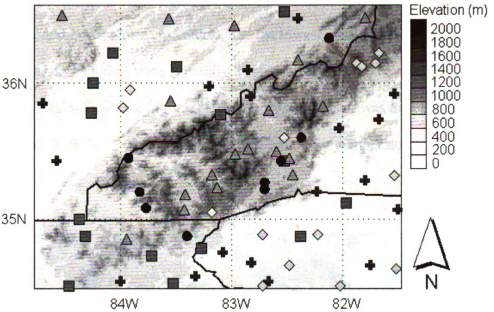

Figure 5.20. July during 1965-1974 with 5 clusters for all variables (minimum temperature, maximum temperature, mean temperature, total precipitation), where Cluster 1 (dot), Cluster 2 (plus sign), Cluster 3 (square), Cluster 4 (triangle), and Cluster 5 (diamond) represent station locations. Elevation in meters is shaded in gray.

Regimes for July (Figure 5.21) during 1995-2004 were less distinct than was the case for January (Figure 5.18). Cluster 1 consisted of stations at varying locations, but most were at low and mid elevations. These locations had moderate temperatures (17.59, 23.81, 29.98°C for minimum, mean, and maximum temperature) and the second highest precipitation receipt (128.72 mm). Cluster 2 stations were located at low elevations on both sides of the Blue Ridge, had the warmest mean and maximum temperatures (18.59, 25.01, and 31.40°C for minimum, mean, and maximum temperature), and lower precipitation (119.94 mm). Cluster 3 stations were at low and mid elevations. Minimum, mean, and maximum temperatures at these locations were 19.34, 24.96, and 30.55°C, while precipitation was the highest of all clusters (133.09 mm). Cluster 4 stations were located at mid elevations, had cooler temperatures (17.01, 23.13, and 29.48°C for minimum, mean, and maximum temperature), and the lowest precipitation total (107.71 mm). Lastly, Cluster 5 stations were generally located at the highest elevations. While the precipitation total was not the highest (127.55 mm), the cluster was the coolest (15.57, 21.13, and 26.65°C for minimum, mean, and maximum temperature).

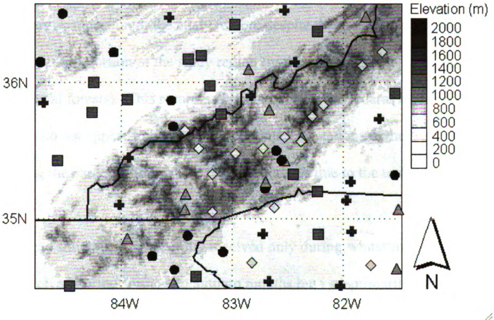

Figure 5.21. July during 1995-2004 with 5 clusters for all variables (minimum temperature, maximum temperature, mean temperature, total precipitation), where Cluster 1 (dot), Cluster 2 (plus sign), Cluster 3 (square), Cluster 4 (triangle), and Cluster 5 (diamond) represent station locations. Elevation in meters is shaded in gray.

5.6. Discussion

Results in this chapter furnish information to help answer Questions 1 and 2. The clusters for all temperature variables and months were closely associated with elevation, and to a lesser extent, latitude. This finding is further supported by the results I presented in Figure 4.6 of Chapter 4 and by previous studies (Shanks, 1954; Mark, 1958; Hicks, 1979; Bolstad et al., 1998). Stations in the warmest regime were located within the Piedmont province of SC at lower elevations. At times the regime also included low-elevation stations within the Ridge and Valley province of TN. A second regime closely followed the base of the Blue Ridge on both the southeast and northwest sides. A third regime was often located at mid elevations, a fourth was located at mid-to-high elevations, and the fifth (and coldest) regime was located at the highest elevations along the Blue Ridge. Often the highest elevation regime was comprised of one or more stations in the northeast portion of the study region, despite the presence of similar high elevations in the central portion of the study region (in the area of GSMNP and its neighboring national forests). This result may occur because the federal lands and the surrounding area do not appear to be as well represented by stations in the high elevations (especially during the early portions of the record), perhaps due to the underdevelopment of the region.

Widespread snowfall was generally received only during winter months. Some snowfall was received during spring and autumn months but was primarily limited to the highest elevations, and cluster results for those months generally reflected that (see Appendix B). Regimes for snowfall were less distinct than those for temperature. However, snowfall totals were usually greatest at the high elevations and lowest in southern and low-elevation locations.

Although my results in Chapter 4 and the results of others (e.g., Whittaker, 1952; Smallshaw, 1953; Shanks, 1954; Mark, 1958; Bogucki, 1972; Hicks, 1979; Gaffin and Hotz, 2000) generally showed that total precipitation varies directly with elevation, that relationship was not always obvious from the spatial patterns displayed by the cluster maps (Figures 5.7-5.12) and may be the result of windward and leeward topographic properties at the higher elevations. Three consistent regimes for precipitation did appear, however, and tended to be more visible during January than July. The first was a maximum located near the union of the NC, SC, and GA borders. Elevation in that area increases sharply from south to north. Any southerly airflow over that region could result in abrupt orographic lifting and precipitation. Gaffin and Hotz (2000) found a similar precipitation maximum in that region that persisted throughout the year (Figures 5.22-5.23). I also found a second maximum located at high-elevation, northeastern stations or along the northwestern side of the Blue Ridge. A minimum generally occurred along the I-40 corridor and at stations to the north of that corridor. Secondary minimum values also occurred at low-lying areas both in the Piedmont province and areas in the northwestern part of the region. These additional maxima and minima were also broadly confirmed by Gaffin and Hotz (2000).

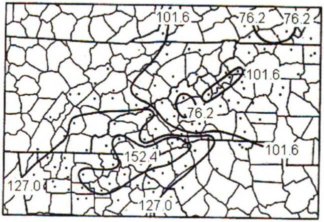

Figure 5.22. Precipitation climatology for January during 1961-1990. Values are reported in mm (adapted from Gaffin and Hotz, 2000; p. 6).

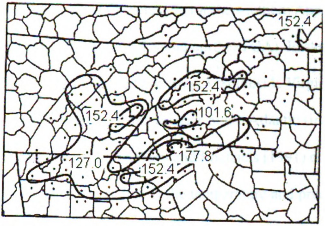

Figure 5.23. Precipitation climatology for July during 1961-1990. Values are reported in mm (adapted from Gaffin and Hotz, 2000; p. 7).

Actual precipitation values calculated in my study were comparable to those reported by Gaffin and Hotz (2000) as well. For January, they found a minimum of 3 inches (76.2 mm) and a maximum of 6 inches (152.4 mm). July values ranged between 4 and 8 inches (101.6 to 177.8 mm). My 1965-1974 decade overlapped with their study and used the same COOP dataset, and my January (77.4 to 153.8 mm) and July (96.0 to 166.9 mm) values were quite similar. My values during 1935-1944 for January (90.5 to 183.5 mm) and July (129.5 to 249.4 mm), as well as January for 1995-2004 (107.6 to 196.0 mm), were somewhat greater than those reported by Gaffin and Hotz (2000). However, my July values during 1995-2004 were similar (94.2 to 167.3 mm).

Although cluster analysis has been used in previous climate studies that included the southern Appalachian region (e.g., Stooksbury and Michaels, 1991; Winkler, 1992; Fovell and Fovell, 1993; Gong and Richman, 1995; Fovell, 1997), all of those studies considered much larger areas. As a result, the southern Appalachian region was usually clustered into four or fewer clusters. The cluster work of Stooksbury and Michaels (1991) was most relevant in that they focused on the southeast U.S. Using temperature and precipitation, the authors found four clusters for the southern Appalachians: Western Appalachian & Valleys (included eastern TN and northern GA), Eastern Appalachian (included western edge of NC along the Blue Ridge), Southside Virginia & Western North Carolina (included western NC), and Interior South Atlantic (included portions of NC, SC, and GA). Unfortunately, Stooksbury and Michaels (1991) did not discuss the differences between the clusters in regards to the temperature and precipitation characteristics. In contrast, my maps presented in this chapter illustrated cluster results for the region, backed by the temperature, precipitation, and snowfall values to allow further comparison of the regimes.

In summary, my results presented in Chapters 4 and 5 suggest that temperature tends to have an inverse relationship with elevation, whereas precipitation and snowfall typically have a direct relationship with elevation, lending to the idea that the region's topography greatly affects the variety of microclimates in the region. The warmest region was the southeastern, low-lying Piedmont and the coolest temperatures were found at the high peaks, particularly in the northeastern portion of the region. Highest precipitation totals were near the union of NC, SC, and GA where a steep topographic gradient exists. Low precipitation values were present in an area of lower elevations that I have referred to as the I-40 corridor. Snowfall totals were greatest in the highest-elevation areas. In this chapter, I provided spatial representations of temperature and snowfall that have not been provided in previous studies. My spatial representation of precipitation was similar to that of Gaffin and Hotz (2000), although I was able to include data for years beyond those included in their study. Their spatial study considered 1961-1990, whereas mine covered the years 1930-2004.

CHAPTER 6

RESULTS AND DISCUSSION OF THE SYNOPTIC CLIMATOLOGY

6.1. Overview

Over the 1979-2006 period, 1437 precipitation events were determined. The frequency of events revealed an increase over time, although the correlation was not statistically significant (Figure 6.1). Eleven clusters were created from the objective classification of the precipitation events (Section 6.2). Although they were based on variables at the 850 hPa level (height, temperature, and dewpoint), 700 hPa level (height, temperature, and dewpoint), and 300 hPa level (height), only the 850 hPa variables are shown here (maps of 700 and 300 hPa variables are included in Appendix D). Eleven clusters also emerged from the subjective (visual) classification (Section 6.3). Subjectively derived clusters were based on variables at the 850 hPa level (height, temperature, dewpoint, and wind), 700 hPa level (height, temperature, dewpoint, and wind), and 300 hPa level (height and wind). The 850 hPa variables are shown in this chapter (maps of 700 and 300 hPa variables are included in Appendix D). A short discussion regarding lifting associated with the subjective clusters is also included (Section 6.4). A hybrid clustering approach will be discussed within Section 6.5 and the results from that method are included in Appendix E. The results of this chapter will help answer Questions 3 and 4 presented in Section 2.5.

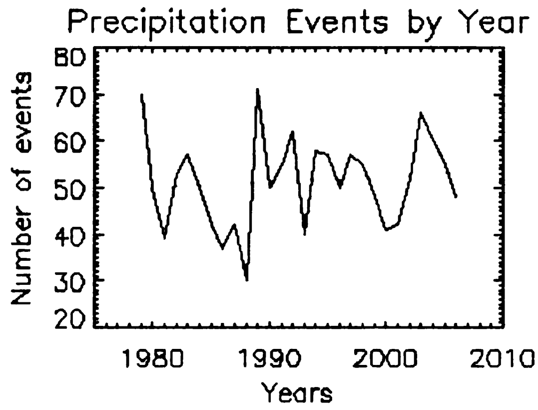

Figure 6.1. Precipitation events by year (1979-2006). Precipitation events were defined as 25 percent or more of available stations reporting 0.5 in (12.7 mm) or more of precipitation in a day.

6.2. Objective Clustering Results

6.2.1. Clusters 2-5 and 7-9

The 11 resulting objective clusters exhibit a large amount of similarity. In fact, the 11 clusters can be visually categorized further into two primary groups. The first group consists of most of the cases and includes Clusters 2-5 and 7-9 (Figures 6.2-6.8). Cluster 2 (345 total cases) and Cluster 3 (319 total cases) depict a warm-season situation with weak temperature and height gradients, warm/moist conditions (10-15°C temperatures and 5-10°C dewpoints), and southwesterly airflow (Figures 6.2-6.3). Cluster 4 (228 total cases), Cluster 5 (208 total cases), and Cluster 7 (102 total cases) occurred most frequently during transition seasons and had stronger gradients, cooler temperatures (5-10°C temperatures), and sometimes a trough present over the study region (Figures 6.4-6.6). Cluster 8 (100 total cases) and Cluster 9 (99 total cases) were most common during the cool season (Figures 6.7-6.8). Tighter gradients, cooler temperatures (0-5°C temperatures), and a trough over the study region were common with cases within those clusters.

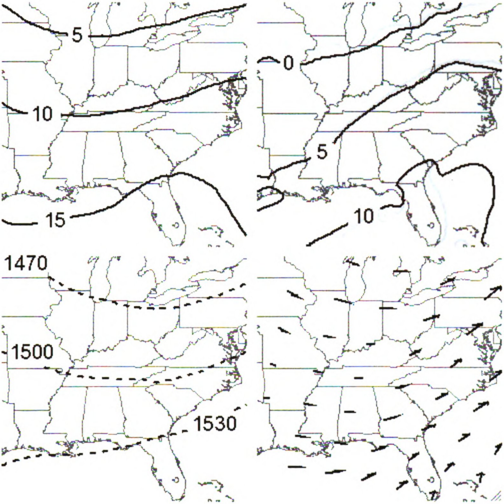

Figure 6.2. Cluster 2. Temperature contoured every 5°C (top left), dewpoint contoured every 5°C (top right), height contoured every 30 m (bottom left), and wind vectors (bottom right) at the 850 hPa level.

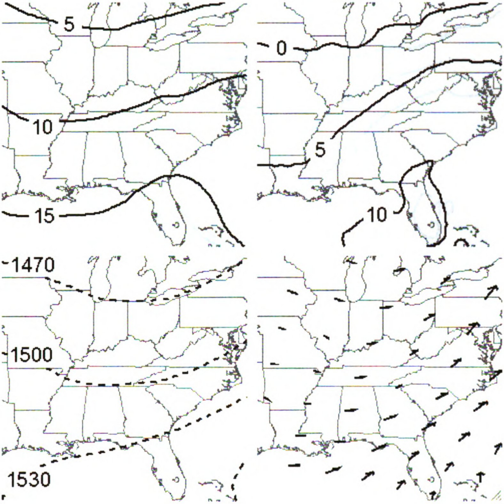

Figure 6.3. Cluster 3. Temperature contoured every 5°C (top left), dewpoint contoured every 5°C (top right), height contoured every 30 m (bottom left), and wind vectors (bottom right) at the 850 hPa level.

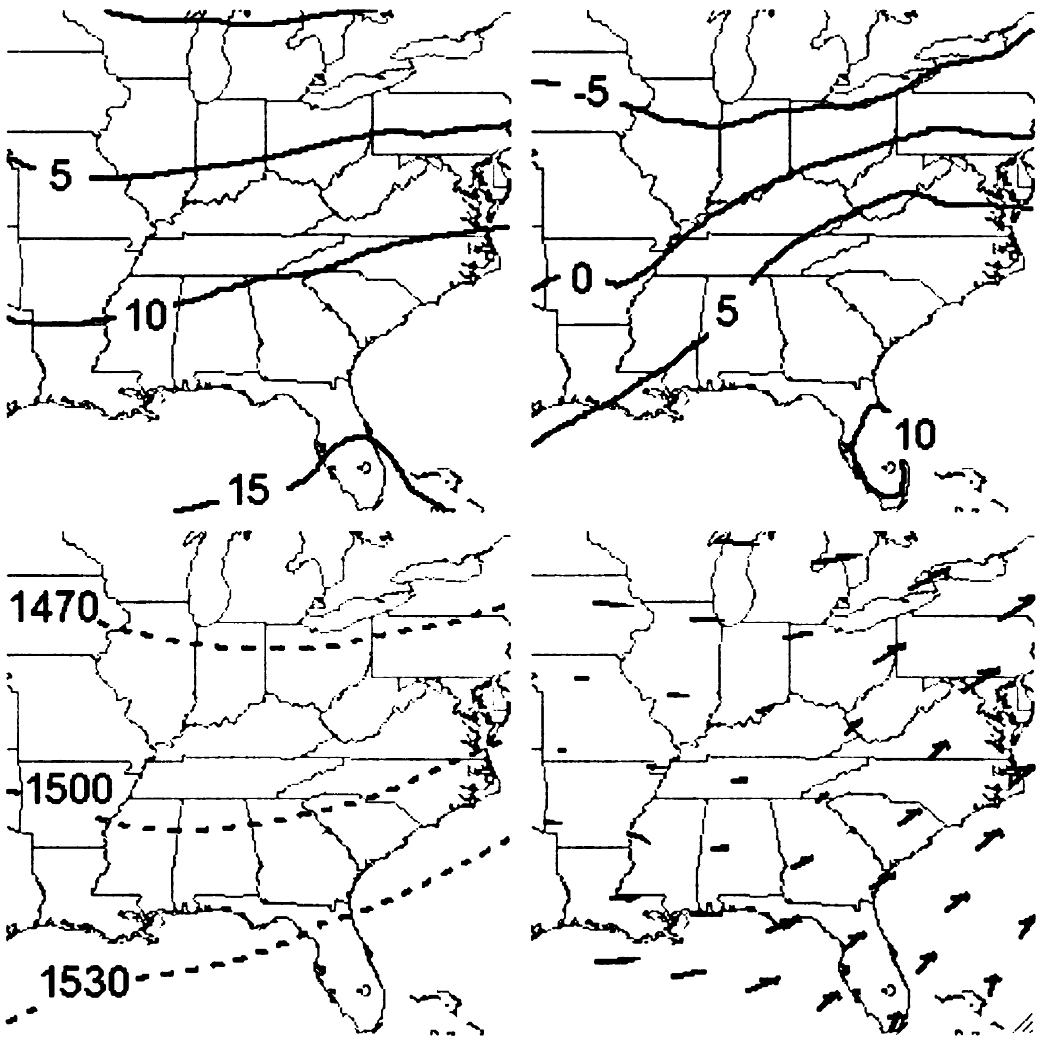

Figure 6.4. Cluster 4. Temperature contoured every 5°C (top left), dewpoint contoured every 5°C (top right), height contoured every 30 m (bottom left), and wind vectors (bottom right) at the 850 hPa level.

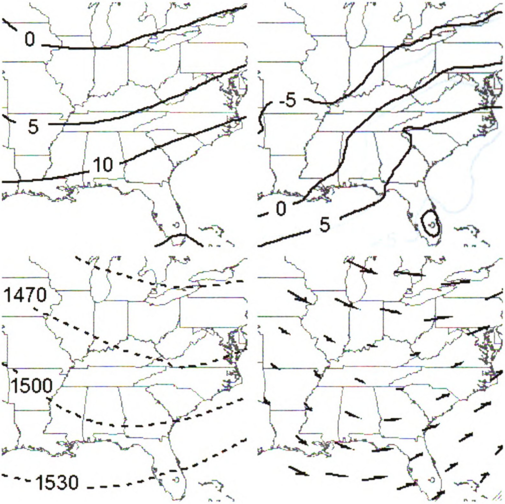

Figure 6.5. Cluster 5. Temperature contoured every 5°C (top left), dewpoint contoured every 5°C (top right), height contoured every 30 m (bottom left), and wind vectors (bottom right) at the 850 hPa level.

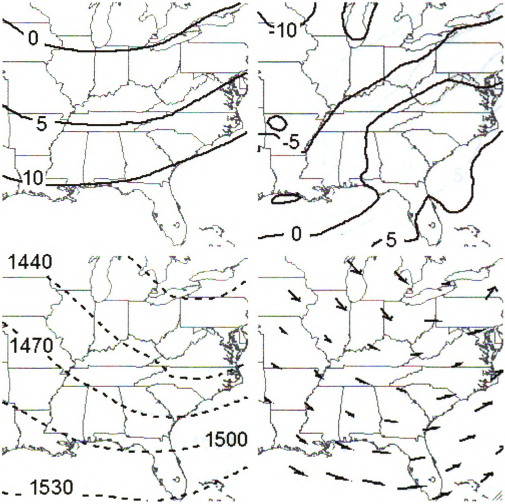

Figure 6.6. Cluster 7. Temperature contoured every 5°C (top left), dewpoint contoured every 5°C (top right), height contoured every 30 m (bottom left), and wind vectors (bottom right) at the 850 hPa level.

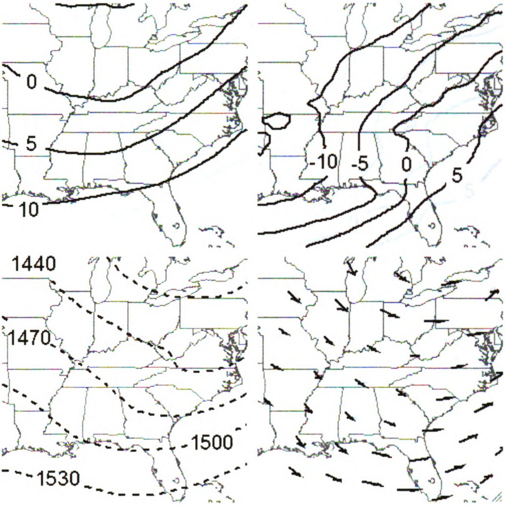

Figure 6.7. Cluster 8. Temperature contoured every 5°C (top left), dewpoint contoured every 5°C (top right), height contoured every 30 m (bottom left), and wind vectors (bottom right) at the 850 hPa level.

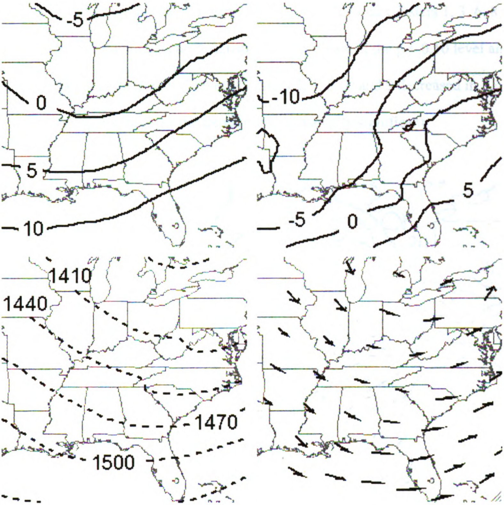

Figure 6.8. Cluster 9. Temperature contoured every 5°C (top left), dewpoint contoured every 5°C (top right), height contoured every 30 m (bottom left), and wind vectors (bottom right) at the 850 hPa level.

6.2.2. Clusters 1, 6, 10, and 11

The remaining clusters consisted of a small number of cases (Figure 6.9-6.12). Cluster 1 (2 total cases), Cluster 6 (3 total cases), Cluster 10 (27 total cases), and Cluster 11 (4 total cases) were similar. In each of the objective clusters, an east-west temperature gradient and strong winds aloft (> 30 m/s) were often present. Most of these cases occurred during winter. Clusters 1, 6, and 10 had particularly low dewpoint values (< -15°C), but these cases occurred infrequently. Of all 11 objective clusters, the frequency of the cases within each objective cluster revealed that Clusters 1, 3, 6, 8, 10, 11 increased over time with Cluster 3 statistically significant at the $p \leq 0.10$ level and Cluster 6 significant at the $p \leq 0.05$ level. Clusters 2, 4, 5, 7, and 9 decreased in frequency over time, but none of the trends were statistically significant.

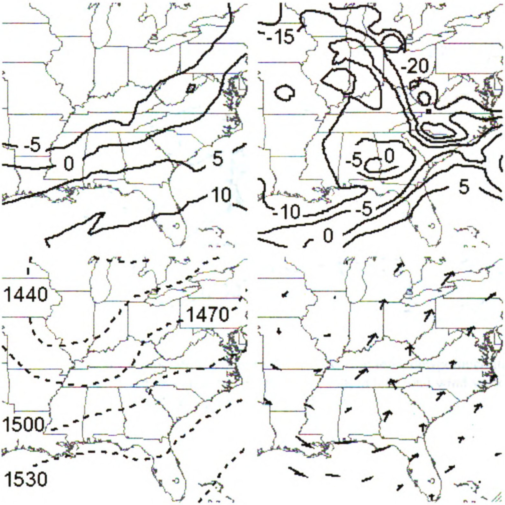

Figure 6.9. Cluster 1. Temperature contoured every 5°C (top left), dewpoint contoured every 5°C (top right), height contoured every 30 m (bottom left), and wind vectors (bottom right) at the 850 hPa level.

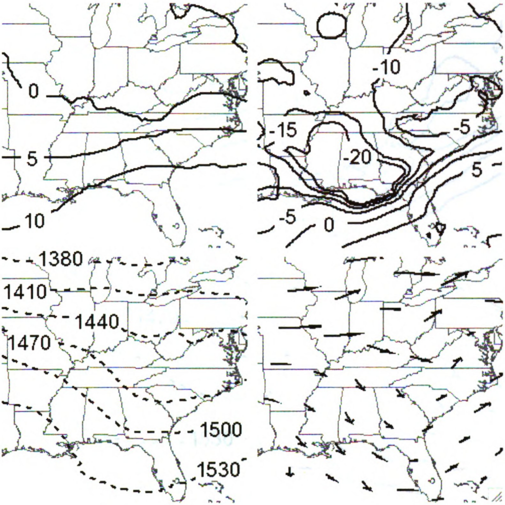

Figure 6.10. Cluster 6. Temperature contoured every 5°C (top left), dewpoint contoured every 5°C (top right), height contoured every 30 m (bottom left), and wind vectors (bottom right) at the 850 hPa level.

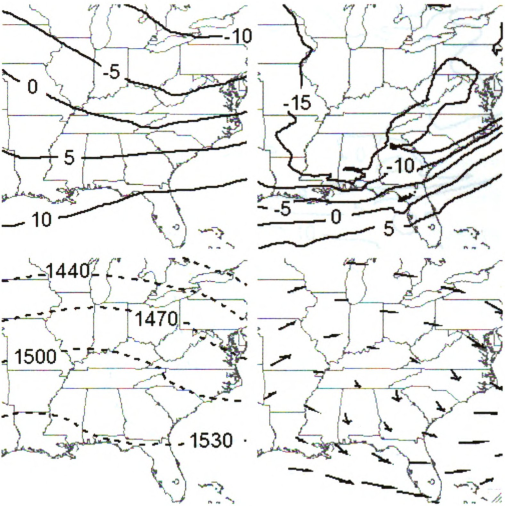

Figure 6.11. Cluster 10. Temperature contoured every 5°C (top left), dewpoint contoured every 5°C (top right), height contoured every 30 m (bottom left), and wind vectors (bottom right) at the 850 hPa level.

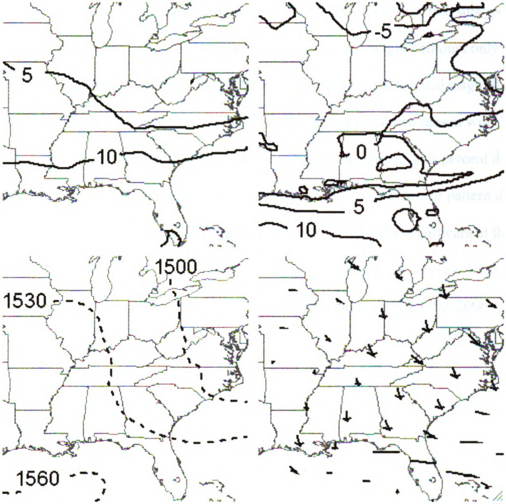

Figure 6.12. Cluster 11. Temperature contoured every 5°C (top left), dewpoint contoured every 5°C (top right), height contoured every 30 m (bottom left), and wind vectors (bottom right) at the 850 hPa level.

6.3. Subjective Clustering Results

6.3.1. Closed Low (CL)

Compared to the objective approach, clusters resulting from the subjective approach tended to be more distinct from one another. "Closed Low" (CL) was a small cluster with 61 total cases (Figure 6.13). For all cases, a closed low was located directly over the southern Appalachian region. Generally, weak cyclonic winds were present at all levels and no discernible fronts were present. Temperatures over the region at 850 hPa were usually 10-15°C and dewpoints were 5-10°C. The cluster had two subtypes. The first was a meso-low or low of tropical origin with closed height contours only at the 850 hPa level. The second was a closed (i.e., cut-off) low of extra-tropical origin that reached up to 300 hPa. CL occurred most frequently during the warm season with 13.1 percent of cases occurring during winter, 24.6 percent during spring, 39.3 percent during summer, and 23.0 percent during autumn. Although CL was an infrequent pattern during precipitation events, its occurrence increased over time (statistically significant at the $p \leq 0.10$ level). During 1979-1992 it accounted for 3.1 percent of the total cases, 4.5 percent of the cases during 1986-1999, and 5.3 percent of the the cases during 1993-2006.

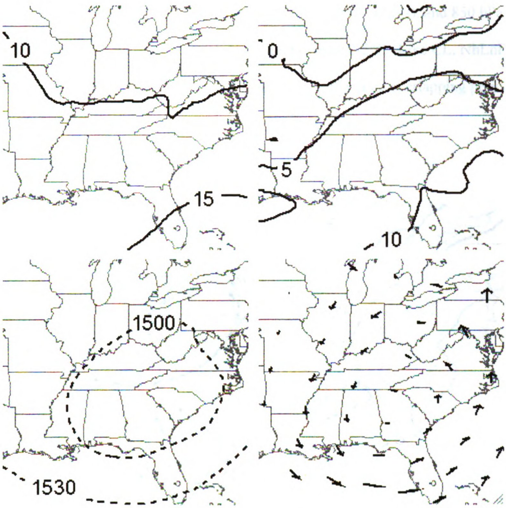

Figure 6.13. Closed low (CL). Temperature contoured every 5°C (top left), dewpoint contoured every 5°C (top right), height contoured every 30 m (bottom left), and wind vectors (bottom right) at the 850 hPa level.

6.3.2. Northerly, Behind Low, No Fronts (NbLnF)

"Northerly, Behind Low, No Fronts" (NbLnF) had 127 totals cases and was a common springtime precipitation pattern, with 21.3 percent of occurrences in winter, 37.8 percent occurring in spring, 21.3 occurring in summer, and 19.7 occurring in autumn (Figure 6.14). Precipitation occurring with NbLnF was associated with a low-pressure system to the northeast of the study region. Cyclonic flow circled around from behind the low bringing northerly or northwesterly flow into the region. No fronts over the study area were obvious, winds were generally weak at 300 hPa (10-20 m/s), and 850 hPa temperatures were generally 5-10°C, while dewpoints were 0-5°C. Like CL, NbLnF also increased in frequency (7.8, 8.1, and 9.9 percent) during the three overlapping periods and the trend was statistically significant at the $p \leq 0.10$ level.

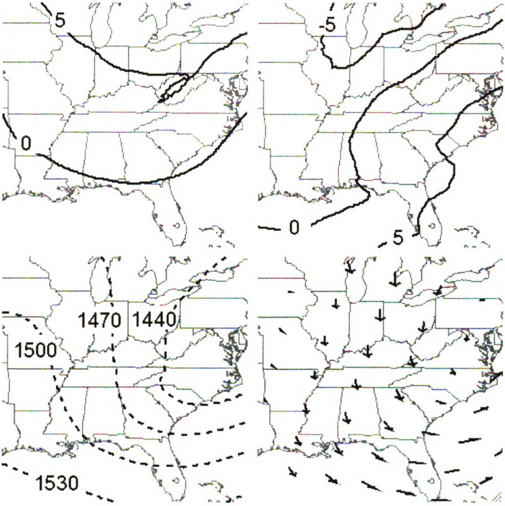

Figure 6.14. Northerly, behind low, no fronts (NbLnF). Temperature contoured every 5°C (top left), dewpoint contoured every 5°C (top right), height contoured every 30 m (bottom left), and wind vectors (bottom right) at the 850 hPa level.

6.3.3. Southerly, Ahead of Low, No Fronts (SaLnF)

A synoptic pattern with 211 total cases was "Southerly, Ahead of Low, No Fronts" (SaLnF; Figure 6.15). The pattern was common during all seasons (26.1 percent during winter, 29.4 during spring, 21.8 during summer, and 22.7 during autumn) and during all three overlapping time periods (14.8, 14.9, and 14.5 percent of total cases) with no statistically significant trend in frequency. The cluster was associated with a low-pressure system located to the west/northwest of the study region. Airflow was generally cyclonic and southerly or southwesterly at all levels. No fronts were present over the study region; however, the region was sometimes within the warm sector of an approaching low-pressure system. Southerly flow was responsible for relatively warm (10-15°C) temperatures and (5-10°C) dewpoints over the region at 850 hPa. Upper-level winds at 300 hPa were still generally weak (~30 m/s).

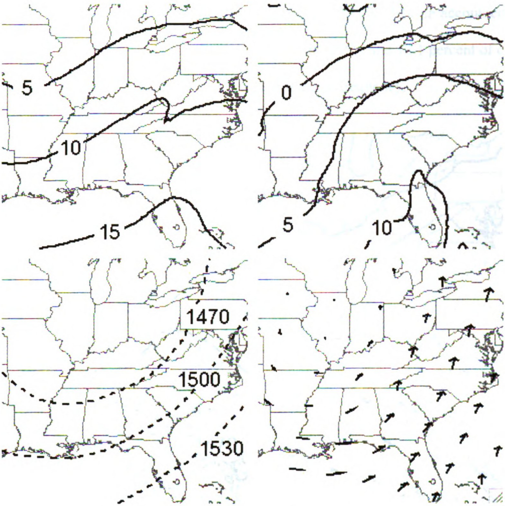

Figure 6.15. Southerly, ahead of low, no fronts (SaLnF). Temperature contoured every 5°C (top left), dewpoint contoured every 5°C (top right), height contoured every 30 m (bottom left), and wind vectors (bottom right) at the 850 hPa level.

6.3.4. Northerly, No Low, No Fronts (NnLnF)

"Northerly, No Low, No Fronts" (NnLnF) occurred 159 times (Figure 6.16). Northwesterly flow at all levels was the most common feature. No low-pressure center or fronts were present, although a trough axis at the 850 hPa level was often present near the study area. A ridge was usually present to the west of the study region. Winds were weak, temperatures were roughly 10°C, and dewpoints were around 5°C. NnLnF was most common in summer (34.0 percent), but did occur during other seasons (15.7 for winter, 28.3 for spring, and 22.0 for autumn). During 1979-1992, NbLnF accounted for 10.0 percent of cases, 12.4 percent of cases during 1986-1999, and 12.1 percent of cases during 1993-2006 with no statistically significant trend in frequency.

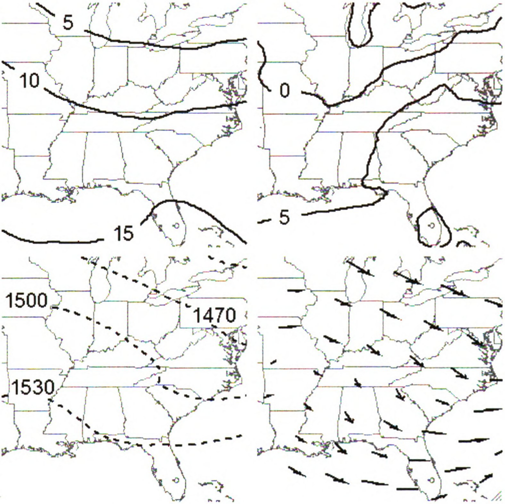

Figure 6.16. Northerly, no low, no fronts (NnLnF). Temperature contoured every 5°C (top left), dewpoint contoured every 5°C (top right), height contoured every 30 m (bottom left), and wind vectors (bottom right) at the 850 hPa level.

6.3.5. Southerly, No Low, No Fronts (SnLnF)

Like NnLnF, the "Southerly, No Low, No Fronts" (SnLnF) pattern was most common during summer (Figure 6.17). There were 186 total cases with 37.1 percent of those during summer. Winter had 16.7 percent, spring had 21.5 percent, and autumn had 24.7 percent. Winds were generally weak at all levels and were southerly or southwesterly. No low-pressure center or fronts were present. Temperatures at 850 hPa were warm (10-15°C). Dewpoints were also high (~10°C) as a tongue of high dewpoint values seemed to be associated with the southerly flow. The frequency of SnLnF did decrease over the study period (14.5 percent of cases during 1979-1992, 13.3 percent during 1986-1999, and 11.4 percent during 1993-2006) although the decrease was not statistically significant.

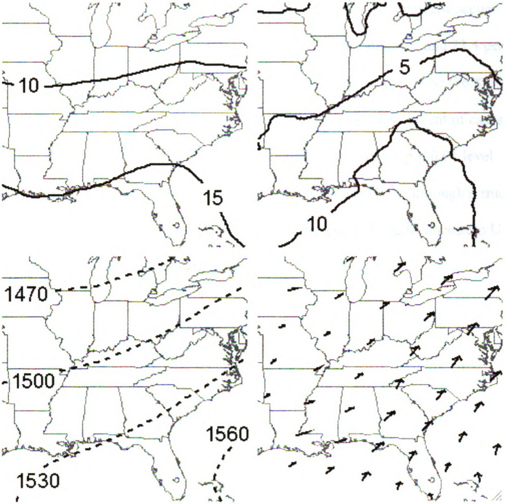

Figure 6.17. Southerly, no low, no fronts (SnLnF). Temperature contoured every 5°C (top left), dewpoint contoured every 5°C (top right), height contoured every 30 m (bottom left), and wind vectors (bottom right) at the 850 hPa level.

6.3.6. Bermuda High (BH)

"Bermuda High" (BH) was similar to SnLnF with the exception that anti-cyclonic flow associated with the Bermuda High was more apparent in the height fields and wind vectors (Figure 6.18). Often easterly flow was present to the south of the study region with anti-cyclonic turning around the Bermuda High, leading to southwesterly flow over the southern Appalachians. Winds were usually weak, 850 hPa temperatures were 10-

15°C and dewpoints were greater than 10°C. Of the 184 cases, 12.0 percent occurred during winter, 24.5 percent during spring, 40.2 percent during summer, and 23.4 percent during autumn. The frequency of the BH pattern has diminished over time (16.8 percent of cases during 1979-1992, 11.8 percent during 1986-1999, and 8.9 percent of cases during 1993-2006) and the trend was statistically significant and the $p \leq 0.01$ level. Most BH cases were associated with a strong summertime Bermuda High, although a small minority of cases were associated with a meso-high present over the southeastern U.S. That subtype was most common during autumn months.

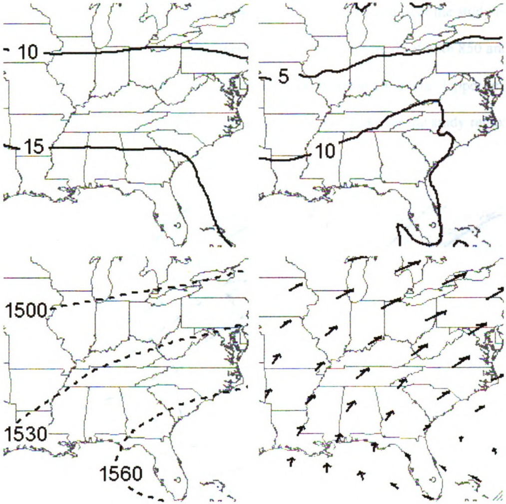

Figure 6.18. Bermuda High (BH). Temperature contoured every 5°C (top left), dewpoint contoured every 5°C (top right), height contoured every 30 m (bottom left), and wind vectors (bottom right) at the 850 hPa level.

6.3.7. North-South Oriented Front (nsF)

The most common synoptic pattern associated with precipitation in the region was "North-South Oriented Front" (nsF), where I found a total of 312 cases (Figure 6.19). Occurrence was most common during winter months (44.2 percent). Spring and autumn both had 27.6 percent and summer only had 0.6 percent of the cases. The overall occurrence of nsF increased over the three overlapping time periods (19.4, 19.7, and 24.0 percent of cases), but the trend was not statistically significant. The nsF pattern was primarily characterized by a north-south oriented cold front located over the study region. The front was usually present in the temperature and dewpoint fields at both 850 and 700 hPa. A trough was also present in the height and wind fields at all levels. Upper-level winds were strong (40 m/s or greater) with a jet streak centered over the study region.

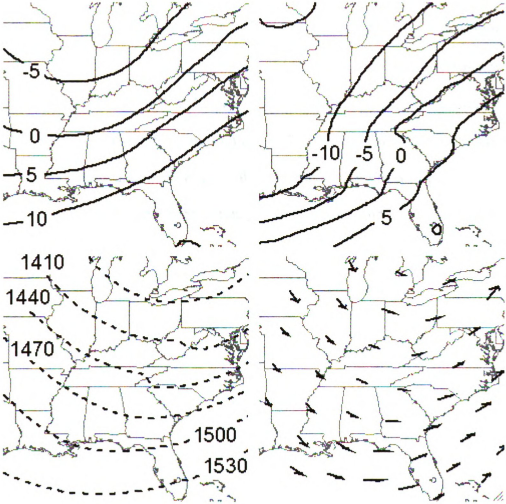

Figure 6.19. North-south oriented front (nsF). Temperature contoured every 5°C (top left), dewpoint contoured every 5°C (top right), height contoured every 30 m (bottom left), and wind vectors (bottom right) at the 850 hPa level.

6.3.8. Northerly, East-West Oriented Front (NewF)

The "Northerly, East-West Oriented Front" (NewF) pattern was similar to the nsF pattern except that the cold front was oriented in a more east-west manner (Figure 6.20). Again, the front was present in the temperature and dewpoint fields for both 850 and 700 hPa. A trough was present over the region at all levels, but the overall flow was more northerly or northwesterly. Upper-level winds at 300 hPa were strong (40-50 m/s) and the study region was located in a region of low-level convergence under the right rear portion of an upper-level jet streak (Harman, 1991; Carlson, 1998). NewF was less common than nsF with only 88 total cases. Of those cases, 51.1 percent occurred during winter, 28.4 during spring, 4.5 during summer, and 15.9 during autumn. Although it was not statistically significant, the frequency of NewF did increase by a small amount over time. The occurrence during the three time periods (6.1, 6.3, and 6.2) did not capture the small increase.

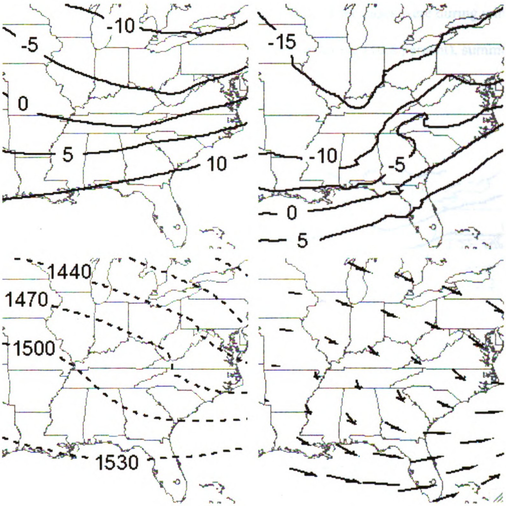

Figure 6.20. Northerly, east-west oriented front (NewF). Temperature contoured every 5°C (top left), dewpoint contoured every 5°C (top right), height contoured every 30 m (bottom left), and wind vectors (bottom right) at the 850 hPa level.

6.3.9. Southerly, East-West Oriented Front (SewF)

"Southerly, East-West Oriented Front" (SewF) was similar to nsF and NewF (Figure 6.21). An east-west cold front was present, but airflow was primarily southerly or southwesterly over the region. Upper-level winds were strong (40-50 m/s) and the region was again located under the right rear of a jet streak. SewF was an uncommon pattern and occurred just 37 times. During 1979-1992, it occurred during 3.0 percent of cases, 3.1 percent during 1986-1999, and 2.2 percent during 1993-2006 and an overall decreasing trend was not statistically significant. Most of the cases were during winter (70.3 percent), although a few occurrences occurred in spring (10.8 percent), summer (2.7 percent), and autumn (16.2 percent) as well.

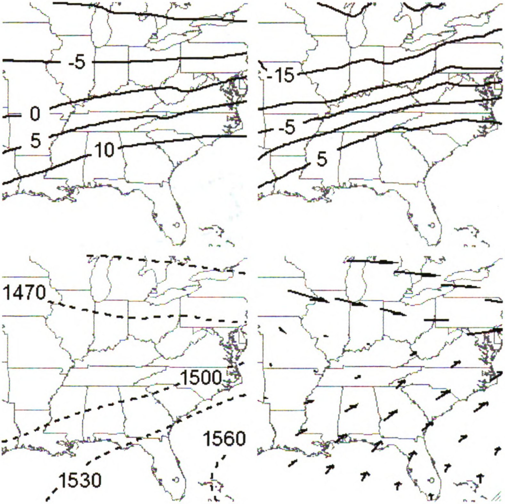

Figure 6.21. Southerly, east-west oriented front (SewF). Temperature contoured every 5°C (top left), dewpoint contoured every 5°C (top right), height contoured every 30 m (bottom left), and wind vectors (bottom right) at the 850 hPa level.

6.3.10. Zonal Flow (Z)

The "Zonal" (Z) pattern was generally one of west-to-east flow at all levels

(Figure 6.22). It was an infrequent pattern with only 51 total cases. Of those, 43.1 percent occurred in winter, 25.5 percent in spring, 17.6 percent in summer, and 13.7 percent in autumn. The frequency trend of the Z pattern did not change much over time and was statistically insignificant (3.2 percent of cases during 1979-1992, 4.2 of cases during 1986-1999, and 3.8 of cases during 1993-2006). Temperatures at 850 hPa were usually 5-10°C and dewpoints were 0-5°C. Upper-level winds at 300 hPa were relatively weak (~30 m/s).

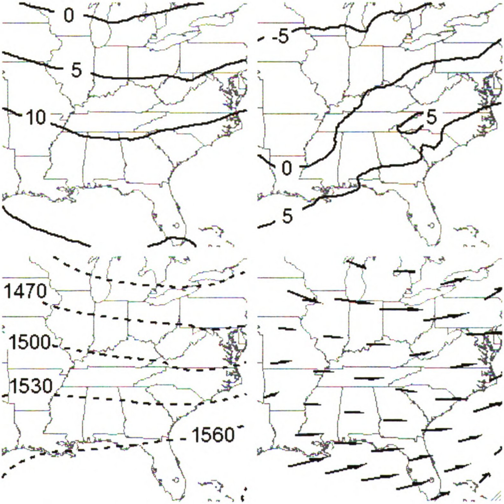

Figure 6.22. Zonal flow (Z). Temperature contoured every 5°C (top left), dewpoint contoured every 5°C (top right), height contoured every 30 m (bottom left), and wind vectors (bottom right) at the 850 hPa level.

6.3.11. Weak flow (W)

Finally, the "Weak" (W) cluster was a collection of 21 remaining cases that did not fully fit any of the previous 10 clusters (Figure 6.23). Cases within the cluster generally had weak airflow circulation over the study area, with no distinct meso-high or meso-low directly over the region. A few of the cases had easterly flow with a low-pressure center to the south and a high-pressure center to the north. Most of the cases occurred during summer (57.1 percent) with warm temperatures and dewpoints. Winter had 4.8 percent of the cases, spring had 9.5 percent, and autumn had 28.6 percent. The frequency of these cases increased slightly over time (1.3 percent of cases during 1979-1992, 1.5 percent of cases during 1986-1999, and 1.6 percent of cases during 1993-2006) although the trend was not statistically significant.

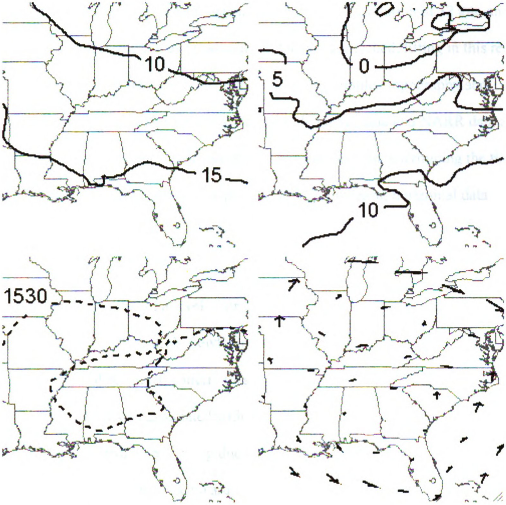

Figure 6.23. Weak flow (W). Temperature contoured every 5°C (top left), dewpoint contoured every 5°C (top right), height contoured every 30 m (bottom left), and wind vectors (bottom right) at the 850 hPa level.

6.4. Speculations Regarding Lifting Mechanisms

Although lifting mechanisms associated with the synoptic patterns were not explicitly considered by the clustering approaches used in this study, the topic is still important to determine the origins of precipitation mentioned in Question 3. The dataset resolutions (once daily COOP observations and NARR data only at 2100 UTC) used here were not necessarily best suited for distinguishing the time or region of lifting since the process can be of short duration or favor certain times of day not captured by the observations. In addition, the NARR data have a horizontal resolution of 32 km, and although that is high resolution as far as climate data are concerned, lifting in this region frequently occurs on a more local scale as a result of the complex topography and warm/moist conditions. Some COOP stations provide hourly data and NARR data are available every 3 hours, which could assist a subsequent study in determining the timing of lifting associated with the above synoptic patterns, but for now, horizontal data resolution remains an obstacle.

Despite the data resolution shortcomings, I was able to create maps of vertical velocity (in Pa/s) at the 700 hPa level. For the subjective clusters, some amount of lifting occurred with the BH, CL, SaLnF, SewF, SnLnF, and W patterns (Figures 6.24-6.29). With the exception of the SewF pattern, these patterns were most often summertime events. Southerly flow was associated with the BH, SaLnF, SewF, and SnLnF types and may have resulted in orographic lifting due to the abrupt increase in elevation along the southern side of the Blue Ridge. Upward motion for the CL pattern makes sense given that a closed low was located over the study area with that pattern. Frontal lifting could be responsible for the upward motion associated with the SewF pattern. Additional lifting may have resulted from the presence of a 300 hPa jet streak located over the study area, which would have promoted lower-tropospheric lifting (Harman, 1991; Carlson, 1998). No lifting was found within the study region for the other patterns, although it still could have occurred at a different time of day or at a scale that was not captured by the 32 km horizontal data. In particular, frontal lifting may have been common with the nsF and NewF patterns (vertical velocity maps not shown). Likewise, some lifting may have been present with objective Clusters 1, 3, 4, 6, 7, 9, and 11 (vertical velocity maps not shown), as some of those patterns were frontal in nature.

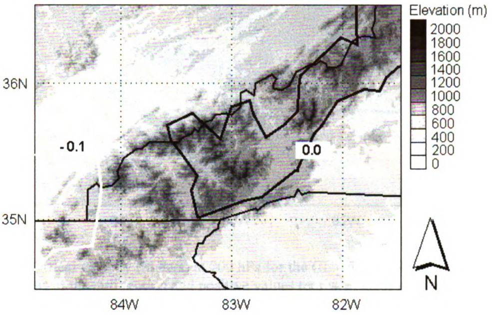

Figure 6.24. Vertical velocity (in Pa/s) at 700 hPa for the BH pattern. Negative values represent areas of upward motion and positive values represent areas of downward motion.

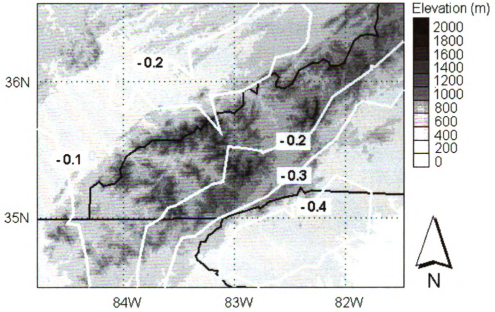

Figure 6.25. Vertical velocity (in Pa/s) at 700 hPa for the CL pattern. Negative values represent areas of upward motion and positive values represent areas of downward motion.

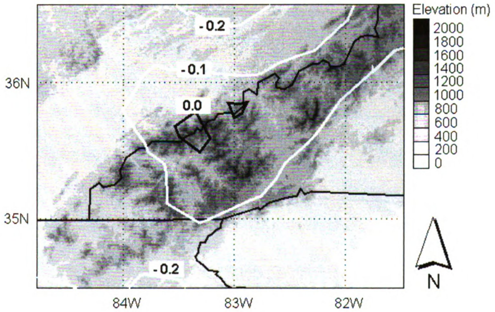

Figure 6.26. Vertical velocity (in Pa/s) at 700 hPa for the SaLnF pattern. Negative values represent areas of upward motion and positive values represent areas of downward motion.

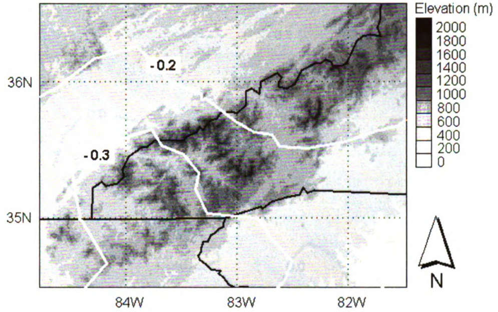

Figure 6.27. Vertical velocity (in Pa/s) at 700 hPa for the SewF pattern. Negative values represent areas of upward motion and positive values represent areas of downward motion.

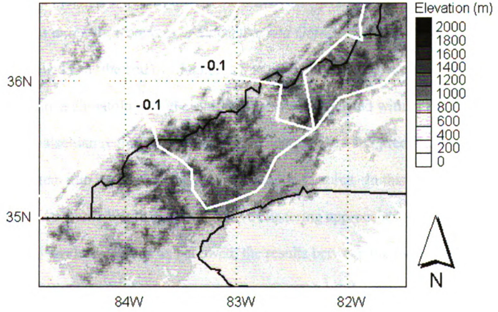

Figure 6.28. Vertical velocity (in Pa/s) at 700 hPa for the SnLnF pattern. Negative values represent areas of upward motion and positive values represent areas of downward motion.

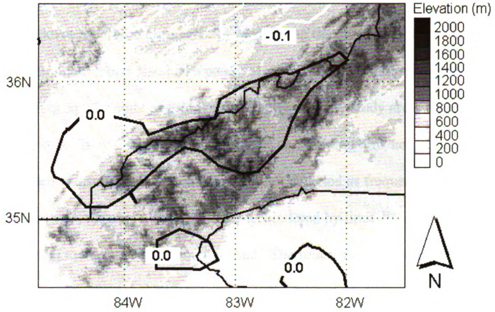

Figure 6.29. Vertical velocity (in Pa/s) at 700 hPa for the W pattern. Negative values represent areas of upward motion and positive values represent areas of downward motion.

6.5. Discussion

6.5.1. Advantages and Disadvantages of Subjective and Objective Clustering

As I outlined near the end of Chapter 2, one of the primary objectives of this study was to create a climatology of the synoptic patterns associated with precipitation in the southern Appalachian region. My intent was to analyze the 1437 precipitation events and categorize them into groups sharing similar synoptic features. In this chapter, I provided the results from objective and subjective clustering approaches. Each approach has strengths and weaknesses, and as I showed, the results between the two approaches differed substantially.

The objective clustering process using IDL and CLUTO provided a hands-free and automated way of clustering the synoptic patterns that was far faster than a subjective approach could ever hope to achieve. The process considered each grid point, variable, and atmospheric level equally to eliminate any bias during the clustering. Unfortunately, this method of eliminating bias also had a potential drawback of giving grid points near the edge of the map equal weight as grid points directly over my study area. In addition, the objective approach may not have been capable of determining how neighboring grid points were related and smaller-scale features were not detected as frequently. As discussed in Chapter 3, the objective approach was hindered by limitations in the software and virtual memory of the computer used. The process of experimenting with smaller grid arrays and fewer variables was perhaps the most time-consuming step of the entire project. Once I determined the appropriate grid sizes and variables, the clustering process moved quickly. The coarse resolution of the data grid (8 x 9) may explain why some smaller features and gradients were not fully captured by the objective approach resulting in many similar cluster patterns. In addition, statistics generated by the CLUTO software provided inconclusive guidance regarding the appropriate number of clusters, so I chose to use 11, which was the same number determined by the subjective approach. In the end, the 11 objective clusters were not nearly as distinct as the subjective clusters. In fact, the objective clusters broadly fit into two main categories, as stated earlier. If, however, the coarse grid used and the inconclusive results regarding the appropriate number of clusters did not hinder the outcome of the cluster patterns, the results from the objective analysis suggest that many distinct synoptic patterns may not affect the precipitation of the region. Such a result would suggest that local features like topography, heat, and moisture have a larger impact on the region's precipitation climatology.

In contrast to the objective approach, the subjective approach allowed me to visually examine each individual case. My general knowledge of synoptic climatology assisted me as I searched for synoptic features such as fronts, high- and low-pressure centers, troughs, ridges, and jet streaks. The benefit of this process was that I considered each case in a holistic way, considering the relationships between values at neighboring grid points. The process also required me, the researcher, to be fully involved in the clustering process. Although it was a time-consuming approach, the act of examining each case provided me the opportunity to monitor the synoptic patterns during precipitation events for my region of study over a 28-year span. A first-hand experience such as that cannot be obtained during objective clustering.

The downsides of the subjective clustering included the time involved, user bias, and user error. I made my best attempt to consider the various cases with an open mind, but certainly my background in synoptic climatology and my review of previous studies of the region may have led me to have some preconceived ideas about what synoptic patterns to expect. In addition, the human eye is likely drawn to certain spatial features (e.g., fronts), certain atmospheric levels, or variables and may lead to bias during the clustering process. For example, I often found myself focusing initially on the temperature and height maps at 850 hPa simply because they were the first two maps I saw based on the way I printed out the maps. If I had arranged the maps in a way that had the 700 or 300 hPa maps first, my results may not have been exactly the same. In order to avoid as much user bias and error as possible in my visual typing, I went through several iterations during the clustering process. Once my clusters were established, I reviewed the clusters multiple times to check for continuity. If one or more cases did not fit in, I would move those cases to a more appropriate cluster. The results from the subjective approach did provide 11 distinct synoptic patterns that resembled traditional synoptic features, suggesting that multiple synoptic patterns often have an impact on the region's precipitation climatology.

6.5.2. Consideration of a Hybrid Clustering Approach

Given the advantages and disadvantages of subjective and objective clustering approaches and the differing results presented here, I am unable to conclude that one approach is superior to the other. My suggestion is that others consider both subjective and objective approaches and if possible use multiple objective approaches to create an ensemble of results. Another option I explored in this study was the idea of a hybrid clustering approach, where I used the objective approach to initially create 50 clusters. I then visually examined the maps for those clusters and subjectively clustered them further to ultimately reach eight clusters (maps are included in Appendix E). The overall resulting patterns had many similarities to the patterns from the subjective approach. The eight resulting hybrid clusters were categorized as BH, CL, NbLnF, SaLnF, SnLnF, nsF, NewF, and SewF. No discernible hybrid patterns resembling NnLnF, Z, or W were found. Of the eight hybrid clusters, BH, nsF, NewF, and SewF had nearly the same number of cases as was found during the subjective approach, whereas the CL, NbLnF, and SaLnF clusters had fewer cases. The largest deviation in terms of the number of cases was the SnLnF cluster, which had 749 cases under the hybrid approach but 186 cases with the subjective approach. Since the hybrid CL, NbLnF, and SaLnF clusters were so few in number, the patterns were likely comprised of outlying cases (e.g., the hybrid CL and SaLnF patterns had very low dewpoint values present) and may not fully represent an average CL, NbLnF, or SaLnF case.

The hybrid approach itself was an experiment and the initial choice of creating 50 objective clusters was simply arbitrary. Increasing the number of initial clusters would allow for more clusters to be found during the subjective process. A future study of the whole cluster analysis issue may wish to explore this topic more thoroughly in order to determine how many initial objective clusters to create. For instance, initially using 50 clusters to represent 1437 cases essentially meant reducing the number of cases to 3.5 percent of the original total. Perhaps using a smaller or larger value, such as 1 percent (14 clusters in this case), 2.5 percent (36 clusters in this case), 5 percent (72 clusters in this case) or 10 percent (144 clusters in this case), would have been a better option.

6.5.3. Comparison with Previous Studies

In regards to the cyclone studies covering the southern Appalachian region (e.g., Miller, 1946; Klein, 1957; Reitan, 1974; Bosart, 1975; Zishka and Smith, 1980), the synoptic pattern that is most relevant here is nsF, since it possesses the typical Norwegian cyclone model cold front. Because I was analyzing the synoptic situation only near the time of precipitation, I did not monitor the synoptic patterns through time to detect the initial timing and location of cyclogenesis. Thus, the nsF pattern may contain cyclones of Colorado, Alberta (Zishka and Smith, 1980), and Atlantic (Miller, 1946; Bosart, 1975) origins. My nsF pattern most closely resembles Miller's (1946) Type B cyclones, Gaffin and Hotz's (2000) Synoptic pattern, and Davis and Rogers's (1992) Cluster 3. Miller (1946) found Type B cyclones to be most common during the winter season, which agrees with my findings for the nsF pattern. The works of Klein (1957), Reitan (1974), and Zishka and Smith (1980) also supported the idea that cyclones in the region were more common during winter, although Davis and Rogers (1992) found their type to be most common in late spring. Zishka and Smith (1980) also found cyclone frequency to decrease during the middle portion of the last century, and some authors speculated in subsequent studies about the potential impact cooling temperatures during that time may have had on that decrease in cyclone frequency (van Loon and Williams 1976a, 1976b; Harvey 1978; Diaz and Quayle, 1978). In contrast, the time period for this study (1979-2006) began shortly after Zishka and Smith's (their study covered 1950-1977). I found that the frequency for the nsF pattern increased over the time period, although the trend was not statistically significant. Other cyclone-related patterns such as CL and NbLnF also increased in frequency and were statistically significant at the $p \leq 0.10$ level. As I discussed in Chapter 4, this time period was accompanied by warming temperatures, which echoes the idea posed by others (e.g., van Loon and Williams 1976a, 1976b; Harvey 1978; Diaz and Quayle, 1978) that cyclone frequency in the region may be related to (though not necessarily caused by) rising temperatures. If true, as temperatures continue to rise in the twenty-first century, cyclogenesis and/or cyclone passage in the region may become increasingly more common (IPCC, 2007a; USGCRP, 2009). The increase in cyclone frequency during 1979-2006 also coincided with a statistically insignificant increase in the number of precipitation events, as defined by this study. The USGCRP found precipitation in the southeastern U.S. to increase over 1970-2008, but the rainfall was received over fewer events, making droughts more common (USGCRP, 2009).

The NewF and SewF patterns found in this study resembled the Type E pattern discussed by Bosart (1975) and the Frontal pattern discussed by Gaffin and Hotz (2000). I was able to distinguish two different patterns based on the low-level flow of the study region and general location of the east-west front. Both Bosart (1975) and Gaffin and Hotz (2000) appear to have grouped these cases together. I found both the NewF and SewF patterns to be most common during the winter months. Although Gaffin and Hotz (2000) considered only heavy rain events, they found their Frontal pattern to be most common during summer. Bosart (1975) did not discuss the seasonal frequency of his Type E pattern.

Of my remaining synoptic patterns, Gaffin and Hotz (2000) had a Meso-High pattern that was similar to my BH pattern. Our studies agree in that those patterns were most common during summer. We both grouped Bermuda High and meso-high cases together, although we opted to name our groups differently. I found Bermuda High cases to be more common during summer with meso-highs being more common during autumn. During a streamline analysis, Bryson (1966) found meso-highs to be common during autumn and winter (September through February). Cluster 1 of Davis and Rogers (1992) was also similar to my BH pattern. They found the pattern to be most common during July and August.

Gaffin and Hotz's (2000) Tropical pattern also shares some similarities to my CL pattern, although their pattern only included tropical lows. In contrast, my CL category included tropical lows and extra-tropical cut-off lows. Similar to my CL pattern, Gaffin and Hotz's Tropical pattern was common during summer and autumn, although I did find some cases occurring during spring as well. Davis and Rogers's (1992) Cluster 6 was similar to my NbLnF pattern. I found that pattern to be most common in spring, and their results agreed, with Cluster 6 most common in April. Their Cluster 9 also resembled some features of my Z and BH patterns. Davis and Rogers (1992) found Cluster 9 to have anticyclonic flow near the surface and zonal flow aloft. No previous studies thoroughly covered the remaining patterns I found in this study (NnLnF, SaLnF, SnLnF, Z, and W).

O'Handley and Bosart (1996) discussed the possible effect that the southern Appalachian topography has on cyclones and fronts. Frontal speed and orientation were found to be affected by the mountains with the fronts developing a "kink" in shape. Because I did not monitor the events over time, I cannot comment regarding the speed of the fronts, but, in many cases, my synoptic patterns did have kinks or distortions in the fronts near the mountainous areas. Frequently, the height fields had a weak trough over the Appalachians (e.g., nsF, NewF, and NnLnF) and the temperature and/or dewpoint fields showed possible impacts (e.g., nsF, NewF, and Z) from the mountains. As I discussed earlier, temporal and spatial trends for temperature, precipitation, and snowfall all appeared to be greatly affected by the region's complex topography.

6.6. Summary

I found 11 distinct clusters using subjective clustering and of those some have been covered in previous studies, but others (e.g., NnLnF, SaLnF, SnLnF, Z, and W) were not covered. An objective clustering approach was also used to determine 11 clusters. Patterns resulting from the objective approach were quite similar and could be qualitatively grouped into two primary categories. I also recommended a combination of an objective method to cluster the cases into a predetermined number of clusters with a subjective (visual) step to combine them further into a smaller number of clusters. In this hybrid approach, I used 50 initial clusters, but recommended more investigation regarding the appropriate initial number is needed. I was able to reduce the 50 clusters down to eight. The resulting hybrid clusters showed many similarities to the subjective clusters.

CHAPTER 7

SUMMARY AND CONCLUSIONS

7.1. Summary

In this dissertation, I presented an expanded climatology of temperature and precipitation for the southern Appalachian region. I undertook this study, in part, because most climatological studies of the region are now dated, and, given its biological importance, I felt that an updated description of the region's recent climate was needed. While we already know that the region is a warm temperate location that receives substantial precipitation, my long-term study provided the opportunity to highlight trends in these climatic conditions, both temporally and spatially.

The need for a thorough climate study of the region was supported further by model projections summarized by the Intergovernmental Panel on Climate Change in its Fourth Assessment Report (IPCC, 2007a) and a recent national report from the U.S. Global Change Research Program (USGCRP, 2009). The IPCC and USGCRP reports briefly covered the southern Appalachians and projected that the region will experience warming temperatures during this century, but precipitation projections were much more uncertain (IPCC, 2007a; USGCRP, 2009).

In Section 2.5, I shared four research questions to be addressed in this dissertation study. In this final chapter, I will now revisit the research questions and summarize the results presented in the previous three chapters in an effort to answer each research question.

1) What is the temperature and precipitation climatology of the southern Appalachians?

Regarding the temporal aspect of Question 1, temperatures were warm during the 1930s and 1940s and then decreased until the mid 1960s to the late 1970s. A two-phase regression analysis unveiled that statistically significant breaks were common spanning the mid 1960s through the late 1970s, showing some support of a 1976/1977 climate shift documented by others (Trenberth, 1990; IPCC, 2007a). In recent decades, a warm trend began that continued until the end of the record. A linear representation of the data revealed an overall cooling trend during the 1931-2006 period. This trend was probably a statistical reflection of extended warmth during the 1930s and 1940s and cooling during the middle portion of the record. Cooling spanning the 1940s to the 1970s was common nationally as sulfur dioxide levels from coal power plants increased nationwide (Delcourt and Delcourt, 2001). Although introduced legislation has led to nationally decreasing sulfur dioxide levels since the 1970s, the increasing population and energy demands, coupled with the region's reliance on coal energy, has kept sulfur dioxide levels high in the southern Appalachian region and is probably an explanatory factor for the region's statistically significant cooling trends over the 1931-2006 period (Delcourt and Delcourt, 2001).

Warming in recent decades was often more strongly developed in the minimum temperature data than it was for maximum temperatures, suggesting that diurnal temperature ranges decreased over the period. In particular, a decreasing diurnal temperature range at high elevations was often statistically significant at the $p \leq 0.01$ level. Also, in recent decades, cool season temperatures tended to increase (e.g., by more than 4.00°C for January), whereas warm season temperatures remained stable or even cooled, suggesting that the annual range of temperature also decreased. At all elevations, temperatures reached an annual maximum during July and a minimum during January. Temperatures were found to be affected by elevation, with temperature values decreasing as elevation increased (see Figure 4.6). Temperature values for the region generally support the Köppen classification of this region as Cfa or humid subtropical (i.e., average temperature of the coldest month was below 18°C, and above -3°C). The recent warming trends also provide some support for the possible projected trends discussed by the IPCC's Fourth Assessment Report and the recent report from the USGCRP (IPCC, 2007a; USGCRP, 2009).

In general, annual precipitation totals increased over the 1931-2006 period, but the values were not statistically significant. Precipitation increased during April through June and September through November, but decreased during most other months. Snowfall totals decreased at low- and mid-elevation stations during most months, but neither trend was statistically significant. In contrast, snowfall increased at high-elevation stations during the period of record and was significant at the $p \leq 0.01$ level. At the high elevations, snowfall decreased during October and November, but increased during other winter and spring months, suggesting that more snow was received in late autumn through the following spring. Intra-annual values of precipitation reached maximum values during March and July with minima common in October and April. The typical snow season spanned October through May at high elevations with a somewhat shorter snow season at lower elevations. Maximum snowfall totals occurred during January for low and mid elevations and during February for high elevations. With

IPCC (2007a) and USGCRP (2009) results remaining uncertain regarding future precipitation trends in the region, the precipitation and snowfall trends found here provide useful information if the trends continue. Spatial aspects of the region's temperature, precipitation, and snowfall climatology lead to Question 2.

2) How many climate regimes exist in this region?

Based on the horizontal resolution of station data, I found temperature to be associated with elevation, and to a lesser extent, latitude. In the end, up to five climate regimes were recognized, and the resulting patterns varied somewhat based on what variable was clustered. Clusters for minimum, maximum, and mean temperature were quite similar. The warmest regime contained stations at elevations generally below 500 m, many of which were in the Piedmont province in the southeastern portion of the study area. The second-warmest regime included stations at an elevation of approximately 500 m on both sides of the Blue Ridge. The third-warmest regime included mid-elevation stations. The fourth warmest regime included mostly mid-to-high elevations, and the fifth warmest (i.e., coldest) regime included stations at the highest elevations.

Precipitation and snowfall generally had fewer than five climate regimes. A precipitation maximum was often present near the confluence of the NC, SC, and GA borders. A second maximum was sometimes present in high elevations along the northeastern portion of the study area and along the northwestern (or TN) side of the Blue Ridge. A precipitation minimum was usually present in the vicinity of the I-40 corridor, which I defined as the area of lower elevations cutting through the Blue Ridge from northwest to southeast. Snowfall was usually received in small amounts for low- and mid-elevation stations, and only two or three snowfall regimes were generally present, with most low-elevation and high-elevation stations clustering separately.

Some amount of intra-annual and inter-annual variability amongst the clusters was present. Cluster patterns were frequently more distinct during winter than summer months. I suspect that varying snowfall totals and a stronger temperature gradient across elevations were largely the reasons for the variability. Nonetheless, most variation in cluster patterns was probably due to the changes in station availability. Specifically, the number of stations in TN and around the area of GSMNP increased over time. Near the beginning of the record, usually only about 30 stations across the study region were available for clustering, but by the last decade more than 70 stations were typically available. The inclusion of more stations near the end of the record made it easier to visualize cluster patterns.

3) What are the synoptic origins of precipitation here?

Using a subjective clustering approach, I found 11 distinct synoptic patterns that led to southern Appalachian precipitation. Common summertime patterns included precipitation associated with a strong "Bermuda High" (BH), a "Closed Low" (CL) situated over the study region, "Southerly, No Low, No Fronts" (SnLnF), or "Northerly, No Low, No Fronts" (NnLnF). A few cases of "Weak Flow" (W) were also most common during summer. A "Northerly, Behind Low, No Fronts" (NbLnF) pattern of northerly flow wrapping around the backside of a low-pressure center had its greatest frequency during spring months. In general, warm season patterns exhibited weaker winds and weaker temperature, dewpoint, and height gradients. On the other hand, cool season patterns were frequently frontal in nature. Of those, one pattern had a typical Norwegian cyclone model cold front with a southwest-northeast or "North-South Oriented Front" (nsF). A second "Northerly, East-West Oriented Front" (NewF) pattern was associated with northerly flow and an east-west oriented cold front located over the study area (NewF). A third "Southerly, East-West Oriented Front" (SewF) pattern had southerly flow and an east-west oriented cold front. A "Zonal Flow" (Z) wind pattern of west-to-east winds was most common during winter. Lastly, a "Southerly, Ahead of Low, No Fronts" (SaLnF) pattern associated with southerly flow in front of an advancing low-pressure center was common during all seasons.

Of these 11 subjective synoptic patterns, six of the patterns were associated with a low-pressure center, frontal zone, and/or an upper-level jet streak (CL, NbLnF, SaLnF, nsF, NewF, and SewF). The number of cases included within those patterns was 836, accounting for roughly 58 percent of the total number of precipitation events. These events favored cooler months. The remaining five patterns (NnLnF, SnLnF, BH, Z, and W) were responsible for 601 precipitation events (42 percent of the total). None of those patterns had a low-pressure system, front, or jet streak present. Many of those cases occurred during warmer months and the precipitation was likely due to orographic lifting resulting from complex topography and other surface irregularities combined with the pronounced warm and moist summer conditions of the region. The CL (statistically significant at the $p \leq 0.10$ level), NbLnF (statistically significant at the $p \leq 0.10$ level), nsF, NewF, NnLnF, SaLnF, and W patterns increased in frequency over the study period, while the BH (statistically significant at the $p \leq 0.01$ level), SnLnF, SewF, and Z patterns decreased in frequency. This overall result suggests that precipitation events associated with cyclone activity increased during 1979-2006, whereas precipitation events resulting from orographic lifting and/or surface heating decreased in frequency during the same period. Although I did not specifically cover the quantity of precipitation received with each synoptic pattern, it is likely that precipitation resulting from cyclonic events was probably more widespread and often impacted all elevations. Precipitation events associated with primarily orographic patterns, however, were probably limited to mid and high elevations. Thus, I may speculate that the trend toward more events associated with cyclonic systems should have resulted in more precipitation received at low elevation areas, which is consistent with results summarized in Table 4.4.

The impact of defining a precipitation event as 25 percent of stations reporting 0.5 in (12.7 mm) in a day should not be overlooked when considering the results above. As shown in Table 3.4, this definition still included just 16 percent of the possible precipitation events. Precipitation in the region was often received in smaller amounts by a smaller percentage of stations. Although the criteria used here were less stringent than those used by others (e.g., Bogucki, 1972; Konrad, 1997; Gaffin and Hotz, 2000), the precipitation events as defined by this study still had a bias toward "major" precipitation events and may in turn have a bias toward synoptic origins of precipitation rather than origins from local topography, heat, and moisture. Nonetheless, the results above illustrate that the combination of heat, moisture, and complex topography within the region appear to be important factors controlling the number of precipitation events and the amount of precipitation received as well. Hypothetically speaking, if the southern

Appalachian Mountains were removed while all other aspects of the region's climate controls were unaltered, the number of precipitation events, the overall amount of precipitation received, and moisture present in the region, would all likely be less than what is experienced currently. Ranges in precipitation would be more uniform across the region with most locales receiving 1000-1300 mm annually. However, given the region's complex terrain and its impact on precipitation, some high-elevation stations receive more than 2000 mm annually. These large precipitation values in high elevations also affect the lower-lying valleys through downslope drainage of rainfall and snow melt, as well as through the resulting increases in humidity. The significant amount of overall moisture brought about by the region's varying topography is at least partially responsible for the lush and diverse environments found there. Consequently, because the topography keeps a substantial moisture supply anchored in the region, we may have some assurance that the region's moisture may be less susceptible to any changes in synoptics during projected changes in global climate.

4) To what extent does the answer to Question 3 depend on whether an objective, subjective, or hybrid clustering approach is used?

The discussion above for Question 3 covered the results from the subjective clustering approach in detail. However, that approach tended to have a bias toward more and distinct synoptic patterns. In contrast, the results from both the objective and hybrid clustering approaches suggested that fewer than 11 clusters may be present and/or that clusters may not be as distinct from one another as those that were subjectively derived. On the one hand, this finding suggests that perhaps precipitation in the region is not affected by synoptic-scale origins as much as the subjective clustering results tend to reveal. On the other hand, however, the finding may be the result of statistical shortcomings in the objective and hybrid approaches used. In regards to the objective approach, statistics for determining the appropriate number of clusters produced inconclusive results, so I ultimately created 11 objective clusters, which was the same number of clusters revealed by the subjective approach.

The resulting 11 objective clusters were less distinct from one another than the subjective clusters were. As shown in Chapter 6, I was able to broadly categorize the 11 objective clusters into non-frontal and frontal groups. The non-frontal group was comprised of most of the cases and some of the clusters highlighted seasonality with varying gradients and temperatures values. The small minority of frontal cases suggested that most precipitation in the region originates locally. This result should be interpreted carefully though since the objective approach utilized a much smaller data grid in order to remain within the computational limits of the software and computer. The use of the smaller grid (8 x 9) may at least partially explain why the objective clusters (and subsequent hybrid clusters) were less distinct than the subjective clusters.

Lastly, I proposed the option of a hybrid approach, wherein I used an objective analysis to first cluster the cases into 50 clusters. I then printed the maps for those 50 clusters and subjectively clustered them further to ultimately arrive at eight clusters. Of those eight patterns, many closely resembled those derived from the subjective approach. However, the "Closed Low" (CL) pattern uncovered by the hybrid approach had only two cases, and the "Southerly, Ahead of Low, No Fronts" (SaLnF) pattern had only one case, so those two patterns should be considered with caution. The hybrid "Southerly, No Low, No Fronts" (SnLnF) also had far more cases (749) than its similar subjective SnLnF pattern (186). The decision to begin with 50 objective clusters was an arbitrary choice. If future studies consider a hybrid approach, it may be beneficial to experiment with increasing or decreasing the number of initial objective clusters.

7.2. Future Climate Change Impacts

Although this dissertation project was not a climate modeling study, the results still provide useful information regarding the region's climate in recent decades and shed some light on possible future climatic trends in the region. In regards to precipitation, an overall trend toward wetter conditions was present during 1931-2006, although drier conditions existed near the end of the study period and in the years since. In general, moister conditions may help moderate temperatures near the ground, particularly in shaded areas, which could offset the effects of increasing temperatures during the twenty-first century. Consequently, this moister trend could help decrease negative impacts on the biodiversity of the region. However, if the recent dry period becomes a new climate regime, then negative impacts on the region's diversity could be more severe in the years to come if low- and mid-elevation species adapt by moving upslope and habitats for high-elevation species decrease.

My results showed that trends in temperature and temperature range were not always consistent by elevation, season, or time of day. Many statistically significant trends were present in the results of this study, but even if those trends continue, they may not necessarily translate to significant ecological change. Conversely, one or more statistically insignificant trends could have a dire impact on a species if the species is already approaching a tipping point. Whether species will adapt by simply moving upward in elevation or adapt in some other way is unclear. However, the loss of grassy bald environments does suggest that sky island shrinkage is occurring. If plant and/or animal species are found to be affected in negative ways, those interested in policy decisions regarding conservation may wish to explore potential mitigation measures that could be taken to minimize impacts, such as the grassy bald restoration projects conducted in GSMNP on Gregory Bald and Andrew's Bald (Houk, 2009).

Some have countered that such restoration projects are never-ending battles against nature that ought not be pursued. Another option includes preserving or creating ecological "corridors" to allow species migration during changing climate conditions (Delcourt and Delcourt 2001; Delcourt, 2002). This option may have some promise given that the Blue Ridge of the southern Appalachian region is already largely connected by various federally-owned properties, creating a large and continuous expanse of potential habitat. However, some studies suggest that such conservation corridors are not always effective when political conflicts arise (Goldman, 2009) or during times of rapid ecological change when species simply do not have enough time to adequately migrate through the corridor (Delcourt and Delcourt 2001; Delcourt, 2002). In addition, even with corridors present, high-elevation sky islands still remain isolated from other potential habitats, making migration for those species unlikely. Based on knowledge of past migration speeds, Delcourt and Delcourt (2001) and Delcourt (2002) have recommended that corridors should be used concurrently with transferring vulnerable species from current sites to new suitable sites in an effort to speed up migration times and improve the survival chances of sky island species. Such experiments of "assisted migration" are already underway within British Columbia (Marris, 2009).

7.3. Recommendations for Future Research

For this project, my goal was to provide an updated and elaborated baseline climatology and synoptic climatology for the southern Appalachian region. I believe I have been largely successful in that task, but nonetheless, areas remain where I feel additional research is needed. First, although station availability increased substantially over the length of my study period, I still recommend that additional COOP stations be added. Particularly, underdeveloped regions, such as GSMNP and the neighboring national forests have fewer stations compared to the surrounding area. Additional stations in those regions may help future projects better understand climate change and variability at those locations.

Second, for the spatial analysis and determination of climate regimes, I focused on five variables (minimum, maximum, and mean temperature, total precipitation, and total snowfall). I chose those variables largely because they were often used in previous studies, so it provided me the ability to compare my results to previous work. Future studies may wish to consider some of the other available variables. I suspect that many of those variables have later starting dates or are reported infrequently, as I found this to be the case with total evaporation and mean soil temperature. The availability of these variables may improve over time.

Third, although I was able to create a synoptic climatology of the area using three different approaches (objective, subjective, and hybrid), each approach did have some shortcomings. Of the seven statistical measures available within CLUTO for determining the appropriate number of objective clusters, none of them provided a conclusive answer regarding the correct number. An exploration of additional statistics, such as those studied by Milligan and Cooper (1985), may be an improvement. Furthermore, the objective analysis was hindered by the computational limitations of the IDL software and the computer I used. Perhaps those with the resources available to handle the large NARR dataset in an objective analysis could provide a better cluster representation of the region since they could utilize a data grid with a higher resolution and/or could include additional synoptic variables. They may also be able to easily conduct a variety of objective analyses in order to create an ensemble of cluster results from which conclusions could be drawn. The hybrid clustering approach I introduced here may also be improved by further experimentation regarding the initial number of objective clusters to create. I started with 50 clusters to represent 1437 cases in this study, but some additional experimentation may improve the hybrid approach.

Fourth, although I did briefly discuss lifting mechanisms for the various synoptic patterns, I feel that some additional research is possible in this area. I used daily COOP precipitation data and NARR data only at 2100 UTC. However, data for some COOP stations are available hourly and NARR data are currently available every 3 hours. A more in-depth analysis, perhaps also including a study of vorticity and divergence, may provide a more thorough depiction of the lifting that occurs with each synoptic system.

Fifth, not only did my temperature results suggest warming trends during the past few decades, but some of my results also pointed toward decreasing ranges in diurnal temperature, as well as in the annual temperature cycle. Because my expertise is not in plant or animal biology, I was unable to adequately cover the potential impacts that the trends in climate have had or could have on the biogeography of the region. Vegetation changes have been documented, however (e.g., Mark, 1958; Allen and Kupfer, 2000; 2001; Delcourt and Delcourt, 2001; Delcourt, 2002), and I hope that additional biogeographical studies of the region's species can shed some light on the potential impacts that changes in temperature range may have on vegetation. In this study, decreasing temperature ranges were most obvious at high elevations with trends often being statistically significant at the $p \leq 0.01$ level, making it crucial to understand whether or not the ecological sky islands of the region are indeed shrinking as others have suggested (Allen and Kupfer, 2000; 2001; Delcourt and Delcourt, 2001; Delcourt, 2002). Delcourt and Delcourt (2001) and Delcourt (2002) discussed sky island shrinkage primarily in terms of temperature and projected that the region's boreal forest could disappear by 2100 or even earlier. However, changes in temperature and temperature range are likely not the only factors that can contribute to or hinder sky island shrinkage. Kupfer and Cairns (1996) suggested that precipitation, soil depth, soil acidity, soil moisture, wind, growing season length, frost-free season length, air pollution, and insect pests are just some of the additional variables that may play a role in whether or not the sky islands of the region will shrink.

Additional areas of research may include more substantial studies of drought, wildfires, or frequency of temperature and precipitation extremes in the region. Decreased precipitation and warmer conditions over the most recent years have coincided with an increased frequency of natural and human-caused fires (Great Smoky Mountains Association, 2007; 2009). Modeling studies may also be able to create projections regarding the risk of fires in the region. If the studies find that fire risk is expected to increase, then local decision makers will have the opportunity to prepare in advance by increasing the number of fire towers, increasing personnel, or purchasing additional equipment, if they choose to do so.

7.4. Final Remarks

Within current discussions of climate change, the southern Appalachian region has gained little attention compared to other regions around the world. In this study, I have provided new evidence indicating that this region has experienced statistically significant temporal trends in temperature, precipitation, and snowfall during decades of the recent past (1931-2006). In particular, I determined that the diurnal and annual ranges of temperature decreased over the period and that significant trends were most common at the highest elevations ($\geq$ 1000 m). Statistically significant increases in high-elevation snowfall also occurred. An objective cluster analysis yielded five common climate regimes for temperature in the region. Fewer than five regimes were common for precipitation and snowfall, although all variables exhibited a relationship to the region's topography. My review of precipitation events over 1979-2006 was more inclusive of smaller events than past studies and revealed up to 11 different synoptic origins of precipitation for the region. A comparison of objective, subjective, and hybrid clustering approaches revealed differing results, suggesting that some uncertainty still remains. However, of those synoptic patterns found, some have experienced statistically significant trends in frequency, which may shed some light on the region's future precipitation trends.

As I have discussed, the significant trends revealed by this study have coincided with negative changes in the region's biodiversity, although the causal connections among these changes remains unclear. Once diminished, the species richness of the area may not return. If the region's species diversity is something we value as a society, we need to understand the processes that affect it, such as natural and anthropogenic climate change. It is my hope that with this dissertation I have built a stronger foundation from which researchers can move forward in that endeavor.

APPENDIX A

ADDITIONAL RESULTS FROM THE TEMPORAL ANALYSIS

A.1. Temporal Results of Temperature

A.1.1. February

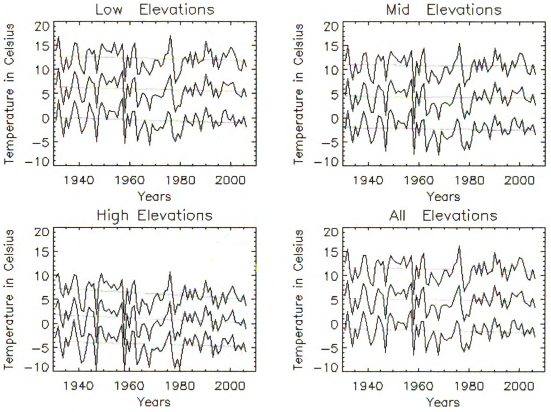

Figure A.1. February minimum (bottom line), maximum (top line), and mean (center line) temperature in °C. A linear fit was calculated for each variable over 1931-2006. Results are included for low elevations (< 500 m; top left), mid elevations (500 – 999 m; top right), high elevations (≥ 1000 m; bottom left), and all elevations (bottom right).

A.1.2. March

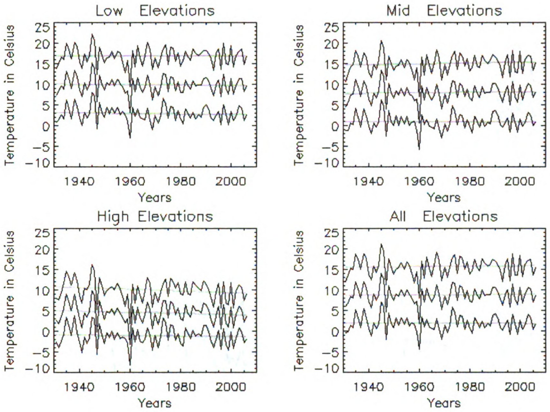

Figure A.2. March minimum (bottom line), maximum (top line), and mean (center line) temperature in °C. A linear fit was calculated for each variable over 1931-2006. Results are included for low elevations (< 500 m; top left), mid elevations (500 – 999 m; top right), high elevations (≥ 1000 m; bottom left), and all elevations (bottom right).

A.1.3. May

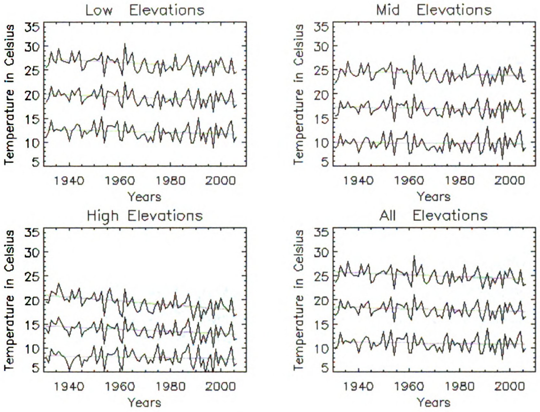

Figure A.3. May minimum (bottom line), maximum (top line), and mean (center line) temperature in °C. A linear fit was calculated for each variable over 1931-2006. Results are included for low elevations (< 500 m; top left), mid elevations (500 – 999 m; top right), high elevations (≥ 1000 m; bottom left), and all elevations (bottom right).

A.1.4. June

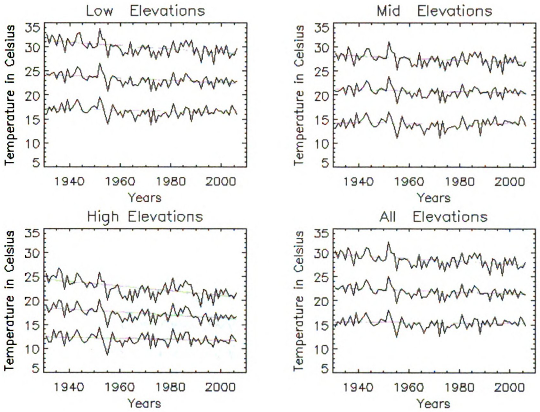

Figure A.4. June minimum (bottom line), maximum (top line), and mean (center line) temperature in °C. A linear fit was calculated for each variable over 1931-2006. Results are included for low elevations (< 500 m; top left), mid elevations (500 – 999 m; top right), high elevations (≥ 1000 m; bottom left), and all elevations (bottom right).

A.1.5. August

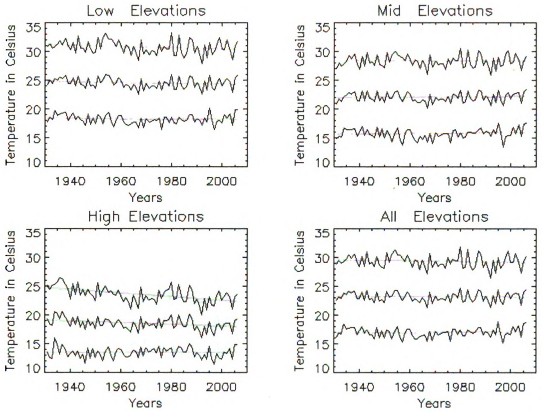

Figure A.5. August minimum (bottom line), maximum (top line), and mean (center line) temperature in °C. A linear fit was calculated for each variable over 1931-2006. Results are included for low elevations (< 500 m; top left), mid elevations (500 – 999 m; top right), high elevations (≥ 1000 m; bottom left), and all elevations (bottom right).

A.1.6. September

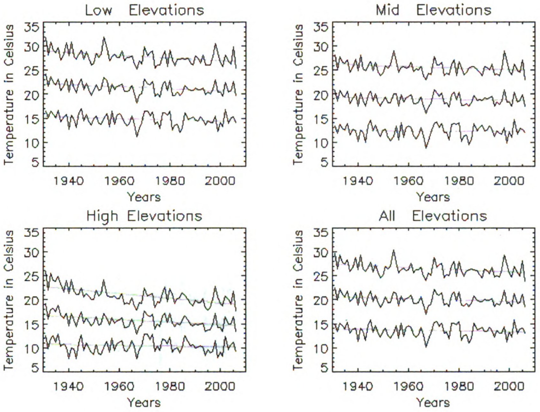

Figure A.6. September minimum (bottom line), maximum (top line), and mean (center line) temperature in °C. A linear fit was calculated for each variable over 1931-2006. Results are included for low elevations (< 500 m; top left), mid elevations (500 – 999 m; top right), high elevations (≥ 1000 m; bottom left), and all elevations (bottom right).

A.1.7. November

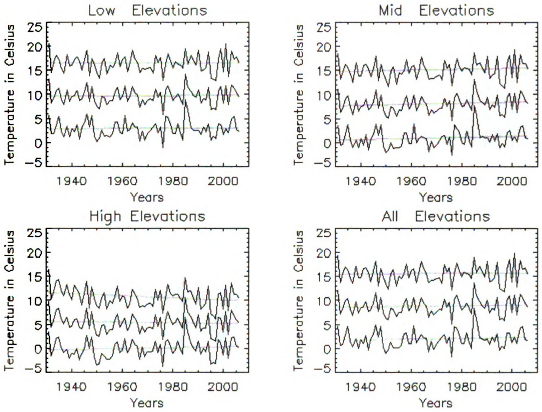

Figure A.7. November minimum (bottom line), maximum (top line), and mean (center line) temperature in °C. A linear fit was calculated for each variable over 1931-2006. Results are included for low elevations (< 500 m; top left), mid elevations (500 – 999 m; top right), high elevations (≥ 1000 m; bottom left), and all elevations (bottom right).

A.1.8. December

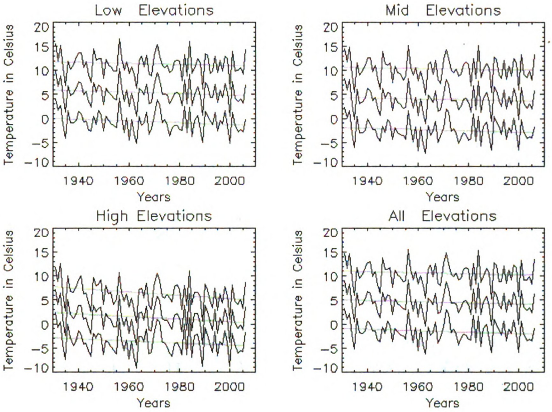

Figure A.8. December minimum (bottom line), maximum (top line), and mean (center line) temperature in °C. A linear fit was calculated for each variable over 1931-2006. Results are included for low elevations (< 500 m; top left), mid elevations (500 – 999 m; top right), high elevations (≥ 1000 m; bottom left), and all elevations (bottom right).

A.1. Temporal Results of Precipitation and Snowfall

A.2.1. February

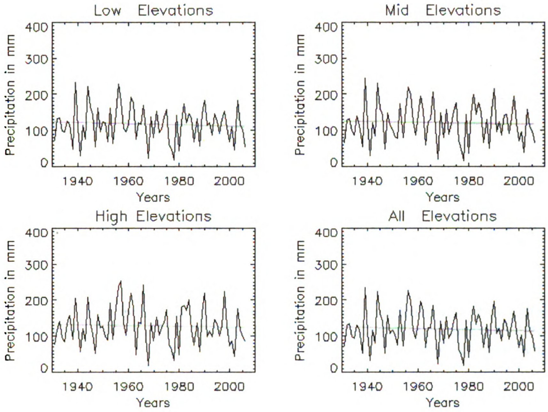

Figure A.9. February precipitation in mm. A linear fit was calculated for 1931-2006. Results are included for low elevations (< 500 m; top left), mid elevations (500 – 999 m; top right), high elevations (≥ 1000 m; bottom left), and all elevations (bottom right).

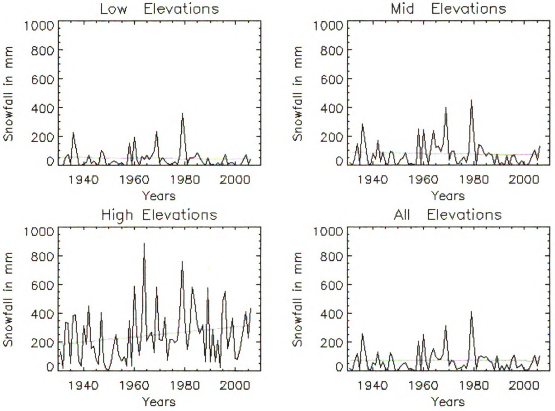

Figure A.10. February snowfall in mm. A linear fit was calculated for 1931-2006. Results are included for low elevations (< 500 m; top left), mid elevations (500 – 999 m; top right), high elevations (≥ 1000 m; bottom left), and all elevations (bottom right).

A.2.2. March

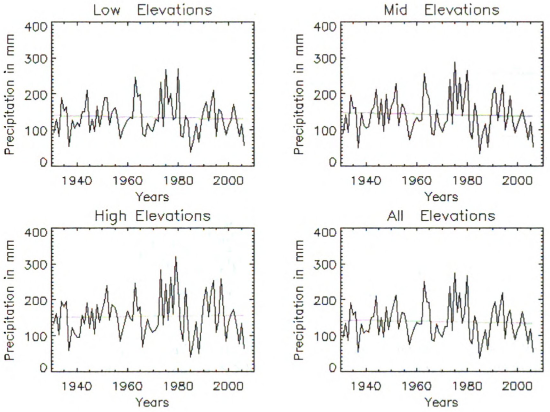

Figure A.11. March precipitation in mm. A linear fit was calculated for 1931-2006. Results are included for low elevations (< 500 m; top left), mid elevations (500 – 999 m; top right), high elevations (≥ 1000 m; bottom left), and all elevations (bottom right).

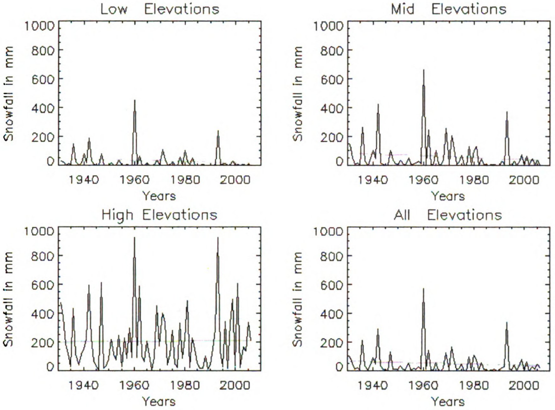

Figure A.12. March snowfall in mm. A linear fit was calculated for 1931-2006. Results are included for low elevations (< 500 m; top left), mid elevations (500 – 999 m; top right), high elevations (≥ 1000 m; bottom left), and all elevations (bottom right).

A.2.3. May

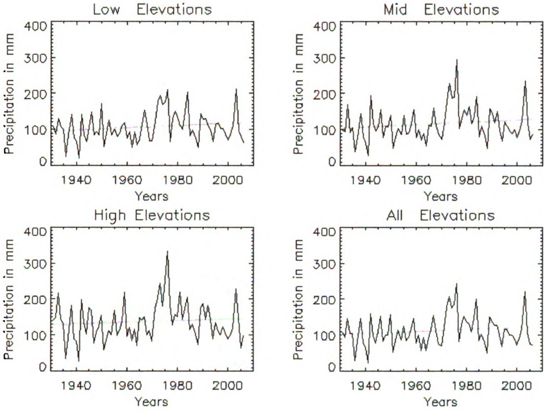

Figure A.13. May precipitation in mm. A linear fit was calculated for 1931-2006. Results are included for low elevations (< 500 m; top left), mid elevations (500 – 999 m; top right), high elevations (≥ 1000 m; bottom left), and all elevations (bottom right).

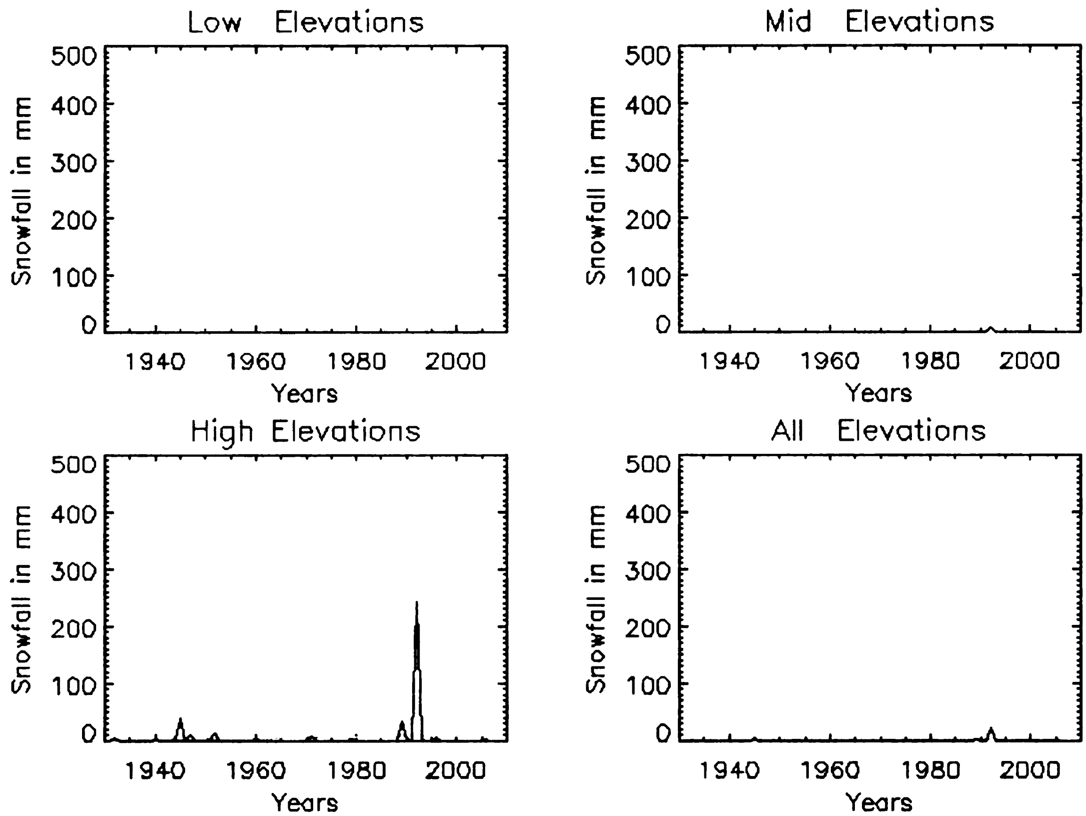

Figure A.14. May snowfall in mm. A linear fit was calculated for 1931-2006. Results are included for low elevations (< 500 m; top left), mid elevations (500 – 999 m; top right), high elevations (≥ 1000 m; bottom left), and all elevations (bottom right).

A.2.4. June

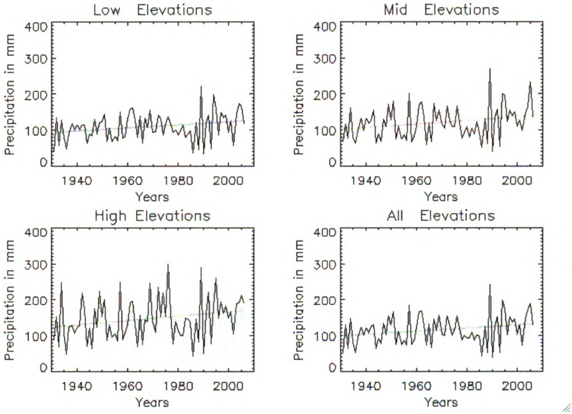

Figure A.15. June precipitation in mm. A linear fit was calculated for 1931-2006. Results are included for low elevations (< 500 m; top left), mid elevations (500 – 999 m; top right), high elevations (≥ 1000 m; bottom left), and all elevations (bottom right).

A.2.5. August

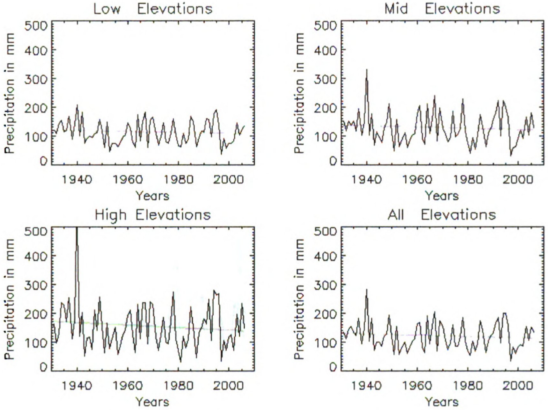

Figure A.16. August precipitation in mm. A linear fit was calculated for 1931-2006. Results are included for low elevations (< 500 m; top left), mid elevations (500 – 999 m; top right), high elevations (≥ 1000 m; bottom left), and all elevations (bottom right).

A.2.6. September

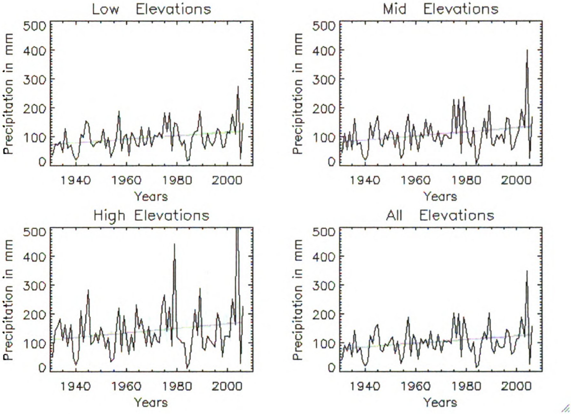

Figure A.17. September precipitation in mm. A linear fit was calculated for 1931-2006. Results are included for low elevations (< 500 m; top left), mid elevations (500 – 999 m; top right), high elevations (≥ 1000 m; bottom left), and all elevations (bottom right).

A.2.7. November

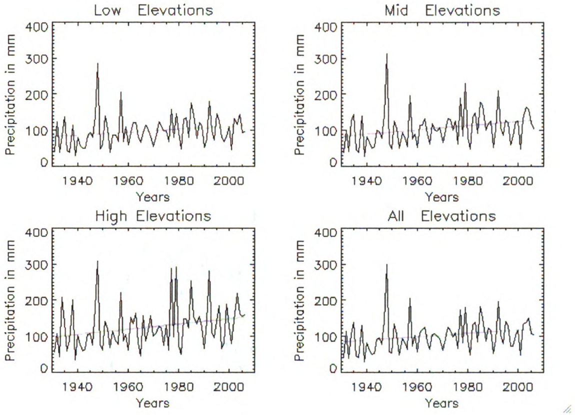

Figure A.18. November precipitation in mm. A linear fit was calculated for 1931-2006. Results are included for low elevations (< 500 m; top left), mid elevations (500 – 999 m; top right), high elevations (≥ 1000 m; bottom left), and all elevations (bottom right).

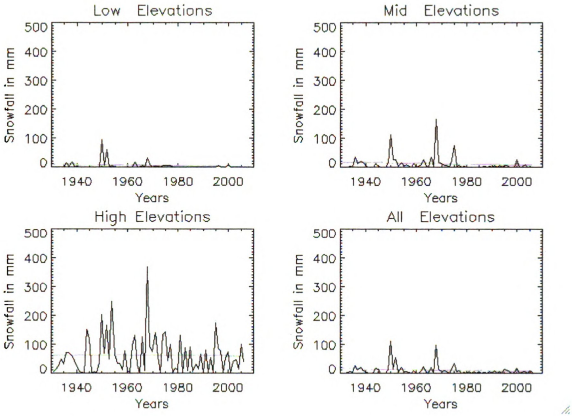

Figure A.19. November snowfall in mm. A linear fit was calculated for 1931-2006. Results are included for low elevations (< 500 m; top left), mid elevations (500 – 999 m; top right), high elevations (≥ 1000 m; bottom left), and all elevations (bottom right).

A.2.8. December

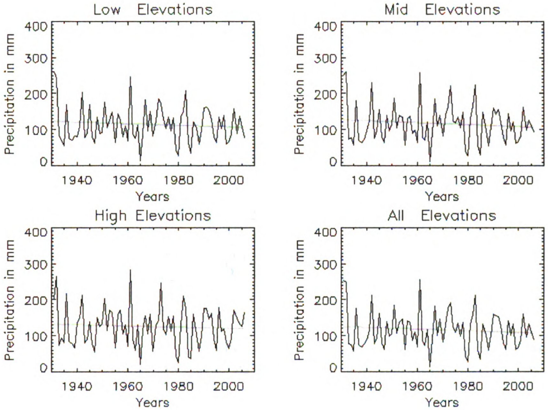

Figure A.20. December precipitation in mm. A linear fit was calculated for 1931-2006. Results are included for low elevations (< 500 m; top left), mid elevations (500 – 999 m; top right), high elevations (≥ 1000 m; bottom left), and all elevations (bottom right).

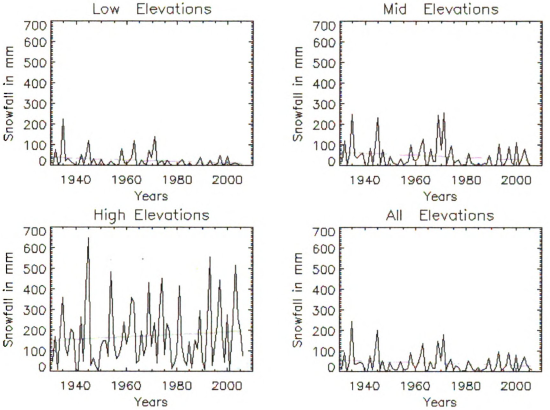

Figure A.21. December snowfall in mm. A linear fit was calculated for 1931-2006. Results are included for low elevations (< 500 m; top left), mid elevations (500 – 999 m; top right), high elevations (≥ 1000 m; bottom left), and all elevations (bottom right).

APPENDIX B

ADDITIONAL RESULTS FROM THE SPATIAL ANALYSIS

B.1. Spatial Results of Temperature

B.1.1. April

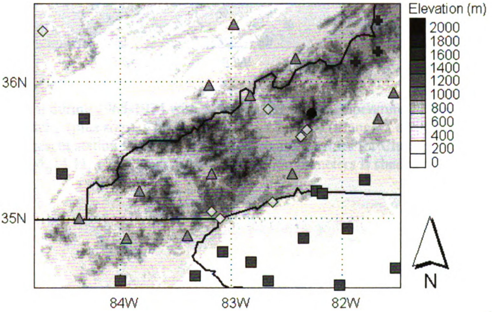

Figure B.1. April during 1935-1944 with 5 clusters for mean temperature, where Cluster 1 (dot), Cluster 2 (plus sign), Cluster 3 (square), Cluster 4 (triangle), and Cluster 5 (diamond) represent station locations. Mean temperature values for Clusters 1-5 were 4.24, 9.65, 15.48, 12.47, and 12.16°C. Elevation in meters is shaded in gray.

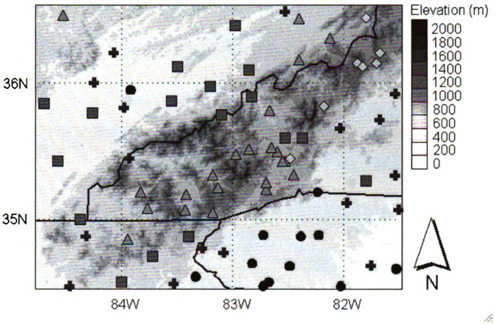

Figure B.2. April during 1965-1974 with 5 clusters for mean temperature, where Cluster 1 (dot), Cluster 2 (plus sign), Cluster 3 (square), Cluster 4 (triangle), and Cluster 5 (diamond) represent station locations. Mean temperature values for Clusters 1-5 were 16.22, 15.06, 14.11, 12.89, and 10.16°C. Elevation in meters is shaded in gray.

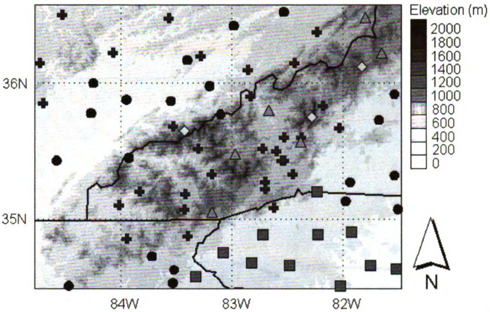

Figure B.3. April during 1995-2004 with 5 clusters for mean temperature, where Cluster 1 (dot), Cluster 2 (plus sign), Cluster 3 (square), Cluster 4 (triangle), and Cluster 5 (diamond) represent station locations. Mean temperature values for Clusters 1-5 were 14.41, 12.88, 15.68, 10.81, and 6.19°C. Elevation in meters is shaded in gray.

B.1.2. October

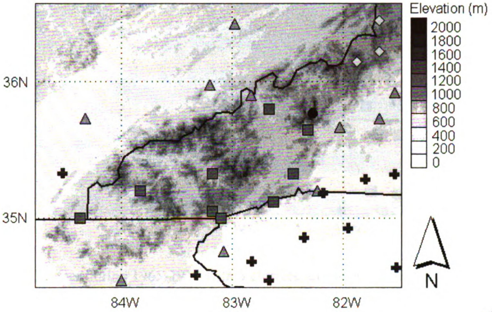

Figure B.4. October during 1935-1944 with 5 clusters for mean temperature, where Cluster 1 (dot), Cluster 2 (plus sign), Cluster 3 (square), Cluster 4 (triangle), and Cluster 5 (diamond) represent station locations. Mean temperature values for Clusters 1-5 were 7.79, 17.06, 13.99, 15.73, and 11.64°C. Elevation in meters is shaded in gray.

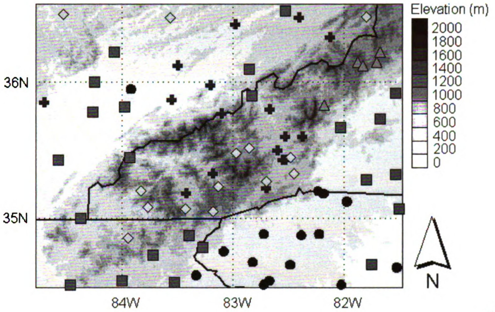

Figure B.5. October during 1965-1974 with 5 clusters for mean temperature, where Cluster 1 (dot), Cluster 2 (plus sign), Cluster 3 (square), Cluster 4 (triangle), and Cluster 5 (diamond) represent station locations. Mean temperature values for Clusters 1-5 were 16.29, 13.80, 14.93, 10.29, and 12.62°C. Elevation in meters is shaded in gray.

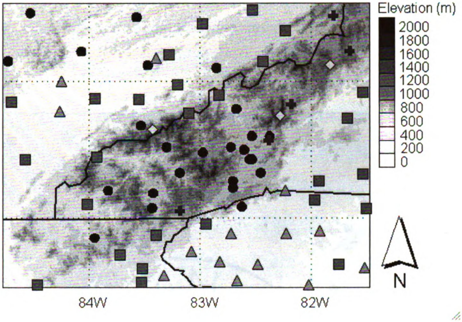

Figure B.6. October during 1995-2004 with 5 clusters for mean temperature, where Cluster 1 (dot), Cluster 2 (plus sign), Cluster 3 (square), Cluster 4 (triangle), and Cluster 5 (diamond) represent station locations. Mean temperature values for Clusters 1-5 were 13.66, 11.59, 15.02, 16.27, and 8.33°C. Elevation in meters is shaded in gray.

B.2. Spatial Results of Precipitation

B.2.1. April

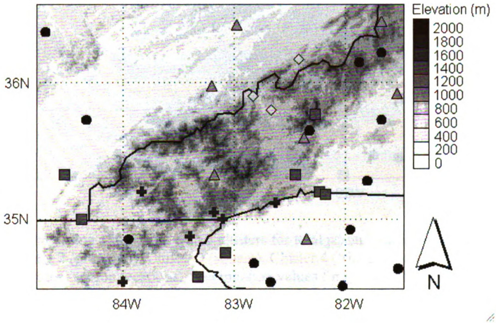

Figure B.7. April during 1935-1944 with 5 clusters for total precipitation, where Cluster 1 (dot), Cluster 2 (plus sign), Cluster 3 (square), Cluster 4 (triangle), and Cluster 5 (diamond) represent station locations. Precipitation values for Clusters 1-5 were 105.42, 147.59, 120.09, 89.45, and 74.75 mm. Elevation in meters is shaded in gray.

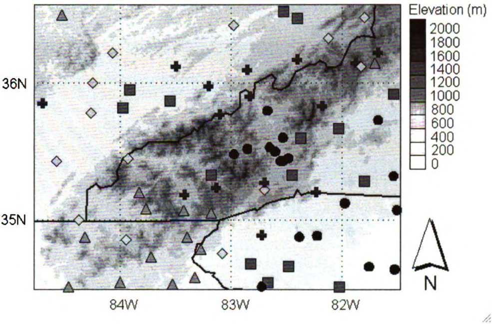

Figure B.8. April during 1965-1974 with 5 clusters for total precipitation, where Cluster 1 (dot), Cluster 2 (plus sign), Cluster 3 (square), Cluster 4 (triangle), and Cluster 5 (diamond) represent station locations. Precipitation values for Clusters 1-5 were 85.44, 111.18, 98.80, 138.72, and 120.93 mm. Elevation in meters is shaded in gray.

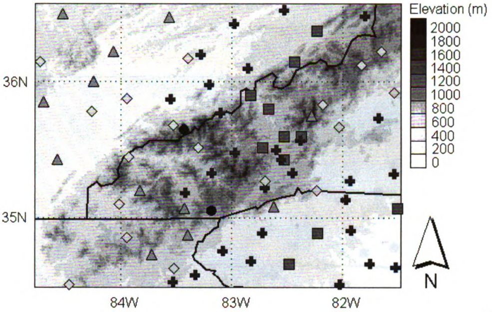

Figure B.9. April during 1995-2004 with 5 clusters for total precipitation, where Cluster 1 (dot), Cluster 2 (plus sign), Cluster 3 (square), Cluster 4 (triangle), and Cluster 5 (diamond) represent station locations. Precipitation values for Clusters 1-5 were 170.35, 103.61, 87.67, 134.18, and 120.04 mm. Elevation in meters is shaded in gray.

B.2.2. October

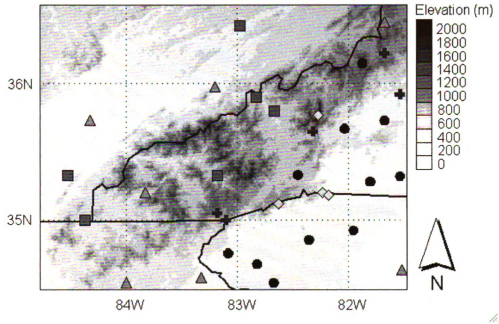

Figure B.10. October during 1935-1944 with 5 clusters for total precipitation, where Cluster 1 (dot), Cluster 2 (plus sign), Cluster 3 (square), Cluster 4 (triangle), and Cluster 5 (diamond) represent station locations. Precipitation values for Clusters 1-5 were 77.80, 87.15, 54.87, 63.34, and 108.94 mm. Elevation in meters is shaded in gray.

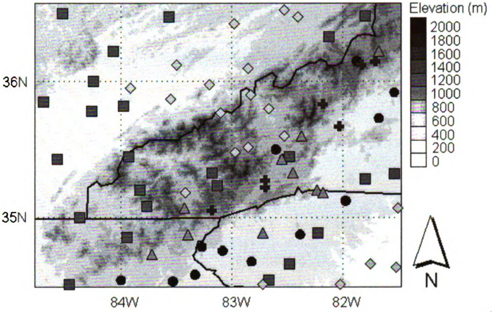

Figure B.11. October during 1965-1974 with 5 clusters for total precipitation, where Cluster 1 (dot), Cluster 2 (plus sign), Cluster 3 (square), Cluster 4 (triangle), and Cluster 5 (diamond) represent station locations. Precipitation values for Clusters 1-5 were 105.25, 158.56, 88.71, 125.91, and 72.51 mm. Elevation in meters is shaded in gray.

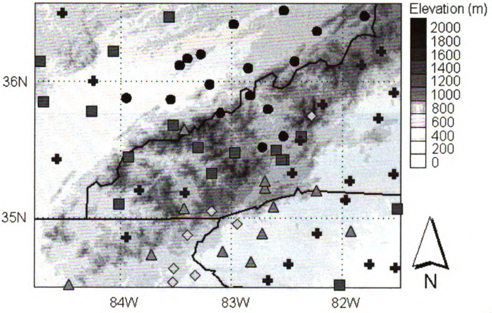

Figure B.12. October during 1995-2004 with 5 clusters for total precipitation, where Cluster 1 (dot), Cluster 2 (plus sign), Cluster 3 (square), Cluster 4 (triangle), and Cluster 5 (diamond) represent station locations. Precipitation values for Clusters 1-5 were 49.77, 77.14, 64.73, 97.19, and 120.84 mm. Elevation in meters is shaded in gray.

B.3. Spatial Results of Snowfall

B.3.1. April

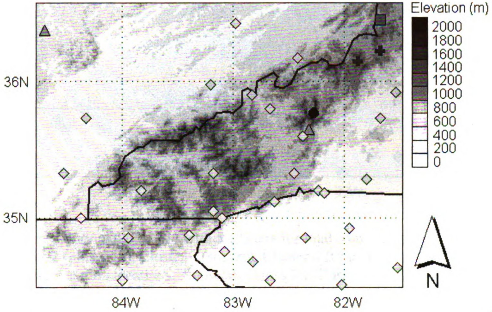

Figure B.13. April during 1935-1944 with 5 clusters for total snowfall, where Cluster 1 (dot), Cluster 2 (plus sign), Cluster 3 (square), Cluster 4 (triangle), and Cluster 5 (diamond) represent station locations. Snowfall values for Clusters 1-5 were 77.22, 26.42, 61.72, 7.50, and 0.12 mm. Elevation in meters is shaded in gray.

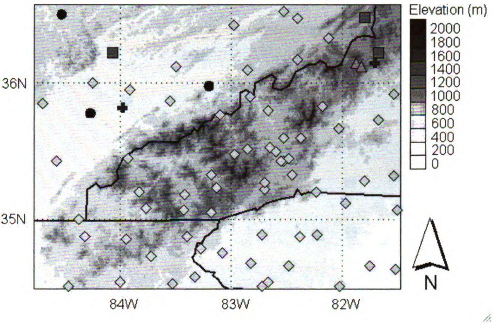

Figure B.14. April during 1965-1974 with 5 clusters for total snowfall, where Cluster 1 (dot), Cluster 2 (plus sign), Cluster 3 (square), Cluster 4 (triangle), and Cluster 5 (diamond) represent station locations. Snowfall values for Clusters 1-5 were 5.93, 16.26, 10.24, 33.66, and 0.19 mm. Elevation in meters is shaded in gray.

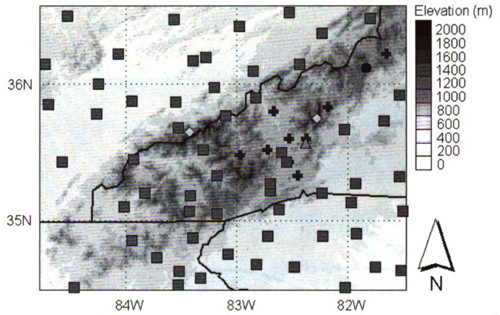

Figure B.15. April during 1995-2004 with 5 clusters for total snowfall, where Cluster 1 (dot), Cluster 2 (plus sign), Cluster 3 (square), Cluster 4 (triangle), and Cluster 5 (diamond) represent station locations. Snowfall values for Clusters 1-5 were 127.51, 12.71, 0.11, 78.99, and 212.26 mm. Elevation in meters is shaded in gray.

B.3.2. October

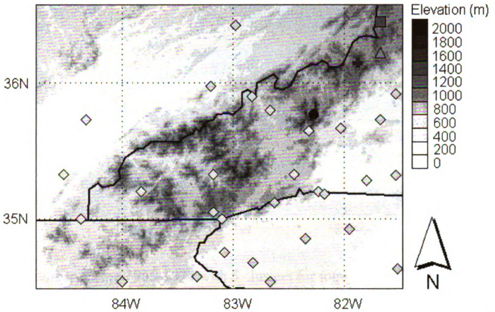

Figure B.16. October during 1935-1944 with 5 clusters for total snowfall, where Cluster 1 (dot), Cluster 2 (plus sign), Cluster 3 (square), Cluster 4 (triangle), and Cluster 5 (diamond) represent station locations. Snowfall values for Clusters 1-5 were 17.02, 5.08, 30.48, 7.62, and 0.00 mm. Elevation in meters is shaded in gray.

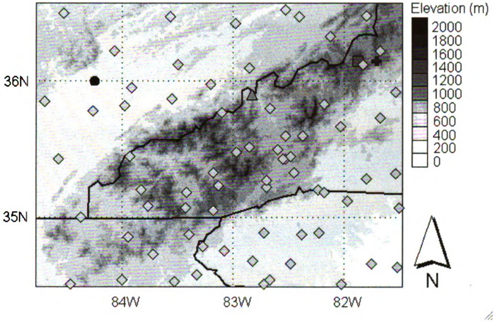

Figure B.17. October during 1965-1974 with 5 clusters for total snowfall, where Cluster 1 (dot), Cluster 2 (plus sign), Cluster 3 (square), Cluster 4 (triangle), and Cluster 5 (diamond) represent station locations. Snowfall values for Clusters 1-5 were 0.00, 0.76, 6.86, 0.00, and 0.00 mm. Elevation in meters is shaded in gray.

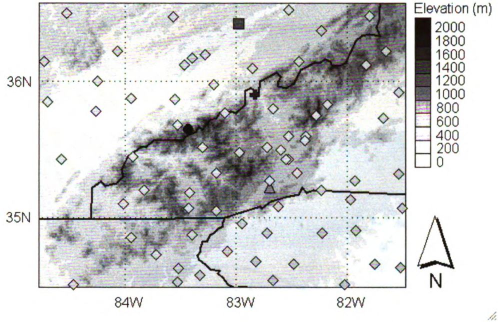

Figure B.18. October during 1995-2004 with 5 clusters for total snowfall, where Cluster 1 (dot), Cluster 2 (plus sign), Cluster 3 (square), Cluster 4 (triangle), and Cluster 5 (diamond) represent station locations. Snowfall values for Clusters 1-5 were 1.27, 0.00, 0.00, 0.00, and 0.00 mm. Elevation in meters is shaded in gray.

B.4. Spatial Results for All Variables

B.4.1. April

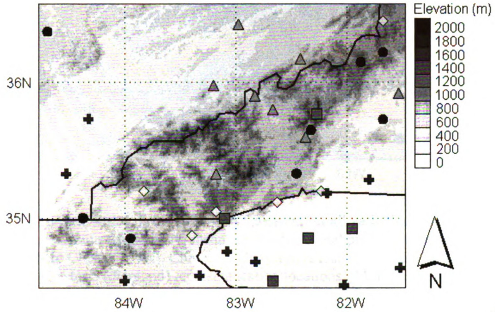

Figure B.19. April during 1935-1944 with 5 clusters for all variables (minimum temperature, maximum temperature, mean temperature, total precipitation, and total snowfall), where Cluster 1 (dot), Cluster 2 (plus sign), Cluster 3 (square), Cluster 4 (triangle), and Cluster 5 (diamond) represent station locations. Minimum temperature values for Clusters 1-5 were 4.72, 8.06, 6.98, 5.48, and 5.43°C. Maximum temperature values for Clusters 1-5 were 19.46, 22.82, 18.47, 20.93, and 19.96°C. Mean temperature values for Clusters 1-5 were 12.09, 15.44, 12.73, 13.21, and 12.71°C. Precipitation values for Clusters 1-5 were 107.66, 116.73, 115.90, 82.59, and 133.06 mm. Snowfall values for Clusters 1-5 were 8.48, 0.08, 15.49, 0.29, and 10.29 mm. Elevation in meters is shaded in gray.

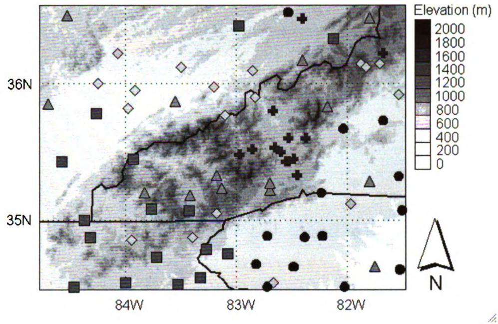

Figure B.20. April during 1965-1974 with 5 clusters for all variables (minimum temperature, maximum temperature, mean temperature, total precipitation, and total snowfall), where Cluster 1 (dot), Cluster 2 (plus sign), Cluster 3 (square), Cluster 4 (triangle), and Cluster 5 (diamond) represent station locations. Minimum temperature values for Clusters 1-5 were 8.41, 5.46, 6.98, 4.72, and 6.60°C. Maximum temperature values for Clusters 1-5 were 23.17, 20.10, 21.86, 21.34, and 20.51°C. Mean temperature values for Clusters 1-5 were 15.81, 12.79, 14.43, 13.04, and 13.57°C. Precipitation values for Clusters 1-5 were 94.35, 87.88, 131.72, 111.89, and 114.70 mm. Snowfall values for Clusters 1-5 were 0.09, 1.11, 0.66, 1.09, and 6.63 mm. Elevation in meters is shaded in gray.

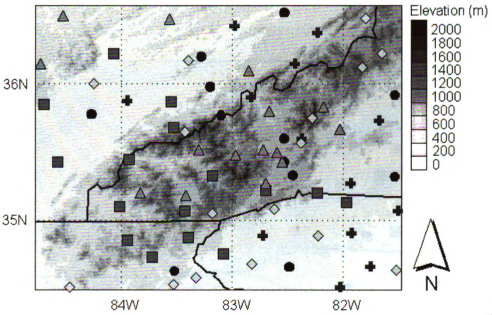

Figure B.21. April during 1995-2004 with 5 clusters for all variables (minimum temperature, maximum temperature, mean temperature, total precipitation, and total snowfall), where Cluster 1 (dot), Cluster 2 (plus sign), Cluster 3 (square), Cluster 4 (triangle), and Cluster 5 (diamond) represent station locations. Minimum temperature values for Clusters 1-5 were 7.07, 6.77, 6.29, 4.53, and 6.03°C. Maximum temperature values for Clusters 1-5 were 20.97, 21.69, 21.53, 20.28, and 18.36°C. Mean temperature values for Clusters 1-5 were 14.03, 14.24, 13.93, 12.42, and 12.21°C. Precipitation values for Clusters 1-5 were 103.58, 99.20, 121.35, 111.15, and 121.20 mm. Snowfall values for Clusters 1-5 were 2.62, 0.97, 0.00, 3.06, and 41.38 mm. Elevation in meters is shaded in gray.

B.4.2. October

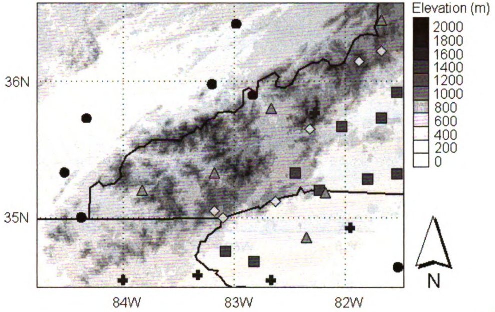

Figure B.22. October during 1935-1944 with 5 clusters for all variables (minimum temperature, maximum temperature, mean temperature, total precipitation, and total snowfall), where Cluster 1 (dot), Cluster 2 (plus sign), Cluster 3 (square), Cluster 4 (triangle), and Cluster 5 (diamond) represent station locations. Minimum temperature values for Clusters 1-5 were 7.83, 9.07, 8.26, 6.79, and 6.62°C. Maximum temperature values for Clusters 1-5 were 23.82, 21.30, 23.75, 22.08, and 19.65°C. Mean temperature values for Clusters 1-5 were 15.83, 15.19, 16.01, 14.50, and 13.13°C. Precipitation values for Clusters 1-5 were 58.77, 80.51, 80.82, 68.08, and 91.69 mm. Snowfall values for Clusters 1-5 were 0.00, 3.40, 0.00, 5.08, and 2.12 mm. Elevation in meters is shaded in gray.

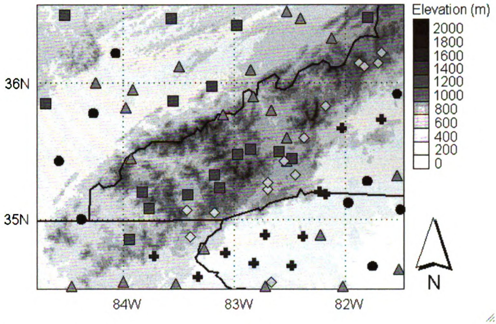

Figure B.23. October during 1965-1974 with 5 clusters for all variables (minimum temperature, maximum temperature, mean temperature, total precipitation, and total snowfall), where Cluster 1 (dot), Cluster 2 (plus sign), Cluster 3 (square), Cluster 4 (triangle), and Cluster 5 (diamond) represent station locations. Minimum temperature values for Clusters 1-5 were 7.09, 9.16, 5.07, 8.27, and 5.80°C. Maximum temperature values for Clusters 1-5 were 22.99, 22.64, 21.00, 21.59, and 19.12°C. Mean temperature values for Clusters 1-5 were 15.05, 15.92, 13.05, 14.94, and 12.45°C. Precipitation values for Clusters 1-5 were 89.19, 116.47, 84.67, 81.53, and 137.00 mm. Snowfall values for Clusters 1-5 were 0.00, 0.00, 0.00, 0.00, and 0.54 mm. Elevation in meters is shaded in gray.

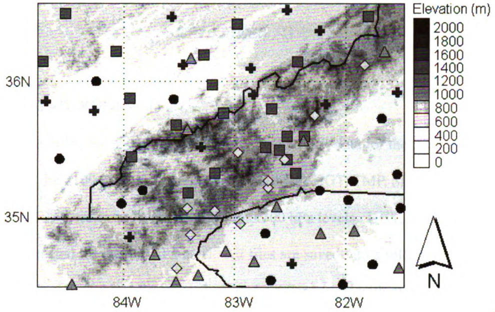

Figure B.24. October during 1995-2004 with 5 clusters for all variables (minimum temperature, maximum temperature, mean temperature, total precipitation, and total snowfall), where Cluster 1 (dot), Cluster 2 (plus sign), Cluster 3 (square), Cluster 4 (triangle), and Cluster 5 (diamond) represent station locations. Minimum temperature values for Clusters 1-5 were 8.17, 6.84, 6.94, 8.59, and 5.97°C. Maximum temperature values for Clusters 1-5 were 22.63, 21.87, 21.08, 20.63, and 19.52°C. Mean temperature values for Clusters 1-5 were 15.42, 14.36, 14.03, 14.63, and 12.76°C. Precipitation values for Clusters 1-5 were 76.96, 61.28, 59.00, 91.53, and 100.66 mm. Snowfall values for Clusters 1-5 were 0.00, 0.00, 0.00, 0.09, 0.00 mm. Elevation in meters is shaded in gray.

APPENDIX C

GRIB FILES

C.1. Automation of GRIB downloads

I used the following sample script to download NARR data for the month of January, 1979 at the 2100 UTC time period. The variables HGT, TMP, SPFH, VVEL, UGRD, and VGRD were extracted for the 850 and 700 hPa levels. HGT, UGRD, and VGRD were extracted for the 300 hPa level. All files are saved into a folder named "1979/" located in the working directory. I created similar scripts with minor edits to download data for other months and years.

```
#!/bin/sh
# download selected variables from NARR 19790101-00Z merged-a data from NCDC
yymm=197901
date=19790101
hr=21
while [ $date != "19790132" ]
do
a="http://nomads.ncdc.noaa.gov/data/narr/$yymm/$date/narr-a_221_${date}_${hr}00_000"
b="narr-a_221_${date}_${hr}00"
./get_inv.pl $a.inv | egrep ":(HGT|TMP|SPFH|VVEL|UGRD|VGRD):850 mb" |
./get_grib.pl $a.grb 1979/${b}_850mb.grb
./get_inv.pl $a.inv | egrep ":(HGT|TMP|SPFH|VVEL|UGRD|VGRD):700 mb" |
./get_grib.pl $a.grb 1979/${b}_700mb.grb
./get_inv.pl $a.inv | egrep ":(HGT|UGRD|VGRD):300 mb" |
./get_grib.pl $a.grb 1979/${b}_300mb.grb
date=`expr $date + 1`
echo "$date"
done
echo "finished downloading variables for $yymm"
```

C.2. Uncompressing GRIB files using WGRIB

Instructions for downloading, compiling, and using WGRIB are located at:

http://www.cpc.ncep.noaa.gov/products/wesley/wgrib.html. Once I downloaded and compiled WGRIB, I used the following command to uncompress 850 hPa data for January 1, 1979.

```
./wgrib.x 1979/narr-a_221_19790101_2100_850mb.grb -d all -text -h -o 1979/narr19790101_850mb.txt
```

The command uncompresses the file and saved it as a .txt formatted file. I used similar commands with minor edits to uncompress files for other days, months, years, and levels.

APPENDIX D

ADDITIONAL RESULTS FROM THE SYNOPTIC CLIMATOLOGY

D.1. Maps of 700 and 300 hPa Variables from the Objective Clustering Approach

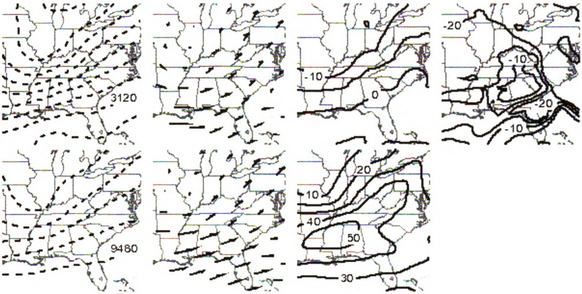

Figure D.1. Cluster 1. Maps in the top row from left to right are temperature (contoured every 5°C) wind vectors, dewpoint (contoured every 5°C), and height (contoured every 30 m) at the 700 hPa level. Maps in the bottom row from left to right are height (contoured every 120 m), wind vectors, and isotachs (contoured every 10 m/s) at the 300 hPa level.

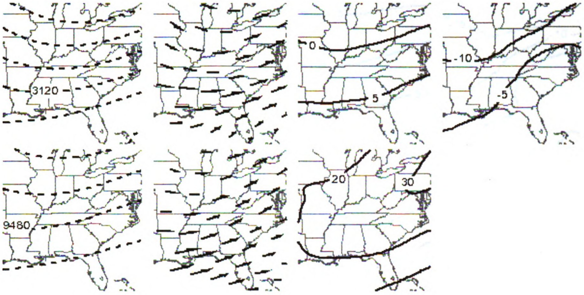

Figure D.2. Cluster 2. Maps in the top row from left to right are temperature (contoured every 5°C) wind vectors, dewpoint (contoured every 5°C), and height (contoured every 30 m) at the 700 hPa level. Maps in the bottom row from left to right are height (contoured every 120 m), wind vectors, and isotachs (contoured every 10 m/s) at the 300 hPa level.

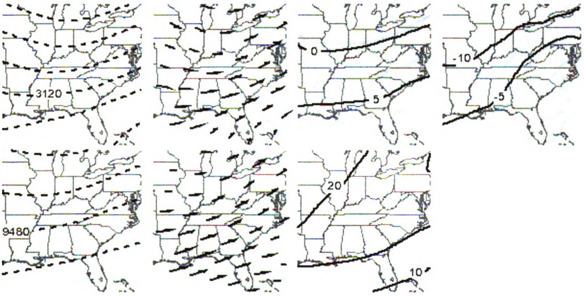

Figure D.3. Cluster 3. Maps in the top row from left to right are temperature (contoured every 5°C) wind vectors, dewpoint (contoured every 5°C), and height (contoured every 30 m) at the 700 hPa level. Maps in the bottom row from left to right are height (contoured every 120 m), wind vectors, and isotachs (contoured every 10 m/s) at the 300 hPa level.

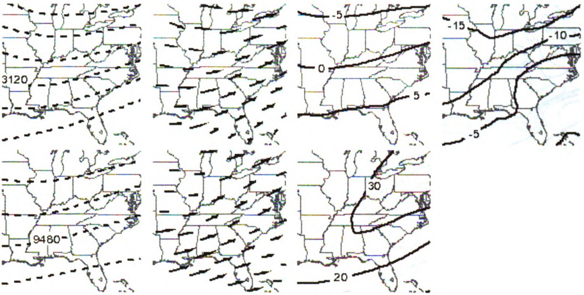

Figure D.4. Cluster 4. Maps in the top row from left to right are temperature (contoured every 5°C) wind vectors, dewpoint (contoured every 5°C), and height (contoured every 30 m) at the 700 hPa level. Maps in the bottom row from left to right are height (contoured every 120 m), wind vectors, and isotachs (contoured every 10 m/s) at the 300 hPa level.

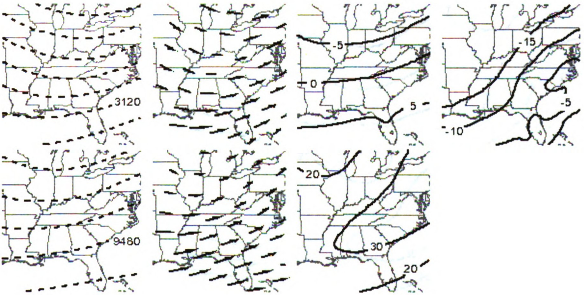

Figure D.5. Cluster 5. Maps in the top row from left to right are temperature (contoured every 5°C) wind vectors, dewpoint (contoured every 5°C), and height (contoured every 30 m) at the 700 hPa level. Maps in the bottom row from left to right are height (contoured every 120 m), wind vectors, and isotachs (contoured every 10 m/s) at the 300 hPa level.

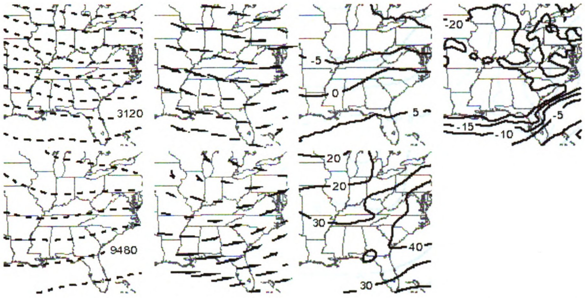

Figure D.6. Cluster 6. Maps in the top row from left to right are temperature (contoured every 5°C) wind vectors, dewpoint (contoured every 5°C), and height (contoured every 30 m) at the 700 hPa level. Maps in the bottom row from left to right are height (contoured every 120 m), wind vectors, and isotachs (contoured every 10 m/s) at the 300 hPa level.

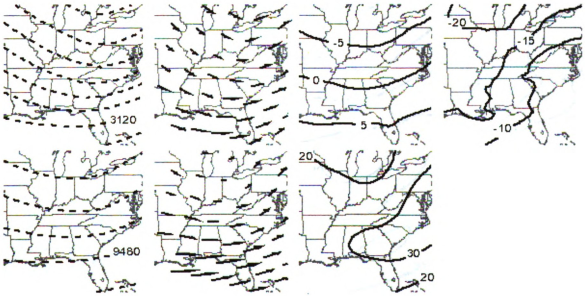

Figure D.7. Cluster 7. Maps in the top row from left to right are temperature (contoured every 5°C) wind vectors, dewpoint (contoured every 5°C), and height (contoured every 30 m) at the 700 hPa level. Maps in the bottom row from left to right are height (contoured every 120 m), wind vectors, and isotachs (contoured every 10 m/s) at the 300 hPa level.

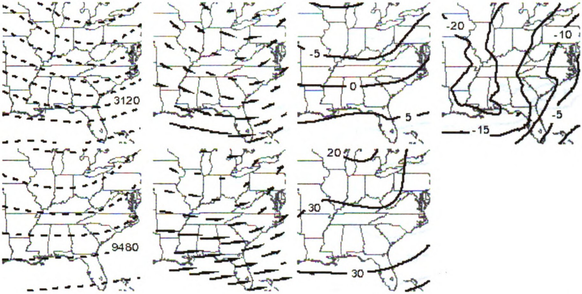

Figure D.8. Cluster 8. Maps in the top row from left to right are temperature (contoured every 5°C) wind vectors, dewpoint (contoured every 5°C), and height (contoured every 30 m) at the 700 hPa level. Maps in the bottom row from left to right are height (contoured every 120 m), wind vectors, and isotachs (contoured every 10 m/s) at the 300 hPa level.

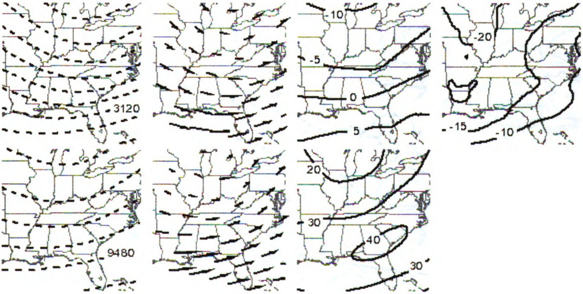

Figure D.9. Cluster 9. Maps in the top row from left to right are temperature (contoured every 5°C) wind vectors, dewpoint (contoured every 5°C), and height (contoured every 30 m) at the 700 hPa level. Maps in the bottom row from left to right are height (contoured every 120 m), wind vectors, and isotachs (contoured every 10 m/s) at the 300 hPa level.

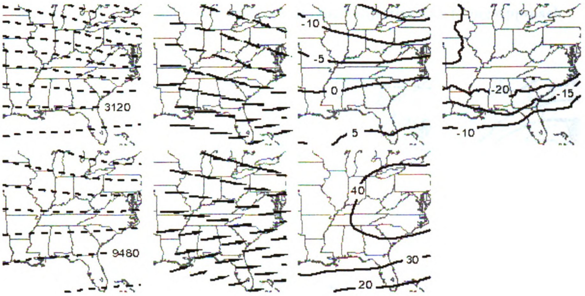

Figure D.10. Cluster 10. Maps in the top row from left to right are temperature (contoured every 5°C) wind vectors, dewpoint (contoured every 5°C), and height (contoured every 30 m) at the 700 hPa level. Maps in the bottom row from left to right are height (contoured every 120 m), wind vectors, and isotachs (contoured every 10 m/s) at the 300 hPa level.

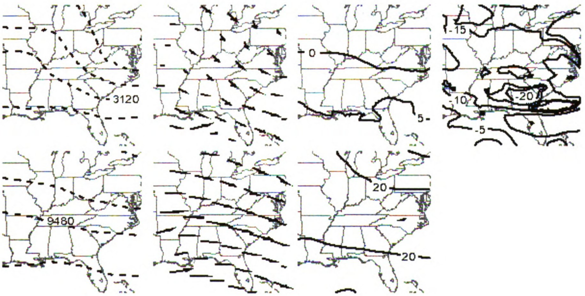

Figure D.11. Cluster 11. Maps in the top row from left to right are temperature (contoured every 5°C) wind vectors, dewpoint (contoured every 5°C), and height (contoured every 30 m) at the 700 hPa level. Maps in the bottom row from left to right are height (contoured every 120 m), wind vectors, and isotachs (contoured every 10 m/s) at the 300 hPa level.

D.2. Maps of 700 and 300 hPa Variables from the Subjective Clustering Approach

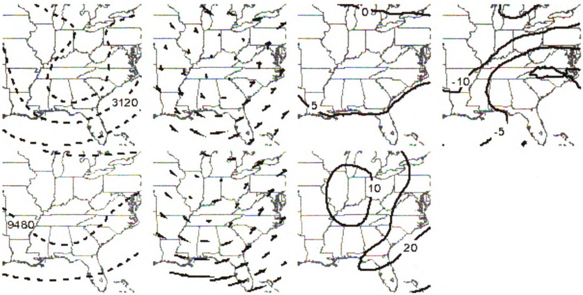

Figure D.12. Closed low (CL). Maps in the top row from left to right are temperature (contoured every 5°C) wind vectors, dewpoint (contoured every 5°C), and height (contoured every 30 m) at the 700 hPa level. Maps in the bottom row from left to right are height (contoured every 120 m), wind vectors, and isotachs (contoured every 10 m/s) at the 300 hPa level.

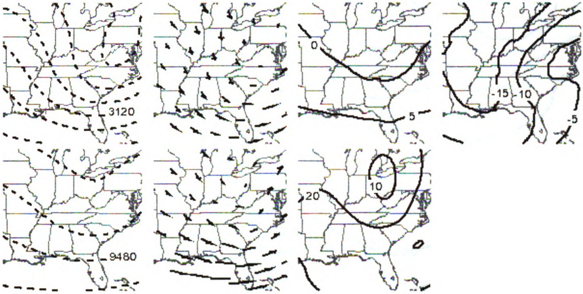

Figure D.13. Northerly, behind low, no fronts (NbLnF). Maps in the top row from left to right are temperature (contoured every 5°C) wind vectors, dewpoint (contoured every 5°C), and height (contoured every 30 m) at the 700 hPa level. Maps in the bottom row from left to right are height (contoured every 120 m), wind vectors, and isotachs (contoured every 10 m/s) at the 300 hPa level.

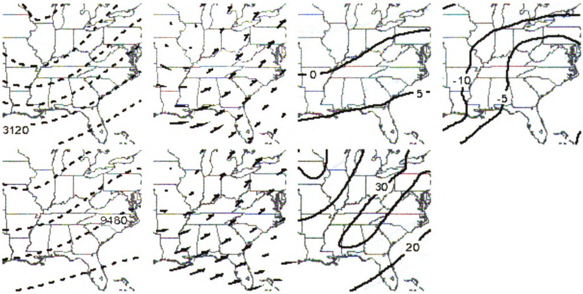

Figure D.14. Southerly, ahead of low, no fronts (SaLnF). Maps in the top row from left to right are temperature (contoured every 5°C) wind vectors, dewpoint (contoured every 5°C), and height (contoured every 30 m) at the 700 hPa level. Maps in the bottom row from left to right are height (contoured every 120 m), wind vectors, and isotachs (contoured every 10 m/s) at the 300 hPa level.

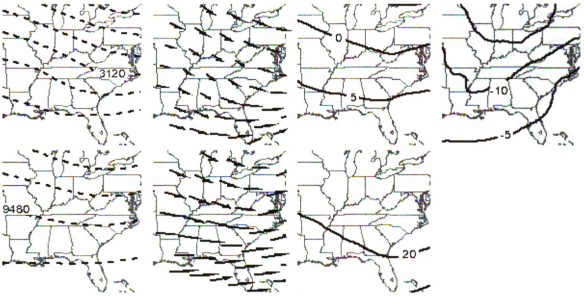

Figure D.15. Northerly, no low, no fronts (NnLnF). Maps in the top row from left to right are temperature (contoured every 5°C) wind vectors, dewpoint (contoured every 5°C), and height (contoured every 30 m) at the 700 hPa level. Maps in the bottom row from left to right are height (contoured every 120 m), wind vectors, and isotachs (contoured every 10 m/s) at the 300 hPa level.

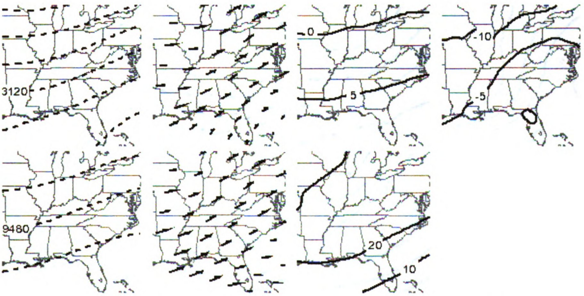

Figure D.16. Southerly, no low, no fronts (SnLnF). Maps in the top row from left to right are temperature (contoured every 5°C) wind vectors, dewpoint (contoured every 5°C), and height (contoured every 30 m) at the 700 hPa level. Maps in the bottom row from left to right are height (contoured every 120 m), wind vectors, and isotachs (contoured every 10 m/s) at the 300 hPa level.

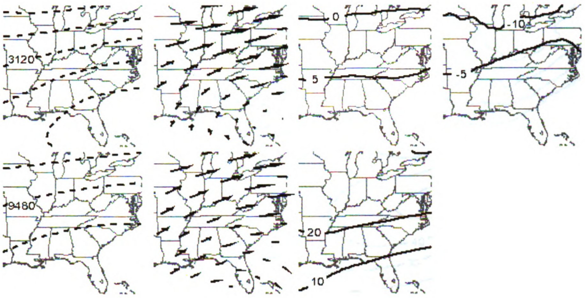

Figure D.17. Bermuda High (BH). Maps in the top row from left to right are temperature (contoured every 5°C) wind vectors, dewpoint (contoured every 5°C), and height (contoured every 30 m) at the 700 hPa level. Maps in the bottom row from left to right are height (contoured every 120 m), wind vectors, and isotachs (contoured every 10 m/s) at the 300 hPa level.

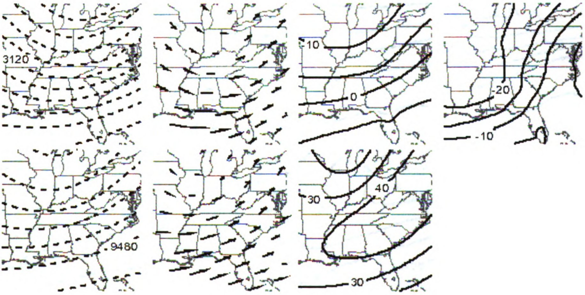

Figure D.18. North-south oriented front (nsF). Maps in the top row from left to right are temperature (contoured every 5°C) wind vectors, dewpoint (contoured every 5°C), and height (contoured every 30 m) at the 700 hPa level. Maps in the bottom row from left to right are height (contoured every 120 m), wind vectors, and isotachs (contoured every 10 m/s) at the 300 hPa level.

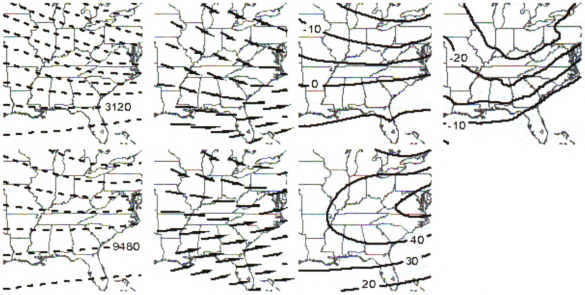

Figure D.19. Northerly, east-west oriented front (NewF). Maps in the top row from left to right are temperature (contoured every 5°C) wind vectors, dewpoint (contoured every 5°C), and height (contoured every 30 m) at the 700 hPa level. Maps in the bottom row from left to right are height (contoured every 120 m), wind vectors, and isotachs (contoured every 10 m/s) at the 300 hPa level.

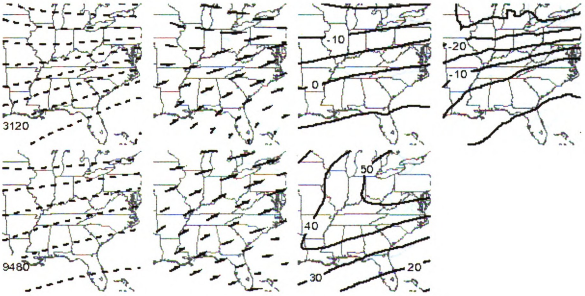

Figure D.20. Southerly, east-west oriented front (SewF). Maps in the top row from left to right are temperature (contoured every 5°C) wind vectors, dewpoint (contoured every 5°C), and height (contoured every 30 m) at the 700 hPa level. Maps in the bottom row from left to right are height (contoured every 120 m), wind vectors, and isotachs (contoured every 10 m/s) at the 300 hPa level.

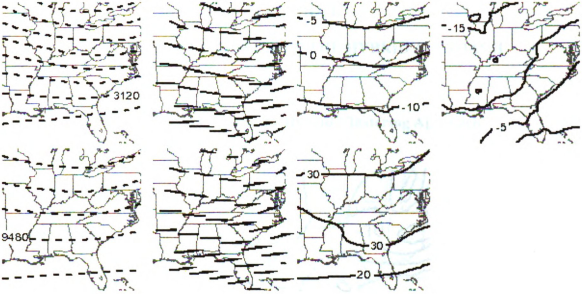

Figure D.21. Zonal flow (Z). Maps in the top row from left to right are temperature (contoured every 5°C) wind vectors, dewpoint (contoured every 5°C), and height (contoured every 30 m) at the 700 hPa level. Maps in the bottom row from left to right are height (contoured every 120 m), wind vectors, and isotachs (contoured every 10 m/s) at the 300 hPa level.

Figure D.22. Weak flow (W). Maps in the top row from left to right are temperature (contoured every 5°C) wind vectors, dewpoint (contoured every 5°C), and height (contoured every 30 m) at the 700 hPa level. Maps in the bottom row from left to right are height (contoured every 120 m), wind vectors, and isotachs (contoured every 10 m/s) at the 300 hPa level.

APPENDIX E

SYNOPTIC PATTERNS FROM THE HYBRID APPROACH

E.1. Maps of 850 hPa Variables from the Hybrid Clustering Approach

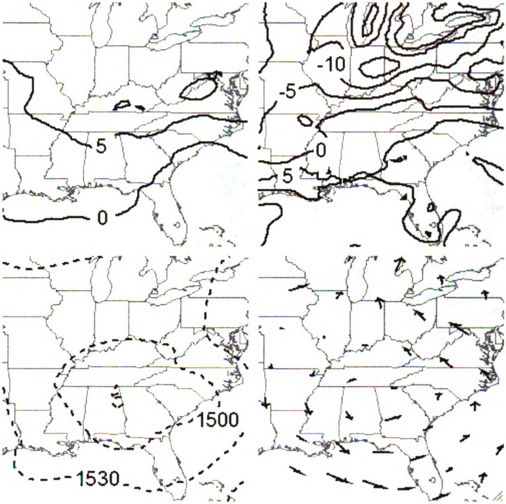

Figure E.1. Closed low (CL). Temperature contoured every 5°C (top left), dewpoint contoured every 5°C (top right), height contoured every 30 m (bottom left), and wind vectors (bottom right) at the 850 hPa level.

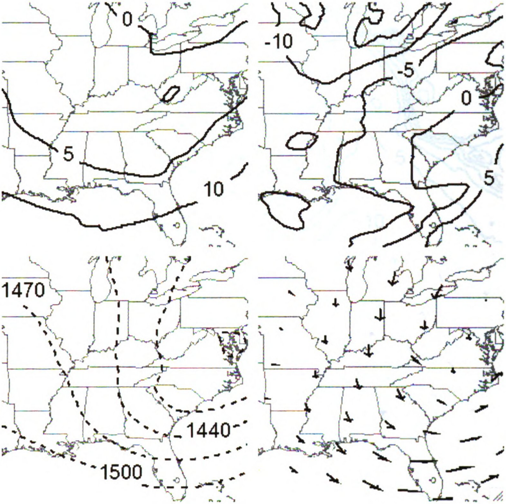

Figure E.2. Northerly, behind low, no fronts (NbLnF). Temperature contoured every 5°C (top left), dewpoint contoured every 5°C (top right), height contoured every 30 m (bottom left), and wind vectors (bottom right) at the 850 hPa level.

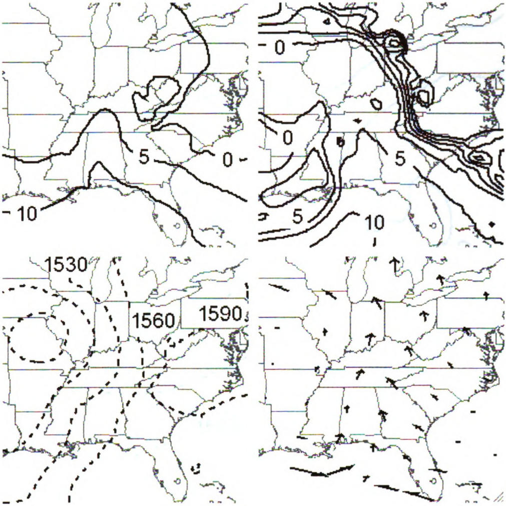

Figure E.3. Southerly, ahead of low, no fronts (SaLnF). Temperature contoured every 5°C (top left), dewpoint contoured every 5°C (top right), height contoured every 30 m (bottom left), and wind vectors (bottom right) at the 850 hPa level.

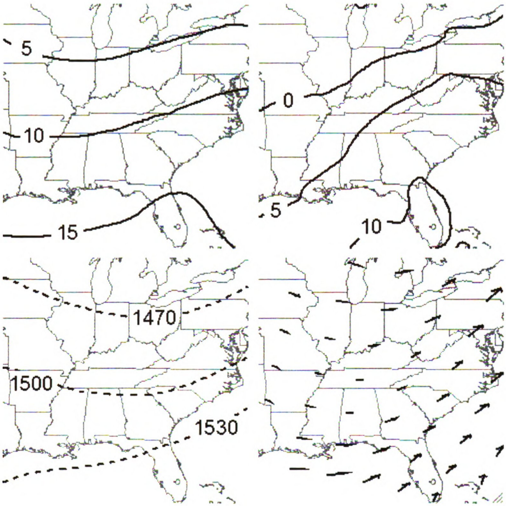

Figure E.4. Southerly, no low, no fronts (SnLnF). Temperature contoured every 5°C (top left), dewpoint contoured every 5°C (top right), height contoured every 30 m (bottom left), and wind vectors (bottom right) at the 850 hPa level.

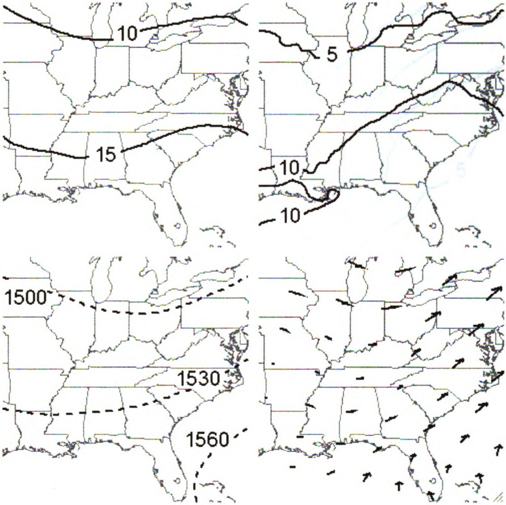

Figure E.5. Bermuda High (BH). Temperature contoured every 5°C (top left), dewpoint contoured every 5°C (top right), height contoured every 30 m (bottom left), and wind vectors (bottom right) at the 850 hPa level.

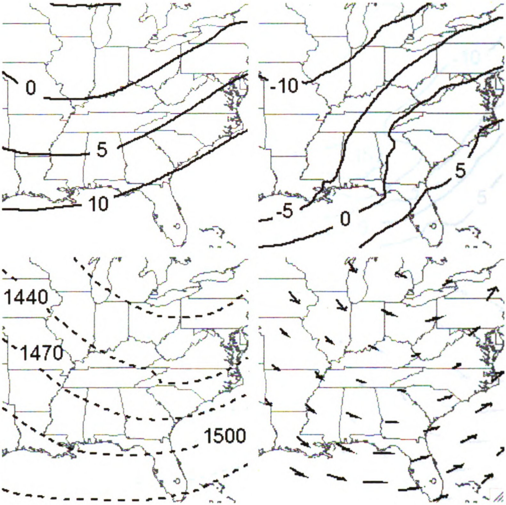

Figure E.6. North-south oriented front (nsF). Temperature contoured every 5°C (top left), dewpoint contoured every 5°C (top right), height contoured every 30 m (bottom left), and wind vectors (bottom right) at the 850 hPa level.

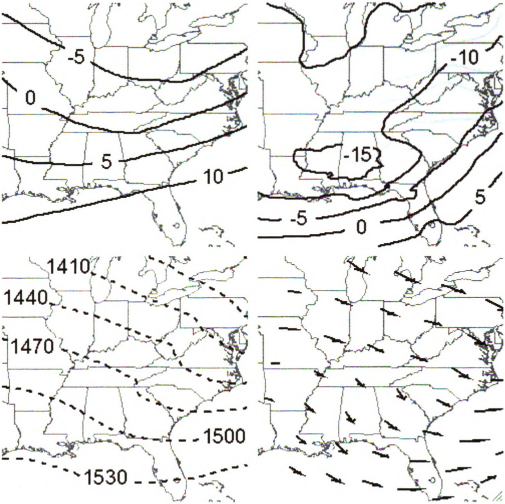

Figure E.7. Northerly, east-west oriented front (NewF). Temperature contoured every 5°C (top left), dewpoint contoured every 5°C (top right), height contoured every 30 m (bottom left), and wind vectors (bottom right) at the 850 hPa level.

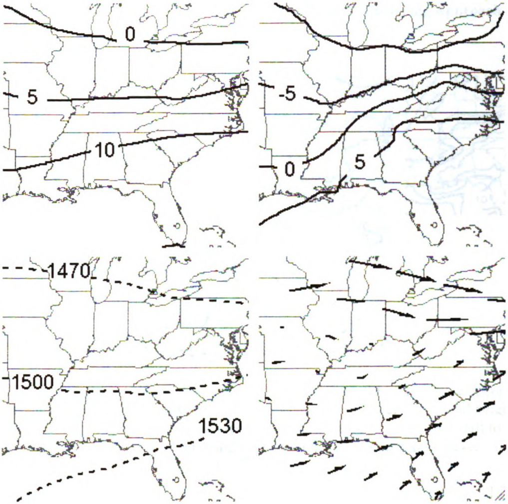

Figure E.8. Southerly, east-west oriented front (SewF). Temperature contoured every 5°C (top left), dewpoint contoured every 5°C (top right), height contoured every 30 m (bottom left), and wind vectors (bottom right) at the 850 hPa level.

E.2. Maps of 700 and 300 hPa Variables from the Hybrid Clustering Approach

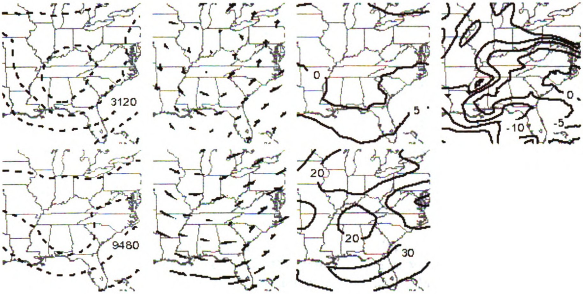

Figure E.9. Closed low (CL). Maps in the top row from left to right are temperature (contoured every 5°C) wind vectors, dewpoint (contoured every 5°C), and height (contoured every 30 m) at the 700 hPa level. Maps in the bottom row from left to right are height (contoured every 120 m), wind vectors, and isotachs (contoured every 10 m/s) at the 300 hPa level.

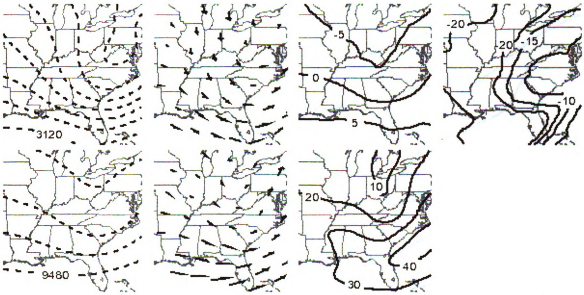

Figure E.10. Northerly, behind low, no fronts (NbLnF). Maps in the top row from left to right are temperature (contoured every 5°C) wind vectors, dewpoint (contoured every 5°C), and height (contoured every 30 m) at the 700 hPa level. Maps in the bottom row from left to right are height (contoured every 120 m), wind vectors, and isotachs (contoured every 10 m/s) at the 300 hPa level.

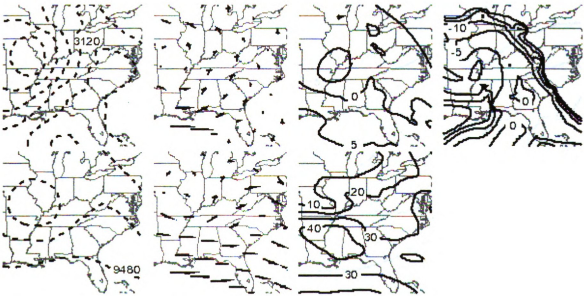

Figure E.11. Southerly, ahead of low, no fronts (SaLnF). Maps in the top row from left to right are temperature (contoured every 5°C) wind vectors, dewpoint (contoured every 5°C), and height (contoured every 30 m) at the 700 hPa level. Maps in the bottom row from left to right are height (contoured every 120 m), wind vectors, and isotachs (contoured every 10 m/s) at the 300 hPa level.

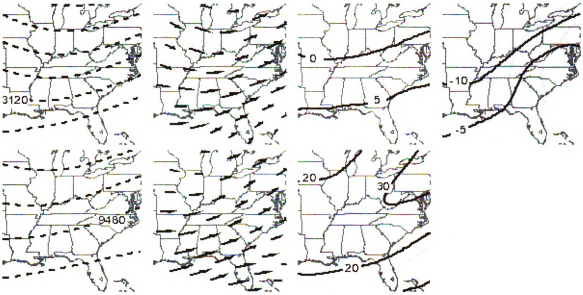

Figure E.12. Southerly, no low, no fronts (SnLnF). Maps in the top row from left to right are temperature (contoured every 5°C) wind vectors, dewpoint (contoured every 5°C), and height (contoured every 30 m) at the 700 hPa level. Maps in the bottom row from left to right are height (contoured every 120 m), wind vectors, and isotachs (contoured every 10 m/s) at the 300 hPa level.

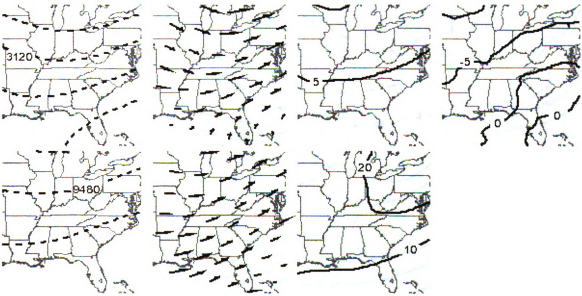

Figure E.13. Bermuda High (BH). Maps in the top row from left to right are temperature (contoured every 5°C) wind vectors, dewpoint (contoured every 5°C), and height (contoured every 30 m) at the 700 hPa level. Maps in the bottom row from left to right are height (contoured every 120 m), wind vectors, and isotachs (contoured every 10 m/s) at the 300 hPa level.

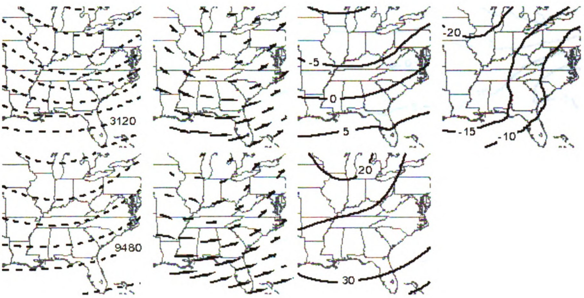

Figure E.14. North-south oriented front (nsF). Maps in the top row from left to right are temperature (contoured every 5°C) wind vectors, dewpoint (contoured every 5°C), and height (contoured every 30 m) at the 700 hPa level. Maps in the bottom row from left to right are height (contoured every 120 m), wind vectors, and isotachs (contoured every 10 m/s) at the 300 hPa level.

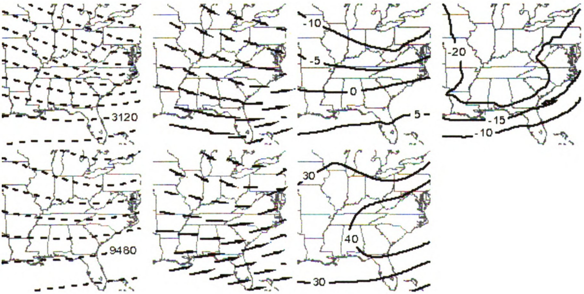

Figure E.15. Northerly, east-west oriented front (NewF). Maps in the top row from left to right are temperature (contoured every 5°C) wind vectors, dewpoint (contoured every 5°C), and height (contoured every 30 m) at the 700 hPa level. Maps in the bottom row from left to right are height (contoured every 120 m), wind vectors, and isotachs (contoured every 10 m/s) at the 300 hPa level.

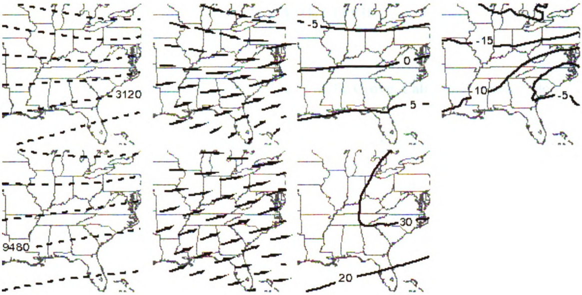

Figure E.16. Southerly, east-west oriented front (SewF). Maps in the top row from left to right are temperature (contoured every 5°C) wind vectors, dewpoint (contoured every 5°C), and height (contoured every 30 m) at the 700 hPa level. Maps in the bottom row from left to right are height (contoured every 120 m), wind vectors, and isotachs (contoured every 10 m/s) at the 300 hPa level.

LITERATURE CITED

Ahrens CD (2003) *Meteorology today*, 7th ed. Pacific Grove, California: Brook/Cole – Thomson Learning.

Allen TR, Kupfer JA (2000) Application of spherical statistics to change vector analysis of Landsat data: Southern Appalachian spruce-fir forests. *Remote Sensing of the Environment*, **74**, 482-493.

Allen TR, Kupfer JA (2001) Spectral response and spatial pattern of Fraser fir mortality and regeneration, Great Smoky Mountains, USA. *Plant Ecology*, **156**, 59-74.

Aneja VP, Businger S, Li Z, Claiborn CS, Murthy A (1991) Ozone climatology at high elevations in the southern Appalachians. *Journal of Geophysical Research*, **96(D1)**, 1007-1021.

Aneja VP, Robarge WP, Claiborn CS, Murthy A, Soo-Kim D, Li Z (1992) Chemical climatology of high elevation spruce-fir forests in the southern Appalachian mountains. *Environmental Pollution*, **75**, 89-96.

Balling RC, Michaels PJ, Knappenberger PC (1998) Analysis of winter and summer warming rates in gridded temperature time series. *Climate Research*, **9**, 175-181.

Bell GD, Bosart LF (1988) Appalachian cold-air damming. *Monthly Weather Review*, **116**, 137-161.

Bogucki DJ (1972) Intense rainfall in Great Smoky Mountains National Park. *Journal of the Tennessee Academy of Science*, **47(3)**, 93-97.

Bolstad PV, Swift L, Collins F, Régnière J (1998) Measured and predicted air temperatures at basin to regional scales in the southern Appalachian mountains. *Agricultural and Forest Meteorology*, **91**, 161-176.

Bosart LF (1975) New England coastal frontogenesis. *Quarterly Journal of the Royal Meteorological Society*, **101**, 957-978.

Braun EL (1950) *Deciduous forests of eastern North America*. New York: Hafner Press.

Bryson RA (1966) Air masses, streamlines, and the boreal forest. *Geographical Bulletin*, **8**, 228-269.

Busing RT, Clebsch EEC, Eagar CC, Pauley EF (1988) Two decades of change in the Great Smoky Mountains spruce-fir forest. *Bulletin of the Torrey Botanical Club*, **115(1)**, 25-31.

Carlson TN (1998) *Mid-latitude weather systems*. Boston, Massachusetts: The American Meteorological Society.

Davis R, Rogers RF (1992) A synoptic climatology of severe storms in Virginia. *The Professional Geographer*, **44(3)**, 319-332.

Deevey ES (1949) Biogeography of the Pleistocene: Part I: Europe and North America. *Bulletin of the Geological Society of America*, **60**, 1315-1416.

Delcourt PA, Delcourt HR (2001) *Living well in the age of global warming*. White River Junction, Vermont: Chelsea Green Publishing Company.

Delcourt HR (2002) *Forests in peril*. Blacksburg, Virginia: The McDonald and Woodward Publishing Company.

Diaz HF, Quayle RG (1978) The 1976-77 winter in the contiguous United States in comparison with past records. *Monthly Weather Review*, **106(10)**, 1393-1421.

Diem JE (2006) Synoptic-scale controls of summer precipitation in the southeastern United States. *Journal of Climate*, **19**, 613-621.

Easterling DR, Horton B, Jones PD, Peterson TC, Karl TR, Parker DE, Salinger MJ, Razuvayev V, Plummer N, Jamason P, Folland CK (1997) Maximum and minimum temperature trends for the globe. *Science*, **277**, 364-367

Fovell RG (1997) Consensus clustering of U.S. temperature and precipitation data. *Journal of Climate*, **10**, 1405-1427.

Fovell RG, Fovell M-YC (1993) Climate zones of the conterminous United States defined using cluster analysis. *Journal of Climate*, **6(11)**, 2103-2135.

Gaffin DM, Hotz DG (2000) A precipitation and flood climatology with synoptic features of heavy rainfall across the southern Appalachian mountains. *National Weather Digest*, **24(3)**, 3-15.

Goldman, M (2009) Constructing connectivity: Conservation corridors and conservation politics in East African rangelands. *Annals of the Association of American Geographers*, **99(2)**, 335-359.

Gong X, Richman MB (1995) On the application of cluster analysis to growing season precipitation data in North America east of the Rockies. *Journal of Climate*, **8(4)**, 897-931.

Great Smoky Mountains Association (2007) A big year for fires. *Bearpaw*, **Fall-Winter 2007-2008**, 4.

Great Smoky Mountains Association (2009) Spring fires scorch hundreds of acres. *Smokies Guide*, **Summer 2009**, 6.

Hack JT, Goodlett JC (1960) Geomorphology and forest ecology of a mountain region in the central Appalachians. *Geological Survey Professional Paper*, **347**, 1-66.

Harman JR (1991) *Synoptic climatology of the westerlies: Processes and patterns*. Washington, D.C.: Association of American Geographers.

Harvey WS (1978) Trends and variations of mean temperature in the lower troposphere. *Monthly Weather Review*, **106**, 413-416.

Heald W (1967) *Sky islands*. Princeton, New Jersey: Van Nostrand.

Hicks DJ (1979) Forest microclimate in the Great Smoky Mountains. *Journal of the Tennessee Academy of Science*, **54(3)**, 84-88.

Houk R (2009) "A" is for azalea. *Smokies Life Magazine*, **3(1)**, 10-17.

Intergovernmental Panel on Climate Change (2007a) *Climate change 2007: The physical science basis*. Cambridge, New York: Cambridge University Press.

Intergovernmental Panel on Climate Change (2007b) *A contribution of Working Group II to the fourth assessment report of the Intergovernmental Panel on Climate Change: Summary for policymakers*.
<http://www.ipcc.ch/pdf/assessment-report/ar4/wg2/ar4-wg2-spm.pdf>.

Karl TR, Jones PD, Knight RW, Kukla G, Plummer N, Razuvayev V, Gallo KP, Lindseay J, Charlson RJ, Peterson TC (1993) A new perspective on recent global warming: Asymmetric trends of daily maximum and minimum temperature. *Bulletin of the American Meteorological Society*, **74(6)**, 1007-1023.

Kalnay E, Kanamitsu M, Kistler R, Collins W, Deaven D, Gandin L, Iredell M, Saha S, White G, Woollen J, Zhu Y, Chelliah M, Ebisuzaki W, Higgins W, Janowiak J, Mo KC, Ropelewski C, Wang J, Leetmaa A, Reynolds R, Jenne R, Joseph D (1996) The NCEP/NCAR 40-year reanalysis project, *Bulletin of the American Meteorological Society*, **77(3)**, 437-471.

Karypis G (2003) CLUTO: A clustering toolkit. *Technical Report: #02-017*. University of Minnesota, Department of Computer Science, Minneapolis, MN 55455.

Klein WH (1957) Principle tracks and mean frequencies of cyclones and anticyclones in the Northern Hemisphere. *Weather Bureau Research Paper No. 40*, 60 pp., U.S. Department of Commerce, NOAA, Washington, D.C.

Konrad CE (1997) Synoptic-scale features associated with warm season heavy rainfall over the interior southeastern United States. *Weather and Forecasting*, **12**, 557-571.

Köppen W (1923) *Die klimate der erde; Grundriss der klimakunde*. De Gruyter.

Kupfer JA, Cairns DM (1996) The suitability of montane ecotones as indicators of global climatic change. *Progress in Physical Geography*, **20(3)**, 253-272.

Kupfer JA, Balmat J, Smith JL (2005) Shifts in the potential distribution of sky island plant communities in response to climate change. In *Connecting mountain islands and desert seas: Biodiversity and management of the Madrean Archipelago II*. Edited by GJ Gottfried, BS Gebow, LG Eskew, and CB Edminster. pp. 485-490. Fort Collins, Colorado: U.S. Department of Agriculture, Forest Service, Rocky Mountain Research Station.

Lewis SL, Lopez-Gonzalez G, Sonke B, Affum-Baffoe K, Baker TR, Ojo LO, Phillips OL, Reitsma JM, White L, Comiskey JA, Djuikouo K M-N, Ewango CEN, Feldpausch TR, Hamilton AC, Gloor M, Hart T, Hladik A, Lloyd J, Lovett JC, Makana J-R, Malhi Y, Mbago FM, Ndangalasi HJ, Peacock J, Peh KS-H, Sheil D, Sunderland T, Swaine MD, Taplin J, Taylor D, Thomas SC, Votere R, Wöll H (2009) Increasing carbon storage in intact African tropical forests. *Nature*, **457**, 1003-1006.

Luyssaert S, Schulze E-D, Börner A, Knohl A, Hessenmöller D, Law BE, Ciais P, Grace J (2008) Old-growth forests as global carbon sinks. *Nature*, **455**, 213-215.

Mark AF (1958) The ecology of the southern Appalachian grass balds. *Ecological Monographs*, **28(4)**, 293-336.

Marris E (2009) Planting the forest of the future. *Nature*, **459**, 906-908.

Mesinger F, DiMego G, Kalnay E, Mitchell K, Shafran PC, Ebisuzaki W, Jović D, Woollen J, Rogers E, Berbery EH, Ek MB, Fan Y, Grumbine R, Higgins W, Li H, Lin Y, Manikin G, Parrish D, Shi W (2006) North American regional reanalysis, *Bulletin of the American Meteorological Society*, **87(3)**, 343-360.

Miller JE (1946) Cyclogenesis in the Atlantic coastal region of the United States. *Journal of Meteorology*, **3**, 31-44.

Milligan GW, Cooper MC (1985) An examination of procedures for determining the number of clusters in a data set. *Psychometrika*, **50**, 159-179.

Mimmack GM, Mason SJ, Galpin JS (2001) Choice of distance matrices in cluster analysis: Defining regions. *Journal of Climate*, **14**, 2790-2797.

National Park Service (2009) *Nature & Science*. <http://www.nps.gov/grsm/naturescience/index.htm>.

O'Handley C, Bosart LF (1996) The impact of the Appalachian Mountains on cyclonic weather systems. Part I: A climatology. *Monthly Weather Review*, **124**, 1353-1373.

Reitan CH (1974) Frequencies of cyclones and cyclogenesis for North America, 1951-1970. *Monthly Weather Review*, **102**, 861-868.

Richwein BA (1980) The damming effect of the southern Appalachians. *National Weather Digest*, **5(1)**, 2-12.

Root TL, Schneider SH (2001) Climate change: Overview and implications for wildlife. In *Wildlife responses to climate change*. Ed. S.H. Schneider and T.L. Root. Washington: Island Press. 1-56.

Shadbolt RP, Waller EA, Messina JP, Winkler JA (2006) Source regions of lower-tropospheric airflow trajectories for the lower peninsula of Michigan: A 40-year air mass climatology. *Journal of Geophysical Research*, **111**, D21117, doi: 10.1029/2005JD006657.

Shanks RE (1954) Climates of the Great Smoky Mountains. *Ecology*, **35(3)**, 354-361.

Skaggs RH (1969) Analysis and regionalization of the diurnal distribution of tornadoes in the United States. *Monthly Weather Review*, **97**, 103-115.

Skroch M (2009) The sky islands of North America. *International Journal of Wilderness*, **15(1)**, 9-14.

Smallshaw J (1953) Some precipitation-altitude studies of the Tennessee Valley Authority. *American Geophysical Union – Transactions*, **34(4)**, 583-588.

Solow AR (1987) Testing for climate change: An application of the two-phase regression model. *Journal of Climate and Applied Meteorology*, **26**, 1401-1405.

Stephenson DB (1997) Correlation of spatial climate/weather maps and the advantages of using the Mahalanobis metric in predictions. *Tellus*, **49A**, 513-527.

Stine AR, Huybers P, Fung IY (2009) Changes in the phase of the annual cycle of surface temperature. *Nature*, **457**, 435-440.

Stooksbury DE, Michaels PJ (1991) Cluster analysis of southeastern U.S. climate stations. *Theoretical and Applied Climatology*, **44(3-4)**, 143-150.

Tan P-N, Steinbach M, Kumar V (2006) *Introduction to data mining*. Boston, Massachusetts: Pearson Education, Inc.

Thornthwaite CW (1931) The climates of North America, according to a new classification. *Geographical Review*, **21**, 633-655.

Trenberth KE (1990) Recent observed interdecadal climate changes in the northern hemisphere. *Bulletin of the American Meteorological Society*, **71(7)**, 988-993.

Tyron RC (1939) *Cluster analysis*. Edwards Brothers.

United States Global Change Research Program (2009) *Global climate change impacts in the United States*. Cambridge, New York: Cambridge University Press.

van Loon H, Williams J (1976a) The connection between trends of mean temperature and circulation at the surface: Part I. Winter. *Monthly Weather Review*, **104**, 365-380.

van Loon H, Williams J (1976b) The connection between trends of mean temperature and circulation at the surface: Part II. Summer. *Monthly Weather Review*, **104**, 1003-1011.

Walters CK, Winkler JA (2001) Airflow configurations of warm season southerly low-level wind maxima in the Great Plains. Part I: spatial and temporal characteristics and relationship to convection. *Weather and Forecasting*, **16(5)**, 513-530.

Walters CK, Winkler JA, Shadbolt RP, van Ravensway J, Bierly GD (2008) A long-term climatology of southerly and northerly jets for the central United States. *Annals of the Association of American Geographers*, **98(3)**, 521-552.

Walters CK, Winkler JA, van Ravensway J, Shadbolt RP (in preparation) Airflow patterns of northerly low-level jets in central North America. Part I: Climatological analysis.

Whittaker RH (1952) A study of summer foliage insect communities in the Great Smoky Mountains. *Ecological Monographs*, **22(1)**, 1-44.

Whittaker RH (1956) Vegetation of the Great Smoky Mountains. *Ecological Monographs*, **26(1)**, 1-80.

Wilks DS (2006) *Statistical methods in the atmospheric sciences*. 2nd ed. Burlington, Massachusetts: Academic Press.

Winkler JA (1992) Regional patterns of the diurnal properties of heavy hourly precipitation. *Professional Geographer*, **44**, 127-146.

Winkler JA (2004) The impact of technology upon in situ atmospheric observations and climate science. In *Geography and technology*, ed. S.D. Brunn, S.L. Cutter, and J.W. Harrington, Jr. Norwell, Massachusetts: Kluwer Academic Publishers.

Zhao Y, Karypis G (2003) Criterion functions for document clustering: Experiments and analysis. *Technical Report #01-40*. University of Minnesota, Department of Computer Science / Army HPC Research Center, Minneapolis, MN 55455.

Zishka ZM, Smith PJ (1980) The climatology of cyclones and anticyclones over North America and surrounding ocean environs for January and July, 1950-77. *Monthly Weather Review*, **108(4)**, 387-401.